University of Stavanger

Faculty of Science and Technology

MASTER'S THESIS

Study program/ Specialization: Offshore Technology, Subsea Technology	Spring semester, 2014 Open / ~~Restricted~~ access
Writer: Lurohman Mamin Masturi	…… (Writer's signature)
Faculty supervisor: Prof. Ove Tobias Gudmestad External supervisor(s):	
Thesis title: Comparison Study of Selected Uncoupled Riser Concepts in Deep Water and Harsh Environment	
Credits (ECTS): 30	
Key words: Deep Water, Uncoupled Riser, COBRA, SLOR, Norwegian Sea	Pages: xviii + 133 + enclosure: 18 Stavanger, 13th June 2014 Date/year

Abstract

Installing deep water risers in harsh environmental conditions even in the icing environment, in the near future seems like inevitable. Especially in the Norwegian Sea, the development of deep water technology requires an urgent solution of how to transfer hydrocarbons from sea bed to the host facility in a remote area with considering hostile environment conditions.

In every subsea production system combined with a floating facility, the need of risers is a must. Deeper water causes various challenges, for instance; higher payload of the vessel, increase probability of collapse failure of the riser, higher probability for riser failure due to buckling and fatigue issue at the touch-down-point (TDP) as well as presence of Vortex Induce Vibration (VIV) in the long suspended riser span. In addition, the polar climate which is occurring in the Norwegian Sea should be considered during designing, installing and operating of the system which caused this area to be different from other places.

In order to reduce excessive floater motions, an uncoupled riser system is introduced. By using buoy elements, the riser system is able decouple the motion effect of the floater, riser and mooring system that may magnify the extreme hull/floater response. This can significantly improve strength and fatigue performance of the riser. This system is widely used in deep water conditions with various riser configurations. In general, an uncoupled riser system consists of two different types of riser concepts (flexible and steel) with buoy in between. There are three main components in this configuration; a flexible jumper that is directly connected to the floater, a sub-surface buoyancy module at the connection point, and a steel riser at the bottom parts. The flexible jumper is used to absorb the floater motions, and the result the configuration gives the optimum riser concept which is best suited for deep water conditions.

In this topic, we limit the uncoupled riser configurations into two types; Catenary Offset Buoyant Riser Assembly (COBRA) and Single Line Offset Riser (SLOR). The difference between these two riser configurations is at the bottom part and at the connection point; COBRA configures the steel pipe as a catenary riser with a long-slender sub-surface buoyancy module on the top which is tethered down to sea bed via mooring lines while SLOR configures the steel pipe as a tensioned riser by using an air can as a buoyancy module to maintain the riser in tensioned position all time. By means of these riser configurations we have the possibility to use different types of riser arrangements since a standalone flexible riser is very expensive to use in deep water conditions. The main advantage of the two uncoupled riser configurations is that they enable possibilities for the floater to drift/side-step in case of drifting icebergs, which will be one of the study cases.

This thesis focuses on a comparison study of the two uncoupled riser configurations based on ultimate limit state (ULS) and accidental limit state (ALS) results by considering the possibility to avoid/prevent iceberg collision. As explained previously, the risers to be studied are set to be installed in the Norwegian Sea which has harsh environmental conditions. Three different water depths have been chosen on purpose, which are 100m, 400m, and 1500m.

In the event of iceberg approach, this thesis work presents two solutions for comparison study. The two solutions are to drift/side-step the floating structure or to disconnect the riser/mooring system using a disconnectable turret. The repot will suggest the optimum solutions; the most suitable uncoupled riser configuration for the Norwegian Sea condition with respect to the riser performance for the case of floater drift off and the geometry of a disconnected riser.

Based on detail strength analysis in operating and accidental conditions, this thesis concludes that COBRA riser concept has robust and efficient design to install in the Norwegian Sea conditions. In addition, the COBRA configuration in 1500 m water depth is feasible to perform a 250 m side-stepping in the event of an iceberg approach.

Keywords: Deep Water, Uncoupled Riser, COBRA, SLOR, Norwegian Sea

Acknowledgment

In the name of Allah SWT, the most precious and the most merciful.

First of all, all praise due to Allah SWT for giving me the 'Rahmat' to complete this thesis which is part of the requirement to achieve my Master of Since degree in Marine and Subsea Technology, University of Stavanger.

I would like to express my sincere gratitude and appreciation to my supervisor, Prof. Ove Tobias Gudmestad for giving me a tremendous support and guidance in this thesis. For all of comments, inputs and patients to read and review my thesis, I would like to say many thanks. In addition, I would also like to thank to my co-Supervisor, Airindy Feslista (PhD Student of UiS), for the discussions and essential comments during the writing process of this thesis. With utmost respect, I would like to thank to Arn Bloch as a Manager, and all my colleges in Avant offshore AS for giving me an opportunity to work part-time during my master's study.

A special thank to all my family in Bandung, for all prayers, loves and supports. Words cannot express how grateful I am for the sacrifices that you have made on my behalf. In this opportunity, I would like to dedicate this thesis for my beloved late mother who was always support and believe in me. Your name is always in my prayers.

Last but not least, my best wish goes to all of my Indonesian friends, 'geng gulfaks', 'geng pengajian', 'geng jernal', 'geng masjid maki', and 'geng AGASTA'. For the experiences we had together, it is priceless. The most beneficial knowledge in this world is the knowledge that will bring you into 'Jannah'.

Stavanger, 13th June 2014

Lurohman Mamin Masturi

Nomenclature

Greek Characters

α_C	Strain hardening
α_{fab}	Manufacturing process reduction factor
γ_A	Load effect factor for accidental loads
γ_C	Condition factor
γ_E	Load effect factor for environmental loads
γ_F	Load effect factor for functional loads
γ_m	Resistance factor for material and resistance uncertainties
γ_{SC}	Resistance factor to take into account the safety class
λ	Wave length
η	Water surface elevation
ζ	Wave amplitude
ω_n	Wave frequency
ω_p	Angular spectral frequency
ρ	Water density
ρ_i	Internal fluid density
ϕ	Roll motion
θ	Pitch motion
φ	Yaw motion
ε	Wave phase angle
σ_ζ^2	Variance of water surface elevations
ν	Poisson's ratio

Symbols

A	Cross section area
A_i	Internal cross-sectional area
A_ω	Normalizing factor

C_D	Drag coefficient
C_M	Inertia coefficient
D	Nominal outside diameter
d	Water depth to still water level
D_{fat}	Accumulated fatigue damage
d_o	Reference depth
deg	Degree
E	Young's modulus
f_k	Force per unit length in tangential direction
f_n	Natural frequency
f_n	Force per unit length in normal direction
f_o	Initial ovality
f_u	Tensile strength
g	Gravity acceleration
$H_{1/3,}$ H_s	Significant wave height
h	Height
k	Surface roughness
k_n	Wave number
KC	Keulegan Carpenter number
kg	Kilogram
kN	Kilogram
kg	Kilo Newton
m	Meter
$m_{0\zeta}$	Area under the spectral curve
$m_{1\zeta}$	First order moment (static moment) of area under the spectral curve
$m_{2\zeta}$	Second order moment (moment of inertia) of area under the spectral curve
M_A	Bending moment from accidental loads
M_E	Bending moment from environmental loads

M_F	Bending moment from functional loads
M_k	Plastic Bending moment resistance
mm	millimeter
MN	Mega Newton
N_{cg}	Number of stress cycles necessary to increase the defect from the initial to the critical defect size
N_{tot}	Total number of applied stress cycles during service or to in-service inspection
p_b	Burst resistance
p_c	Resistance for external pressure (hoop buckling)
p_d	Design pressure
p_e	External pressure
p_{el}	Elastic collapse pressure
p_i	Internal (local) pressure
p_{ie}	External (local) pressure
p_{inc}	Incidental pressure
p_{Id}	Local internal design pressure
p_{li}	Local incidental pressure
p_{min}	Minimum internal pressure
p_p	Plastic collapse pressure
p_{pr}	Resistance against buckling propagation
R_e	Reynolds number
R_k	Generalized resistance
s	Second
$S(\omega)$	Spectral density
S_A	Load effect from accidental loads
S_d	Sum of design load factor
S_E	Load effect from environmental loads
S_F	Load effect from functional loads

$S_J(\omega)$	JONSWAP spectrum
S_P	Pressure load
$S_\zeta(\omega)$	Wave energy spectrum
t	Time
t_1	Minimum required wall thickness for a straight pipe without allowances
t_{corr}	Corrosion allowance
T_{eA}	Effective tension from accidental loads
T_{eE}	Effective tension from environmental loads
T_{eF}	Effective tension from functional loads
t_{fab}	Fabrication negative tolerance
T_k	Plastic axial force resistance
t_{nom}	Nominal wall thickness
T_P	Wave peak period
T_W	True wall tension
T_z	Wave zero-crossing wave period
U_M	Free stream velocity amplitude of the oscillatory flow
$v_c(z)$	Total current velocity at level z
$v_{c,tide}(0)$	Tidal current velocity at the still water level
$v_{c,wind}(0)$	Wind-generated current velocity at the still water level
z	Distance from still water level

Abbreviations

ALS	Accidental Limit State
API	American Petroleum Institute
BSR	Buoyancy Supported Riser
COBRA	Catenary Offset Buoyant Riser Assembly
DFF	Design Fatigue Factor
DNV	Det Norske Veritas

DOF	Degree of Freedom
FE	Finite Element
FLS	Fatigue Limit State
FPSO	Floating Production Unit
FSHR	Free Standing Hybrid Riser
JONSWAP	Joint Operation North Sea Wave Project
LF	Low Frequency
LRFD	Load and Resistance Factor Design
MBR	Minimum Bending Radius
RAO	Response Amplitude Operator
SCF	Stress Concentration Factor
SCR	Steel Catenary Riser
SHRT	Single Hybrid Riser Tower
SLOR	Single Line Offset Riser
SLS	Serviceability Limit State
SMYS	Specified Minimum Yield Stress
TCR	Tethered Catenary Riser
TDP	Touch Down Point
TLP	Tension Leg Platform
ULS	Ultimate Limit State
VIV	Vortex Induce Vibration
WF	Wave Frequency
WSD	Working Stress Design

Table of Contents

List of Table

List of Figure

1. Introduction

1.1 Background

The development of the offshore oil and gas industry in recent decades grows toward deep water. Fixed platforms become less favorable as the water depths increase. In order to fulfill the market demand that is continuously increasing, the oil and gas industry requires new frontier exploration. Therefore, the scientists have been challenged to establish solutions of how to produce hydrocarbons from deep water fields in absence of dry trees on fixed platforms.

The journey of offshore for oil and gas industry was begun in the middle of the 19th century. In 1947, Kerr McGee completed the first offshore well platform in the Gulf of Mexico (GoM), 17 km off Louisiana in 6 m of water depth (Palmer & King, 2004). The first concept subsea system was suggested in the early 1970s, it was a pilot project by placing a wellhead and xmass tree on the seabed in a sealed chamber near an existing platform (Bai & Bai, 2010). Since the subsea wellhead and the platform were located in separate places, it required a tubular pipe to flow the hydrocarbon production from the subsea well connected to the platform which later we called a riser.

From the time when the subsea technology was introduced, exploration and production activities have increased dramatically in deep water. Hydrocarbon production in the areas such as the Gulf of Mexico (GoM), West of Africa (WoA), Brazil, and on the Norwegian Continental Shelf (NCS) continuous to move into ever increasing water depths by utilizing the advantage of the subsea technology. To date, the deepest offshore drilling and production activity is the Pertindo platform at water depth 2450 m (8000 ft), located 320 km from Texas coast in Alaminos Canyon Block 857 (Shell, 2011), see also Fig. 1.1.

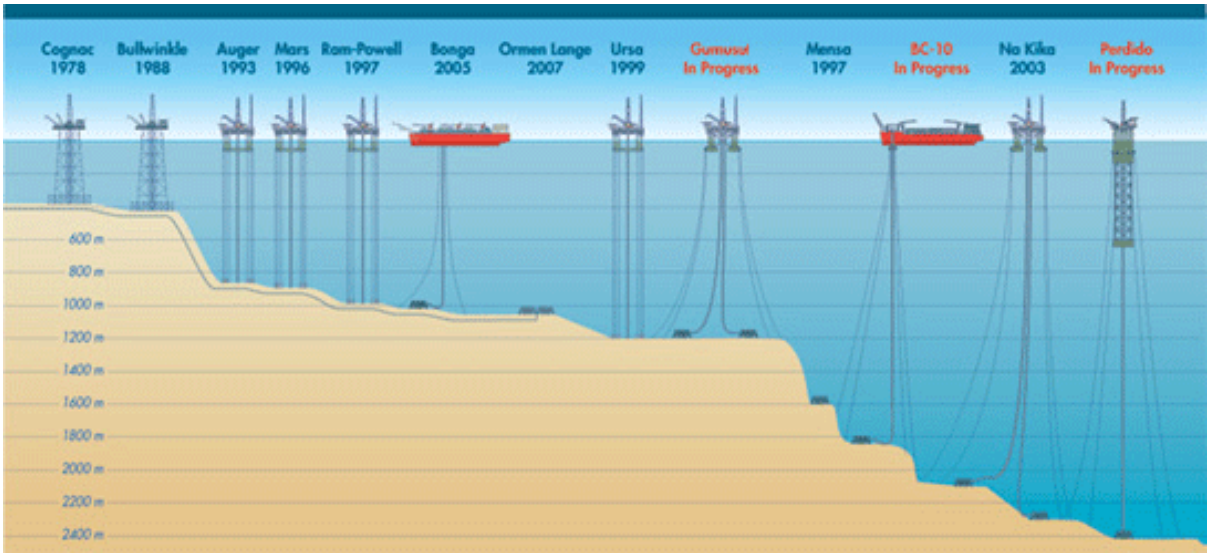

Figure 1-1 Deep water developments (Shell, 2013)

The Norwegian Continental Shelf (NCS) is a proven exploration area for petroleum resources, the area can be divided into three main petroleum regions; The North Sea, The Norwegian Sea and The Barents Sea. Refer to Fig. 1.2, the petroleum production totaling 225.14 million Sm^3 of oil equivalents produced from NCS in 2013, which leads Norway as the seventh largest oil exporter and the fourteenth largest oil producer in the world. Moreover, the petroleum activity in Norway is a benchmark of a highly competent technology in the oil and gas industry. Through active explorations and current field developments the Norwegian offshore industry sector increased from 248 to 361 billion NOK from 2009 to 2011 (NPD, 2013).

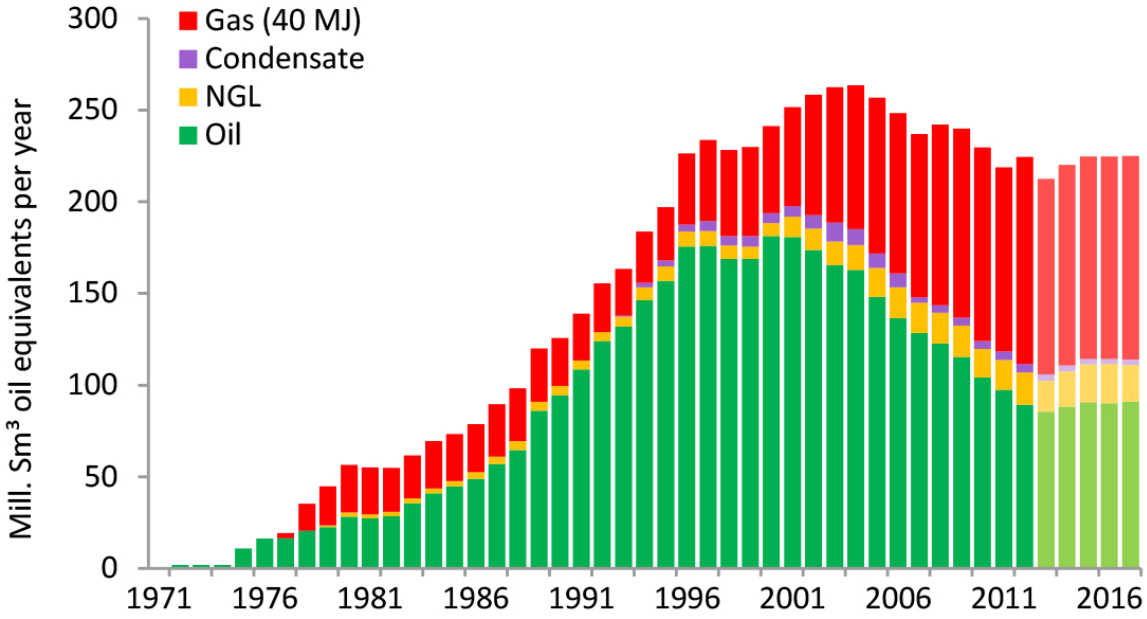

Figure 1-2 Historical production of oil and gas, and prognosis for production in coming years (NPD, 2013)

Today, one of the mature fields in the Norwegian Sea located in the Haltenbanken area, which is enclosed by a large area of deep water with potential significant amounts of hydrocarbon resources. The harsh environment challenges should be addressed to develop the area where waves exceeding 30 meters, wind speeds up to 39 m/s and sea currents up to 1.8 m/s, make the Norwegian Sea more challenging than the North Sea (Totland, Pettersen, Grini, & Utengen, 2007). In terms of the deep water, the Haltenbanken area has more than 1,000 m water depth, thus the subsea production systems are certainly required to develop new fields in this area. Except the Ormen Lange field where the first hydrocarbon production came on stream in 2007, large potential of undiscovered resources in the deep water areas of the Norwegian Sea remain untouchable.

Recently, the deep water risers have been developed for calm to moderate environmental conditions such as the GoM, WoA, and Brazil. None of the deep water riser configurations are installed in harsh environment conditions such as in the Norwegian Sea. An innovative technology and further research of the riser configurations, to convey hydrocarbons from sea

bed to the host facilities in the deep water and harsh environment conditions, are going to be an important aspect in the further development of the Norwegian Sea.

The Norwegian Sea, especially in the Haltenbanken area is weather sensitive due to the environmental conditions as mentioned above. The use of floaters in this area generates excessive floater motions that may harm the risers during extreme environmental conditions. The solutions for the riser configurations to reduce the large motions due to the extreme environmental conditions are presented in this thesis. The uncoupled riser which is utilizing buoy elements in the riser configuration is effective to decouple large motions of the floater and hence the riser becomes less susceptible to fatigue damage. Among the many uncouple riser configurations, the thesis will focus on two selected uncoupled riser configurations; Catenary Offset Buoyant Riser Assembly (COBRA) and Single Line Offset Riser (SLOR).

In general, an uncoupled riser presents a combination between the steel riser at the bottom part and flexible jumpers at top part, with a long and slender sub-surface buoyancy module attached in between. The flexible jumper has the ability to accommodate high curvature due to excessive motion of the floater with low bending stress, and then the steel riser is dissipating any floater motion that is going to transfer to the bottom part. Therefore, with the presence of the buoyancy module, the steel riser at the bottom part is largely decoupled from the floater motions. Typically, the buoyancy module is located at sufficient depths (100-400 m below the MWL), away from the wave zone and the surface current region, thus the direct environmental loading on the buoyancy module is low. The main advantages of the two uncoupled riser configurations is that they enable possibilities for the riser to temporary disconnect from the floater and for the floater to drift/side-step in order to prevent/avoid iceberg collision.

The main idea of this thesis is to compare the performances of the two uncoupled riser configurations based on strength analyses results in harsh environmental conditions. And as a sensitivity study, we will compare the risers' performance in the event of an iceberg approaching by using two selected solutions; first, when the floater drifts off and second, when the riser/mooring system is disconnected from the floater using a disconnectable turret.

1.2 Purpose and Scope

The Norwegian Sea has plenty of room for application of the deep water technology for harsh environmental conditions. Further exploration in this area will continue to require the newest development of the subsea technology in the remote area which also means the need of risers to transport hydrocarbons from seabed to the floater is a must. This thesis presents two uncoupled riser configuration; COBRA and SLOR for a comparison study to obtain the optimum type of the uncoupled riser configuration for the Norwegian Sea conditions. In this thesis we will also capture a sensitivity study for COBRA and SLOR in the event of iceberg approach. Two solutions have been decided, either using drift/side-step of the floater or to disconnect the riser/mooring system using a disconnectable turret to propose a best solution to avoid/prevent iceberg collision.

The final result of this thesis will suggest the optimum type of the uncoupled riser configuration and the solution in term of iceberg approach. Orcaflex software is mainly used to perform a static and dynamic analysis in conjunction with the above mentioned cases.

The scope of thesis will consist of:

- Chapter 2 gives an overview of uncoupled riser systems, challenges in deep water conditions, components of the riser, including a review of COBRA and SLOR riser concepts.
- Chapter 3 provides an overview of the environmental conditions in the Norwegian Sea and the physical aspect of the marine environment.
- Chapter 4 gives design codes that are used to design the riser. Mainly, the riser is designed based on the relevant DNV code by using the LRFD method.
- Chapter 5 provides theoretical backgrounds that are relevant for this thesis.
- Chapter 6 presents design basis for the uncoupled riser. This chapter includes analysis methodology, design parameters, computer models, and also the design acceptance criteria.
- Chapter 7 provides detailed information of the COBRA and SLOR concepts, and the analysis which includes static, and dynamic.
- Chapter 8 demonstrates the comparison study of COBRA and SLOR configurations in the event of iceberg approach. This chapter will also conclude an optimum solution to prevent/avoid iceberg collusion.
- Chapter 9 presents the conclusion and recommendation from the study.

2. Uncoupled Riser Overview

2.1 Overview

Risers can be defined as conductor pipes connecting floaters on the surface and the wellheads at the seabed (Bai & Bai, 2010). The function of risers depends on the type of the risers. A production riser has the function to provide conduits for conveying of hydrocarbons or injection fluids between the subsea equipment and the floater. Other types of risers have different functions such as marine drilling risers and completion/workover risers, which are not related for this thesis.

Based on API (2009), the risers are defined as having following functions:

1. To convey fluids between the wells and the floating production system.
2. To import, export, or circulate fluids between the floating production system and remote equipment or pipeline system.
3. As guide drilling or workover tools and tubulars to and into the wells.
4. To support auxiliary lines.
5. To serve as, or be incorporated in the mooring element.

The riser system can be distinguished by the type of host facilities, where the risers are tied back. In the deep water, the motions of the host facilities will have significant impact on the risers' designs and configurations. The production risers tied back to floating structures are inherently more complex that those tied back to fixed structures, since they need to be able to accommodate the motions of the floating structures. For this reason such risers are commonly referred to as dynamic risers (Lien, 2010).

The dynamic riser motions are created from complex combinations between floaters, risers, and also mooring systems as a response to the environmental loadings. These interaction effects are called coupling effects. All portions of the riser configuration which is directly affected by this effect are called coupled riser configurations. For some riser configurations, the coupling effects may magnify the extreme hull/floater responses (Chakrabarti, 2005).

Traditional coupled riser configurations become more challenging when installed in deep water and hash environment conditions; hence there is an interest to develop new riser configurations to overcome the challenges. A hybrid riser was installed in the first floating production system in the late 1980s on the Placid Green Canyon Block 29field, Gulf of Mexico in 470m of water depth. The riser consisted of a vertical steel pipe connected to a foundation assembly at the seabed and was tensioned by means of a subsurface buoyancy can. While at the top end, the riser was connected to the platform via flexible jumper. The floater motions are effectively absorbed by the flexible riser and the buoyancy can, hence the steel pipe becomes less susceptible to fatigue damage. Because of the capability of the riser configurations to decouple the floater motions, this riser configuration is characterized as uncoupled risers.

Uncoupled risers in deep water are mainly developed from the hybrid riser tower configurations. A number of different uncouple riser configurations have been installed, some examples are the Free Standing Hybrid Riser (FSHR), Single Line Offset Riser (SLOR), Groped SLOR, Buoyancy Supported Riser (BSR), Catenary Offset Buoyant Riser Assembly (COBRA), Tethered Catenary Riser (TCR), and Saipem's RCS configuration. Since the successful installation of hybrid risers in WoA, GoM and Brazil, uncoupled riser configurations have been largely adopted for deep water fields worldwide as shown in Table 2-1.

Table 2-1 Uncoupled Riser Installations (Maclure & Walters, 2006).

Field	Riser Type	Location	Water Depth (m)
Placid Green Canyon	Bundle	Gulf of Mexico	470
Enserch Garden Bank	Bundle	Gulf of Mexico	670
Total Girassol	Bundle	West of Africa	1350
Kizomba A	SLOR	West of Africa	1200
Kizomba B	SLOR/COR	West of Africa	1200
Petrobas P-52	SLOR	Brazil	1800
Cascade & Chinook	FSHR	Gulf of Mexico	2515

In this chapter, the general uncoupled riser system is discussed with the challenges that are presented in the deep water environment conditions. In the last part of this chapter, the detailed review of uncoupled riser geometries are highlighted for SLOR and COBRA configurations as the selected riser configurations among the uncoupled riser concepts.

2.2 Deepwater challenges

As the offshore oil and gas industry has to move into ever increasing water depth, the deep water environmental challenges should be considered in designing, constructing and installing a riser. Some of the challenges that are affecting to the riser behavior are presented below.

2.2.1 Water depth

In the deep water, installation of fixed-base offshore platforms becomes prohibited from economical point of view. The total investment cost for building a fixed-base platform in Norway varied from 14.0 to 32.0 US dollars per barrel of production (2013's value). If the conventional technology is applied to build a platform in 400 m water depth, the total investment would have reached 40.0 US dollars per barrel (Lappegaard, Solheim, & Plummer, 1991). That indicates that the total CAPEX for building fixed platforms rises as the water depths increase, which means the investment would be less interesting or even not acceptable for the economists. Hence, for the deep water development, the use of floating structures is obligatory.

When it comes to risers which are tied back to the floating facility, various challenges exist due to water depth, for instance; riser weight, riser sizing, and spreading area of the riser. The explanations are presented below in detail.

Riser Weight

The riser weight increases due to increased depth, because of the suspended length of the riser is significantly longer in the deep water. When the pipe is hanging on the floater that has a longer unsupported pipe length, there will be a higher top tension force in the floater. The top tension force is one of the important factors in the floater's design. The floater load capacity to sustain the tension forces from the tied back riser is known as vessel pay load.

Accounting for the top tension force and the top inclination angle of the riser, the vessel payload in deep water may be 10% to 30% larger in nominal conditions and 50% to 100% larger in extreme conditions (Howells & Hatton, 1997).

Riser Sizing

In shallow water depths, the pipe wall thickness is often driven by internal pressure. While in the deep water the riser's wall thickness design may be based on external pressure (Hydrostatic pressure). The hydrostatic pressure increases proportionally with water depth. The consideration of hydrostatic pressure is related to the installation method that the risers are generally laid in empty condition (unflooded risers).

During the installation conditions, the unflooded risers should have sufficient wall thickness to resist collapse and local buckling due to the hydrostatic pressure. In which case, high bending stress may also appear in the region of the sagbend in conjunction with external pressure at maximum depth.

Spreading Area of the Riser

The risers require area to spread on the seabed. Since the water depth increases, the risers need to set down in a large area to maintain the proper configurations.

For the steel catenary riser (SCR) configurations, the increased water depth can be a particular challenge. The steel catenary riser configuration has a typical radial spread of 1.0 to 1.5 times the water depth. Hence, in a 1500 m water depth, this would result in a total spread between diametrically opposed risers of 3000 to 4500 m. This could be a key factor when selecting riser system arrangement and positioning (Howells & Hatton, 1997).

2.2.2 Dynamic Response

The direct effect of wave loading is reduced when water depth increases, but the indirect effect of the waves may prove more severe. The large motions of the floater due to combination of waves, currents, and winds create great challenges in designing the risers in harsh environment conditions. The dynamic heave and surge motions of the floaters generate buckling issues at touchdown point (TDP) and fatigue problems, the conditions may vary in

different locations according to soil-riser interactions. For the top tensioned risers, variation of tension load due to heave motions lead to fatigue problem near the bottom assembly.

In the deep water conditions, other dynamic cases should give more attention to Vortex Induced Vibration (VIV). For certain current speeds, VIV gives significant contributions to fatigue damage on the risers. In order to reduce the risk of VIV, strakes along the critical area of the riser are normally needed. In addition, the small near bottom current should not be ignored. Although, the small currents do not give significant contribution to the fatigue damages, the riser drag force is greatly increasing (Howells & Hatton, 1997).

2.2.3 Riser/Floater Interaction

Selection of the riser concept is highly dependent on the floating facility. The riser arrangements should have capability to accommodate the floater drift offset and motion responses. As the water depth increases, the horizontal offsets increase accordingly and this results in more severe dynamic motions.

For a SPAR or a tension leg platform (TLP) with relatively small horizontal offset, the top tensioned riser and steel catenary risers may be suitable. However, in the harsh environment and deep water conditions, the horizontal offsets can be increased significantly. The uncoupled riser configurations with buoyancy can assistance may be necessary to control large floater offsets.

2.2.4 Installation

Different technologies and methods are adopted to install offshore pipelines and risers. The installation method of the top tensioned risers on a SPAR or a TPL is run in a similar manner as to workover/drilling riser. The production risers can be installed when the floater responses to dynamic loading produce a relatively small horizontal offsets. Another method to install the risers is the S-lay, J-lay, and Reel lay methods. These three installation methods for the risers have to use a dedicated installation vessel that is designed for each method as the installation methods is dependent on the capacity of the installation vessels.

In another aspect, the installation window in the Norwegian Sea is usually limited to summer period and some days in spring when air pressures and temperatures are constant. A greater water depth requires longer riser length, and hence longer installation time will be. Based on above explanation, the installation challenges in deep water are summarized as follows:

- Limited number of installation vessels.
- Limited installation windows.
- High installation costs.
- Complex installation methods.

The uncoupled riser configurations may have efficient installation time as well as installation cost. An advantage of the uncouple risers is that some part of the risers can be pre-installed prior to the floater installations.

2.2.5 Harsh Environment

The most challenging aspect in a Norwegian Sea project development is the harsh environment conditions. The extreme conditions are enforcing the engineers to design a robust riser configuration. Waves exceeding 30 m, wind at speeds up to 39 m/s and sea currents up to 1.8 m/s all make the Norwegian Sea a rather extreme location to develop an offshore oil and gas field. The water depth of the Norwegian Sea is varying with the deepest water depth at Haltenbanken reaching more than 1000 m (Totland et al., 2007). The most suitable facility concept to be used to develop fields in harsh environment conditions could be the gravity based concrete platform, which has been so successful in the North Sea, but when it comes to deeper water (more than 150 m water depth) the concept is not commercially feasible anymore.

In addition, in particular areas of the NCS such as in the Barents Sea, there is a possibility of drifting icebergs. In this case, the riser configurations should be designed to prevent/avoid iceberg collisions. In this thesis, a comparison study is presented in chapter 8 to provide solutions in the event of icebergs approach.

2.3 Review of Uncouple Riser Geometry

In recent years, the oil and gas industry presence has increased dramatically in deep water fields. As the riser weight increases with the water depth, the installation issue arises when the payload of the installation vessel and water depth turn into limitation factors to install the risers in the deep water. The uncoupled riser concept has been established and improved with a focus on the important issues; robustness of the riser design and considerations of the installation points of view.

The uncoupled riser configurations will minimize the payload and dynamic constraint of the floaters in large water depths. As shown in table 2-1, the uncoupled riser configurations have been applied worldwide as an economically feasible and field proven concept. The benefit of the uncouple riser configurations offers the best solution for project development on the Norwegian Sea with special characteristics and harsh environmental conditions.

The uncoupled risers were mainly developed from the free standing hybrid riser. They are called hybrid risers because they are using flexible and steel materials in the riser configuration. Three main components are used in these configurations; flexible pipes, steel pipes and buoyancy cans. The flexible pipes (or flexible jumper) perform as a decoupling component of the floater motions, which makes the risers having excellent fatigue performances.

The research is still developing in order to optimize the functionality of uncouple riser concepts. In the following sections is provided a review of uncoupled riser geometries for the

field proven uncoupled riser configurations: Single Line Offset Riser (SLOR) and a new riser uncoupled concept that has not been applied yet: the Catenary Offset Buoyant Riser Assembly (COBRA) as the selected uncoupled riser concepts for this thesis.

2.3.1 Single Line Offset Riser (SLOR)

The Single line offset Riser and the Free Standing Hybrid Riser (FSHR) are similar riser concepts. The main difference between SLOR and FSHR is that in SLOR design, the steel pipe runs through the buoyancy can and the flexible jumper connects to the gooseneck connection located at the top of the buoyancy can while the FSHR design has a lower gooseneck connection than SLOR then adding a top riser assembly and a tether chain which connects to the buoyancy tank on the top of it. Figure 2-1 shows an illustration of SLOR and FHSR concepts.

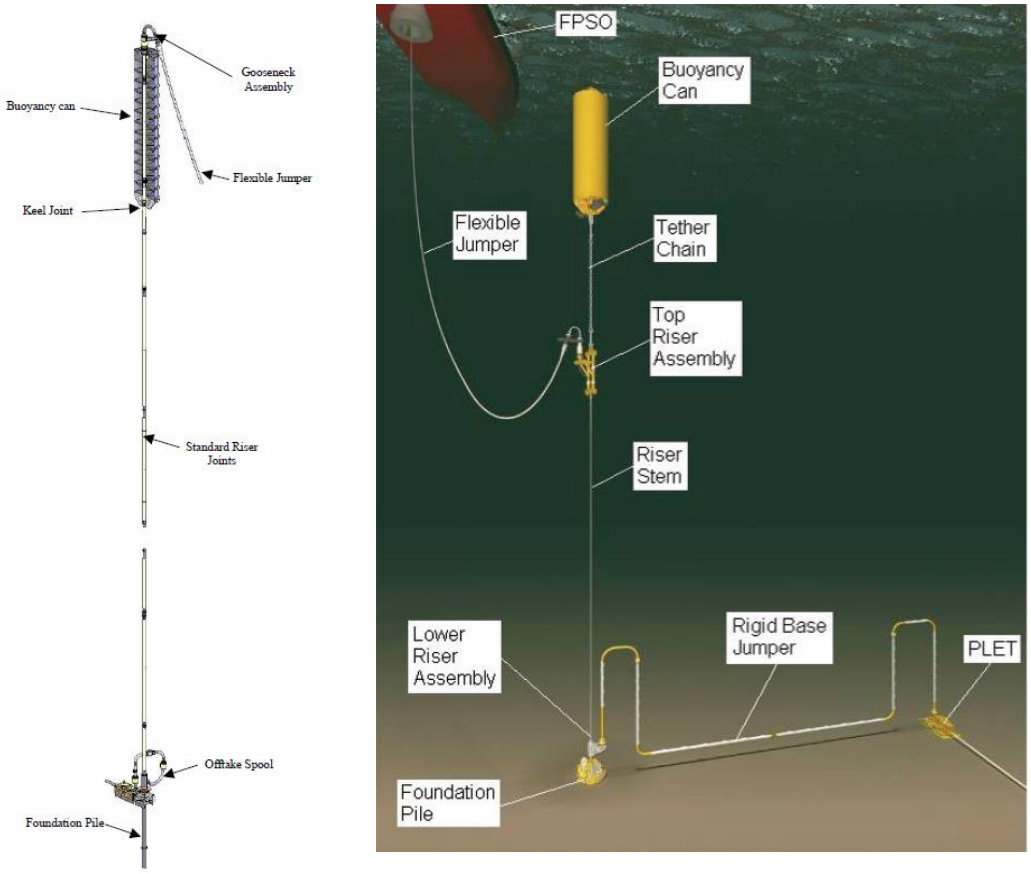

Figure 2-1 Comparison of SLOR and FSHR Arrangements. Picture courtesy of (McGrail & Lim, 2004) and (Reitze, Mandeville, & Streit, 2011)

Both of risers are developed based on hybrid a riser tower concept which is previously installed in 4 field developments in WoA by the end of 2007. The success of this riser concept is increasing the industry demands to install similar concepts in deep water developments around the world. The company 2H offshore Inc. http://www.2hoffshore.com/ developed the Single Line Offset Riser (SLOR) to be an enabling technology for deep water field development due to the robustness and flexibility of installations inherent with the design.

The SLOR consist of a single vertical steel pipe as the bottom part connected to a foundation pile at the seabed. The system is tensioned using a buoyancy can, which is mechanically connected to the flexible jumper at the top part via a gooseneck (McGrail & Lim, 2004). The steel riser runs through the bore of the buoyancy can, which is normally located between 50 – 200 m below the Mean Water Level (MWL). As a result, the riser arrangement reduces the effect of waves and surface currents on the steel riser, whilst maintaining access for inspection and ease of the flexible jumper installations. Although a relatively new technology, the SLOR design is field proven on the number of projects in WoA and GoM. A SLOR arrangement design for the Gulf of Mexico is shown in figure 2-2. The main SLOR components are described in the following sections.

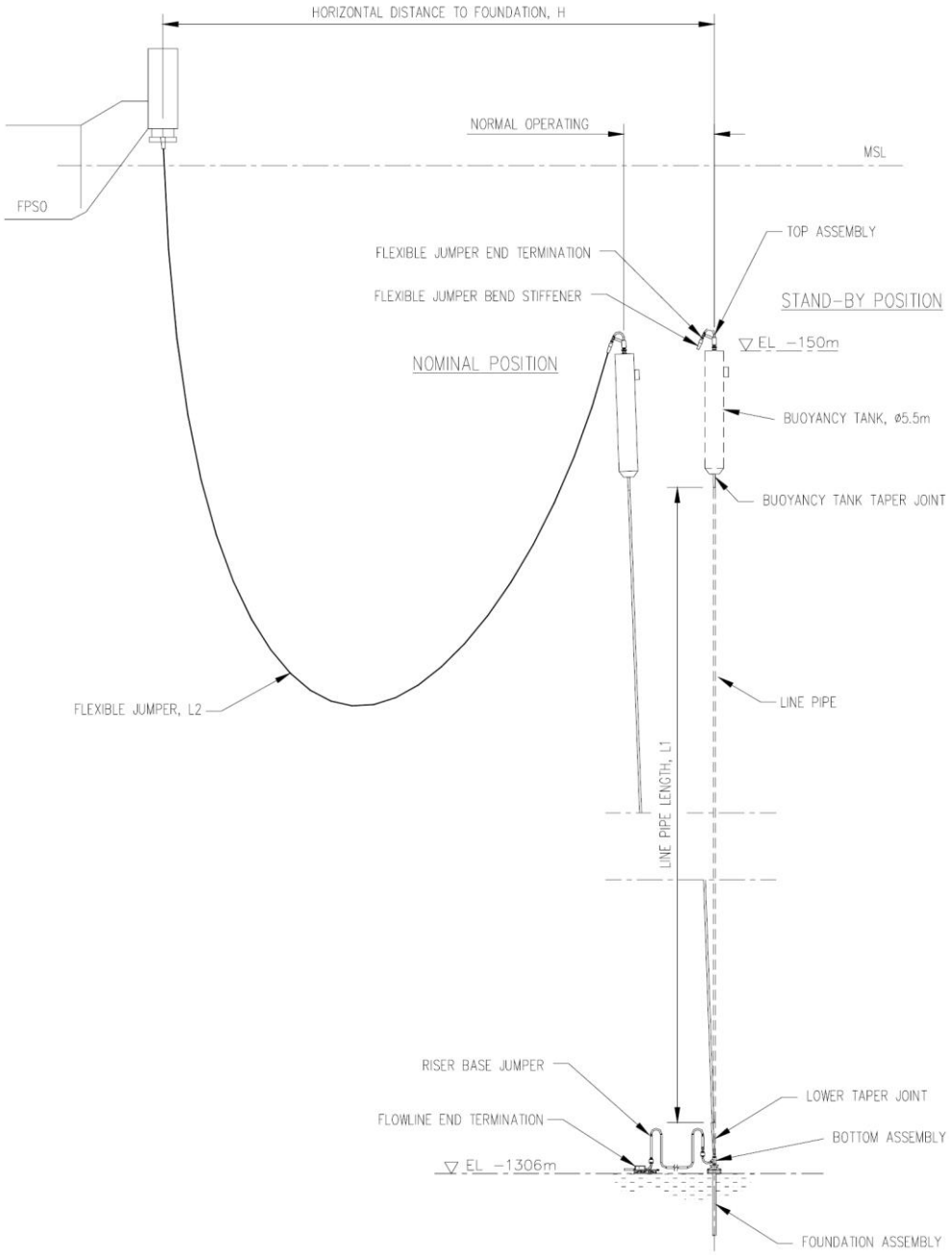

Figure 2-2 SLOR Arrangements. Picture courtesy of (Maclure & Walters, 2006)

Foundation

Typically, A SLOR foundation consists of either a suction anchor or a grouted pile to which the steel riser is connected on the connector mandrel located at the top of the foundation assembly. The connector mandrel provides orientation of the steel riser to align with the rigid based jumper. The horizontal motions of the steel pipe can lead to large bending loads at the base of the riser. To reduce bending loads transfer to the foundation, a low stiffness elastomeric material called flex elements are used.

The preferred solution are suggested to use a small diameter drilled and grouted pile (typically 30-40 in). The small diameter foundation pile suits to accommodate large banding loads which results in a less critical rigid based jumper design.

Lower Riser Assembly

The lower riser assembly consists of the lower offtake spool, and the lower taper joint. The offtake spool has a component with an internal flow path from the side of the spool to which an introduction bend is attached. A rigid based jumper is attached to the end of the introduction bend by using either a horizontal or a vertical connection system. The based jumper contains a number of loops that has a function to accommodate the flowline expansions due to temperatures, operational conditions and shut down conditions.

On the top of the offtake spool is attached the lower taper joint. This joint is a high specification component that is designed to accommodate the long term fatigue loading and to control the bending loads at the bottom of the riser due to horizontal motions from the upper parts. A sample of the lower riser assembly can be seen in Figure 2-3.

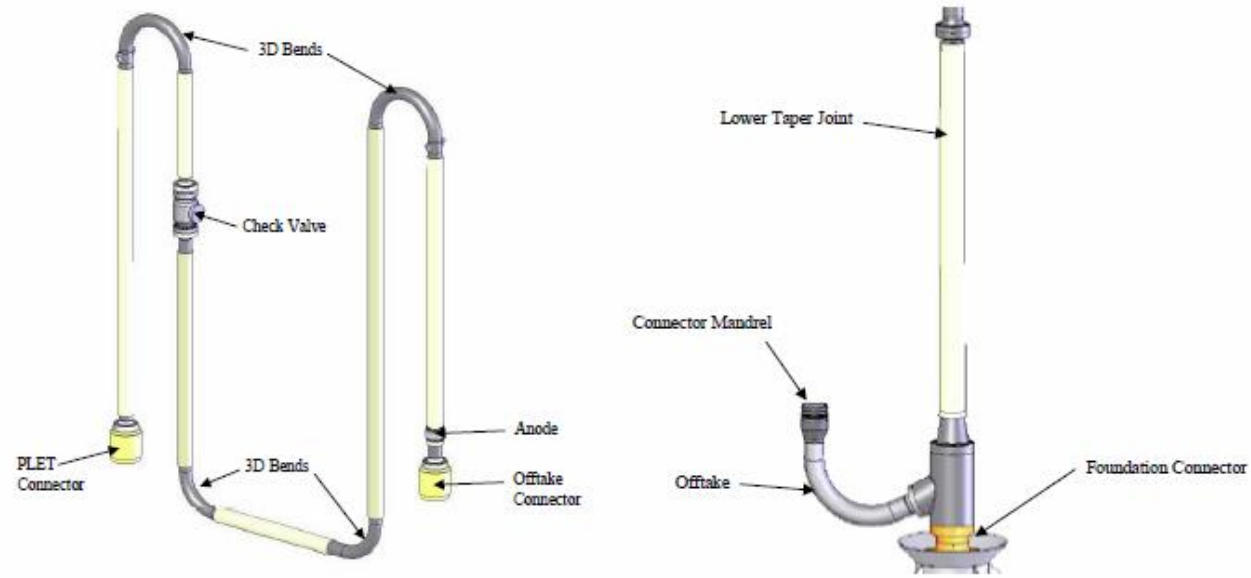

Figure 2-3 SLOR Lower Assembly Details. Picture courtesy of (Maclure & Walters, 2006)

Buoyancy Can and Keel Joint

The SLOR is tensioned by a buoyancy can filled with air or nitrogen. The can contains a numbers of compartments with bulkheads as a separator. The pipe runs through the central of the cans that acts as the main structural component. The buoyancy can should be designed to be able to resist external pressures as well as content pressures. To reduce the weights and obtain optimum buoyancy forces, the buoyancy can shall be limited to minimal wall thickness. The stiffeners may be needed to provide an additional stiffness of the buoyancy can. The buoyancy can is designed such that at least one compartment is maintained permanently water filled as a contingency (Maclure & Walters, 2006).

As shown in Figure 2-4, the steel riser is set in the top of the buoyancy can by a load shoulder and thus the upward tension forces produced by the buoyancy can is transmitted directly to the vertical steel riser.

A keel joint arrangement is used to control the bending moment transferred to the riser string due to horizontal riser motions. The joint is located at the base of the buoyancy can. The keel joint has a similar function as the taper joint at the lower riser assembly. In order to reduced fatigue damages and large bending loads, the keel joint arranges the two tapered steel riser sections joined back to back.

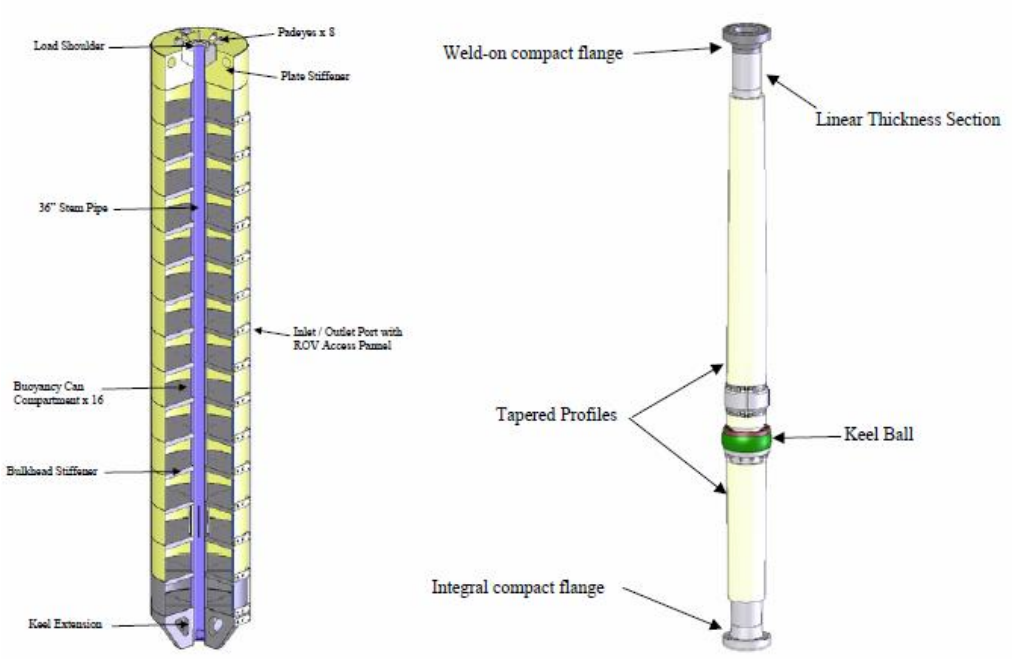

Figure 2-4 Buoyancy Can and Keel Joint Details. Picture courtesy of (Maclure & Walters, 2006)

Gooseneck Assembly

The gooseneck assembly, which is located on the top of the buoyancy can, provides fluids off-take flow from the vertical steel riser to the flexible jumper. The gooseneck is created of an induction bend pipe and it is structurally braced back to the gooseneck support spool at the

base of the assembly. The structural assembly of the gooseneck shall have enough strength to sustain the loads from the flexible jumper reactions.

The bend radius of the gooseneck is typically configured as 3D and 5D bends. These bends can allow the pigging balls through the risers and prevent flow restrictions during pigging operations. For production risers, depending on the type of fluids, it may be designed to consider an erosion allowance.

Flexible Jumper

A flexible jumper is used to convey the fluids between the steel riser and the floaters. A bend stiffener is used to restrict the bend radius of the jumper at the floater and gooseneck termination points (as shown in Figure 2-5). The flexible jumper effectively absorbs the floater motions and hence minimum dynamic motions are transferred to lower part of the riser configurations. Therefore, the riser configuration has excellent performance in term of long term fatigue loadings.

The flexible jumper materials and bend stiffeners are very much dependent on the individual riser service, insulation and pigging requirements.

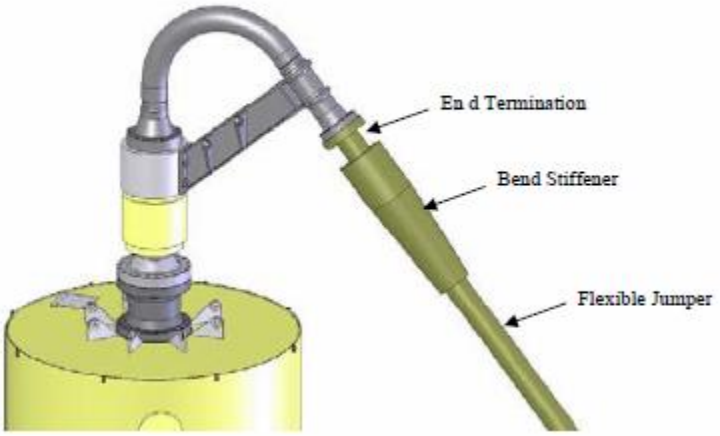

Figure 2-5 Flexible Jumper and Gooseneck Assembly. Picture courtesy of (Maclure & Walters, 2006).

2.3.2 Catenary Offset Buoyant Riser (COBRA)

A new uncoupled riser configuration has been developed called Catenary Offset Buoyant Riser (COBRA). The riser consists of a steel catenary riser (SCR) on the bottom section with a long-slender subsurface buoyancy can on the top of the SCR section, which is tethered down to sea bed via mooring lines. To connect the SCR sections to the floater, a flexible jumper is installed from the top of the buoyancy can via a gooseneck assembly. Figure 2-6 shows the general arrangement of COBRA.

The COBRA has similar advantages with the other uncoupled riser configurations, by using the flexible jumpers on the top sections, the floater motions is effectively absorbed and hence the SCR section has minimum impact of dynamic motions from the floaters. By means of these, the riser improves both the strength and the fatigue performance on the overall system. The subsurface buoyancy can be positioned at a sufficient depth in such a way that the effect of surface waves and currents can be reduced.

Based on Karunakan (Karunakaran & Baarholm, 2013), the riser concept combines the advantages of the SCR and the Single Hybrid Riser Tower. This concept has better dynamic performance compared to SCR, and hence eliminates fatigue damage at TDP. Compared to the Single Hybrid Riser Tower, this concept avoids all the expensive bottom assembly, and the complex bottom connection which is generally required for Single Hybrid Riser Concept. However, the riser configuration demands a large field layout as the Catenary Configurations radially spread away from the host facilities.

The main components of COBRA are listed as follow:

- Flexible Jumper
- Gooseneck Assembly
- Buoyancy Can
- Foundation Assembly (for the mooring lines)
- Steel Catenary Riser

For the buoyancy can, the gooseneck assembly and the flexible jumper are the same that are used in the SLOR. Therefore, detail explanations of COBRA will be limited to the bottom parts of the riser arrangement.

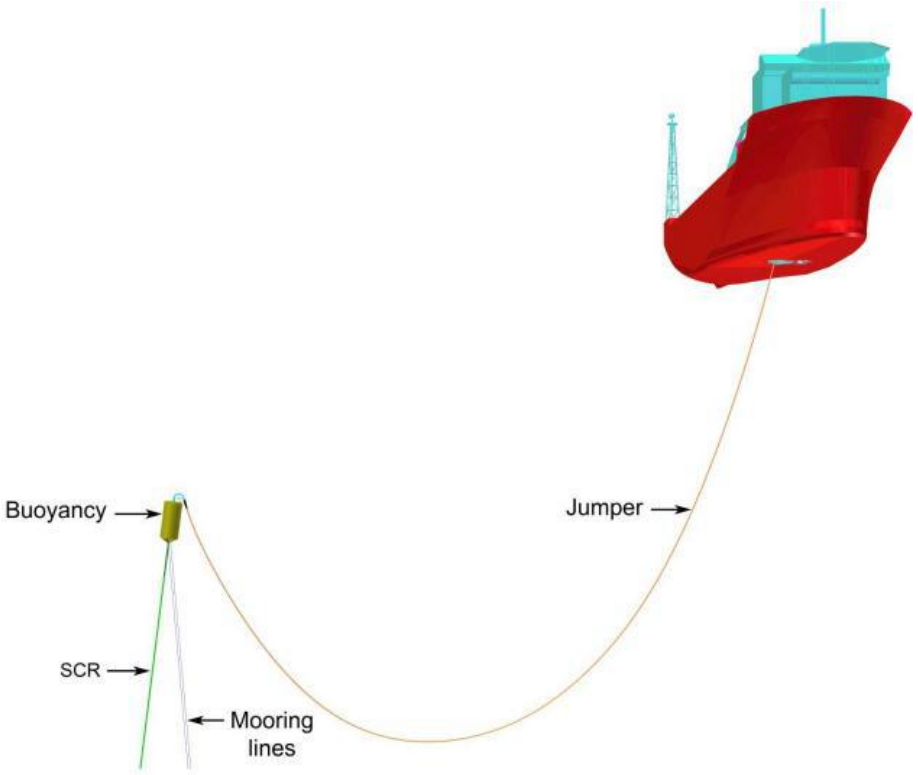

Figure 2-6 COBRA Riser Arrangements. Picture courtesy of (Karunakaran & Baarholm, 2013)

Foundation Assembly

A suction anchor (as shown in Figure 2-7) is proposed for mooring lines foundation assembly. In order to maintain the buoyancy can in the intended positions, two mooring lines are connected at the bottom of the buoy at the both sides of the SCR connection points. Furthermore, an equal distance between the two lines shall be maintained on both connection points; at the anchor point and the buoy point.

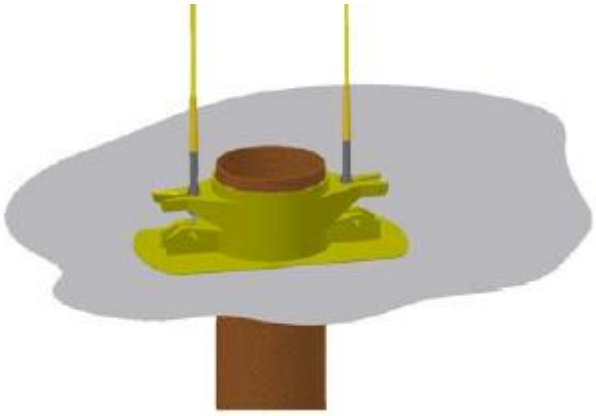

Figure 2-7 Suction Anchor for Mooring Lines. Picture courtesy of (Karunakaran & Baarholm, 2013)

Steel Catenary Riser

Use of a Steel Catenary Riser (SCR) is an economically attractive choice for a deepwater field, since the configuration of the riser and the installation operations are considered relatively simple compared to the hybrid riser concept. However, the design of the SCR in harsh environmental conditions remains a significant challenge due to fatigue issues near the hang-off and the touch down point (TDP). A COBRA concept offers a solution to bring down the SCR connection points far below the wave zone and the current regions by using the buoyancy can as the connection point of the SCR. The buoyancy can is tethered down to the seabed and the flexible jumper is used to connect the SCR to the floaters. In this way, the fatigue issues at the TDP and connection point can be eliminated.

The COBRA concept is a modified of the SCR concept, in which the aim is to combine simplicity and economical features of the SCR with motion handling capabilities of the hybrid riser tower. The result is the new uncoupled riser arrangement able to handle deep water and harsh environment conditions (Karunakaran & Baarholm, 2013). The sample arrangement of SCR for 1500 m water depth can be seen in Figure 2-8.

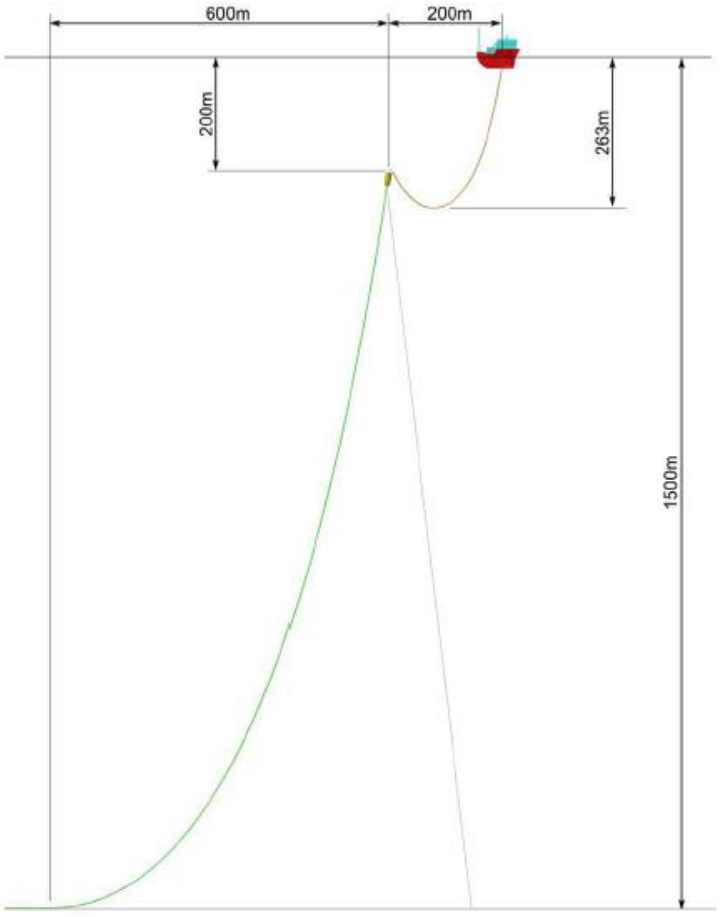

Figure 2-8 COBRA Riser Configurations. Picture courtesy of (Karunakaran & Baarholm, 2013).

3. Environmental Conditions in the Norwegian Sea

3.1 General

The first hydrocarbons was coming on stream from the Norwegian Sea region is in 1993, which indicates that this area is a relatively recent petroleum regions. In the last 20 years, hydrocarbon productions from the Norwegian Sea have increased significantly. Five new discoveries were made in this area in 2012 while accumulated production in the same year totaled 69 million Sm^3 o.e. The PDO for Aasta Hansteen was submitted in the last year making the gross hydrocarbon recoverable reserves increasing to 100 million Sm^3 o.e (NPD, 2013). This petroleum region is likely to be a new hydrocarbons resource for Norway in the next decades.

The subsequent development of the Norwegian Continental Shelf (NCS) is representing one of the largest oil and gas investment projects in the world. However, the environmental conditions of the NCS are categorized as of the Atlantic Frontier type (See Figure 3-1) which is considered as a hostile environment area. The development in this type of area is set to be a challenge for the engineers to produce and contribute highly competitive and innovative technologies for the oil and gas industry. Developing a new technology requires observation of the design limitations. One of the design limitations in this case is the environmental conditions of the Norwegian Sea. The importance of observations in the environmental aspects is to obtain proper engineering design that is dedicated for the particular environmental condition.

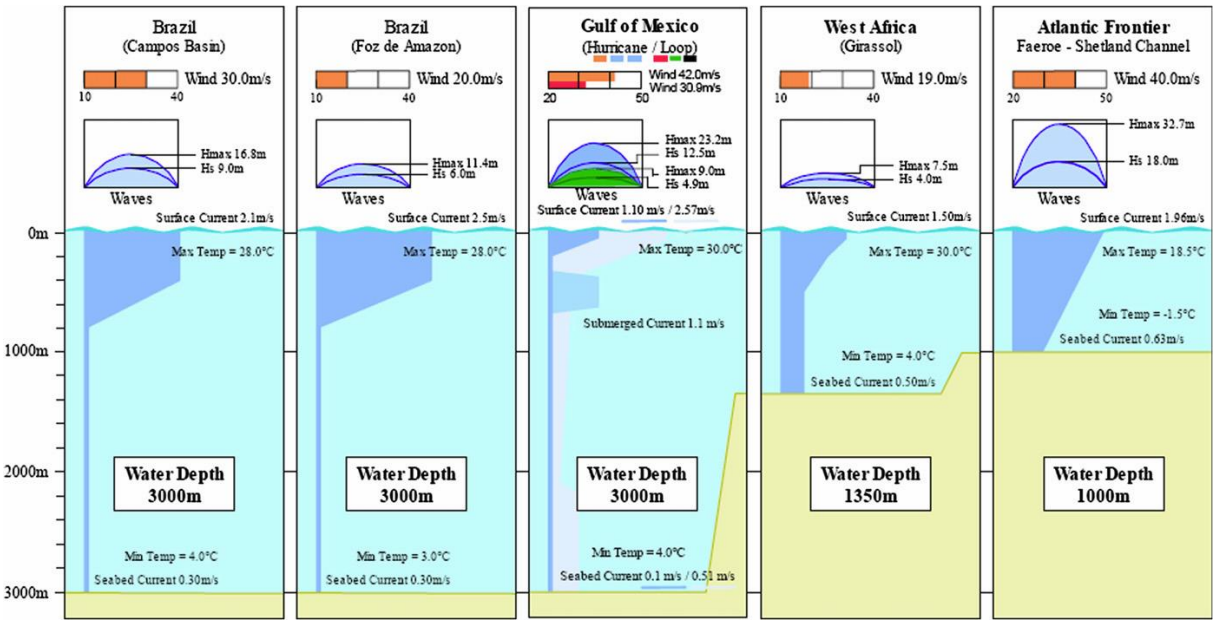

Figure 3-1 General Metocean Data for Some Hydrocarbon Produced Areas. Picture courtesy of (Bai & Bai, 2010)

The environmental aspects of the Norwegian Sea that have to be considered for designing the risers are presented in the following section. It explains characteristic of existing wind,

currents, waves, sea ice and icebergs in this region. According to that, the Norwegian Sea has a unique environmental condition that makes it different from other areas in the world.

3.2 Geography

The Norwegian Sea is bordered by the North Atlantic Ocean on the northwest of Norway, the Greenland and the North Sea together with the North Atlantic to the west, and the Barents Sea to the northeast. In the southwest, it is separated from the Atlantic Ocean by a submarine ridge running between Iceland and the Faroe Islands and to the north, the Jan Mayen Ridge separates it from the Greenland Sea. Meanwhile the Norwegian Sea is considered as a marginal sea in the North Atlantic Ocean, the most part of the sea shares the continental shelf with the Norwegian's main island and the Lofoten Basins where water depths at this area can reach approximately 3000 m (Chakrabarti, 2005).

The majority area of the Norwegian Sea lies on the Upper Triassic-Middle Jurassic, Upper Cretaceous and Paleocene plays, where the deep water region is located at the Upper Cretaceous to Upper Palaeocene plays (see Figure 3-2). For these specific plays, the deep water regions just have been explored since 1997, and the biggest discovery is the Ormen Lange gas field. Thereafter several appraisal wells were drilled as part of the Aasta Hansteen development in 2011. However, up to today, a limited number of exploration activities have been done in the deep water area of the Norwegian Sea which believed to have a large potential of undiscovered hydrocarbons.

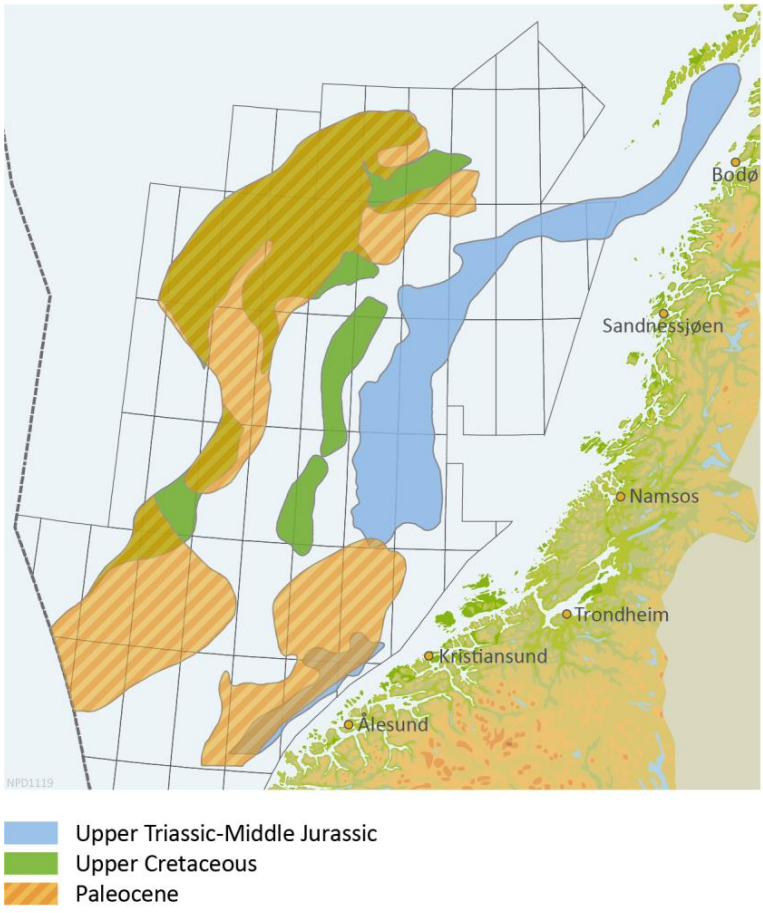

Figure 3-2 The Plays in the Norwegian Sea. Picture courtesy of [15]

3.3 Wind

The NORSOK Standard: N-003 has been used to obtain the wind data for this thesis. The wind data is determined based on annual probability of exceedance of 10^{-2}. The average wind velocity on the Norwegian Continental Shelf at 10 m above sea level is taken as 41 m/s (10 min average) or 38 m/s (1 h average) (NORSOK, 2007).

3.4 Sea Water Temperatures

The geographical position of the Norwegian Sea is located in the relatively high latitude ($61^0$00' N – $71^0$10' N), however the sea water temperature is considered as a mild condition. This could be due to the Thermohaline Circulation affects the climate in the Norwegian Sea, when the warm North Atlantic current flow from the equator. The Thermohaline Circulation (THC) is an ocean current across the globe that is driven by fluxes of heat and freshwater across the sea surface and subsequent interior mixing of heat and salt which are the main factor to determine the density of sea water (Rahmastorf, 2003).

In this thesis, the sea water temperatures in the Norwegian Sea are selected based on the NORSOK Standard N-003 as presented in Figure 3-3. The sea surface temperatures vary in the winter from 2 to 6^0 C and in the summer from 10 to 15^0 C with an annual probability of exceedance of 10^{-2} (NORSOK, 2007).

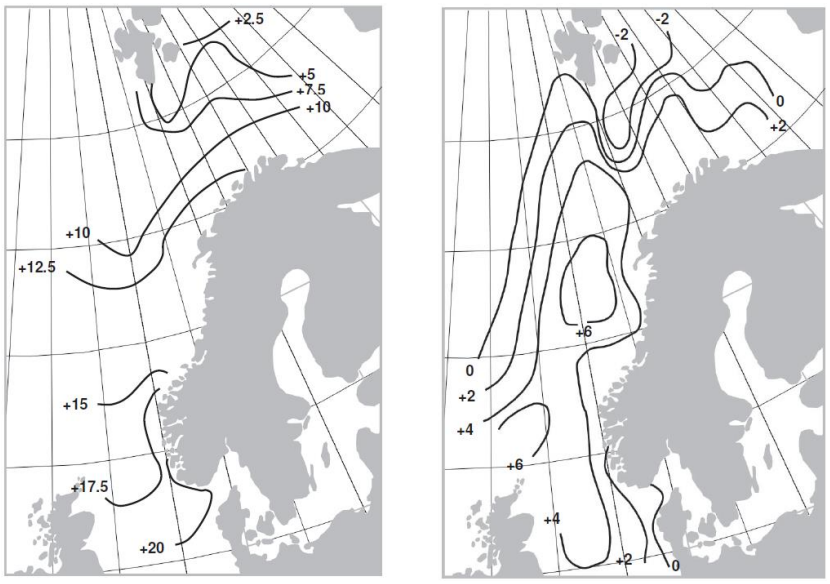

Figure 3-3 The Highest and the Lowes Sea Surface Temperature in the NCS. Picture courtesy of (NORSOK, 2007)

3.5 Currents

The Norwegian Sea current originates in the North Atlantic current that flows from the European Continental slope and brings a warm European climate with high salinity. As explained above, the current condition in the Norwegian Sea is affected by the global ocean currents. Therefore, in the Norwegian Sea, the current velocity at the surface can reach 1.8 m/s and will reduce exponentially with the water depths increase (Totland et al., 2007).

In this thesis, the selected current data are taken from the design basis of COBRA an Uncoupled Riser Study (Karunakaran & Baarholm, 2013). The current data which were presented in the design basis are representing typical current data for Northern Sea Location. According to Figure 3-4, in the Northern North Sea area one has similar current profiles as in the Norwegian Sea area.

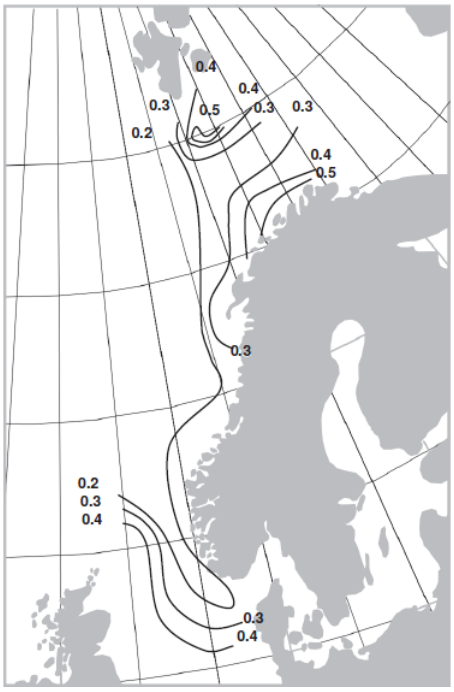

Figure 3-4 . The surface current velocity with 100 year return period in m/s. Picture courtesy of (NORSOK, 2007)

3.6 Waves

The wave loads for the global strength design may be based on selected short-term seastates. The design storm approach with annual exceedance probability of 10^{-2} is considered for the thesis. The design storm approach is especially relevant in connection with nonlinear action effects (NORSOK, 2007). This approach requires information about the significant wave height (H_s) and spectral peak period (T_p) to complete the formulations. The NORSOK N-003 has been used to select appropriate H_s and T_p values for a seastate of 3 h duration which will be used in the analysis. H_s and T_p contour in the Norwegian Sea with annual probability of exccedance of 10^{-2} can be found in Figure 3-5.

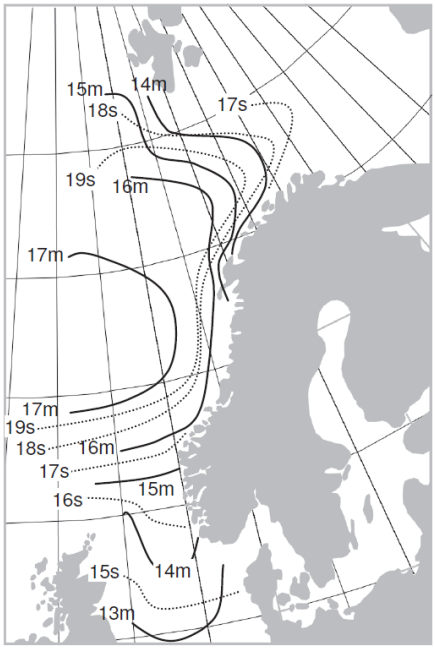

Figure 3-5 . The Significant Wave height, H_s (in m) and Related Maximum Peak Period, T_p (in s) for seastates of 3 h duration. Picture courtesy of (NORSOK, 2007)

3.7 Sea ice and Ice Berg

The sea in the Norwegian Sea has relatively stable and high water temperature. The thermohaline effect brings warm sea waters from the North Atlantic regions, so that unlike the Artic Seas, the Norwegian Sea is ice-free throughout the year. On the other hand, in conventional theory, the Gulf Stream brings warm weather northwards and gives Norway a relatively higher temperature than other places so far north. However, recent research found that there is no unambiguous correlation between the Gulf Stream on one side and the temperatures in the Norwegian Sea on the other. The large volume of water in the Norwegian Sea itself absorbs vast quantities of heat from the sun in the spring and summer, and then releasing that heat into the air in the autumn and winter (Amundsen & Lie, 2012).

Sea ice conditions on the NCS can be found only in the Barents Sea area. Although, the Norwegian Sea is ice free throughout the year, the northern and eastern part of the Barents Sea is covered by sea ice for much of the year. In open water, the combination of ice, winds and waves initiate icebergs drifting. When, an iceberg collides with a structure, the icebergs collision will cause large forces which could damage the structure. According to DNV recommendation, the Barents Sea can be divided into eight regions based on the physical and geographical aspects in related to ice formations.

The division of the Barents Sea can be seen In the Figure 3-6, which is divided into 8 regions as followed.

1. Spitsbergen : Usually ice every winter
2. Norwegian Sea : Generally ice free

3. Franz Josef Land : Usually ice every winter
4. Kara : Usually ice every winter
5. Novozemelsky : In between
6. Kola : In between
7. Pechora : Usually ice every winter
8. White Sea : Usually ice every winter

Figure 3-6. The Barents Sea Regions based on Ice Formations. Picture courtesy of (Gudmestad & Karunakaran, 2012)

3.8 Precipitation

In the summer months, the Norwegian Sea is often experiencing the wettest month over the year whereas the late spring months, around May and June, are expected to be the driest months. In the spring and summer seasons, the Norwegian Sea is affected by a warm air from the northern part of the North Sea. The warm air flows over the cold sea which is a suitable condition for the appearance of fog formations. This condition may present a transportation problem related to safety flight. The flight distance may be so long that the helicopter passes the "point of no return" (Gudmestad, Olufsen, & Strass, 1995).

3.9 Sea Bottom and Soil

The detailed characteristics of the soils such as soil stiffness, strengths and capacity may vary in every place. By means of that, it is important to conduct soil investigations, because of every soil layer has different properties based on the particular area where the soil is located. In designing the bottom assembly in a certain area, the selection of foundation type either using a suction anchor or a piled foundation is also depending on the soil characteristics at

that site. Furthermore, in the SCR configuration, the soil data plays important aspects in designing the riser due to a complex interaction between the riser movement and the seabed soil at the touchdown point (TDP).

In general, the soils on the Norwegian Continental Shelf are compact with upper layers usually consisting of stratified dense sands and hard clays, followed by further over consolidated clays, silts and sands (de Ruiter & Fox, 1975).

4. Design Code for Riser

4.1 Introduction

The risers should be designed based on acknowledged standards and regulations, which also take into consideration the various design conditions that may involve during the service life of the risers. The minimum requirements for the design conditions of the risers are to be given for fabrication, installation, commissioning, operation, maintenance, requalification, and abandonment. According to the definition, the function of the risers is to ensure transport of gas, oil and water in pipes safe, uninterrupted and simultaneous from the seabed to the floating facilities. In the other words, the riser is part of flow assurance chain. The flow assurance has broad definitions. The definition of flow assurance is a multi-discipline activity for multiphase transport, which covers the transmission of oil, gas and water in the same pipeline from the reservoir to the processing plant ("About Flow Assurance," 2007). In order to achieve the "successful flow", the riser should be designed, manufactured, fabricated, operated and maintained based on standardized design codes.

In the oil and gas industry, the risers should be designed in accordance with safety philosophy related to human life, environment and financial issues. According to DNV, the integrating safety philosophy for different aspects is illustrated in Figure 4-1 (DNV, 2010a). This safety philosophy will also be implemented in the design of risers which are dedicated to the oil and gas industry. The basic requirements of the risers are to design these in such a way that they will remain fit for use as intended and will sustain all foreseeable load effects and other influences likely to occur during the service life (DNV, 2010a).

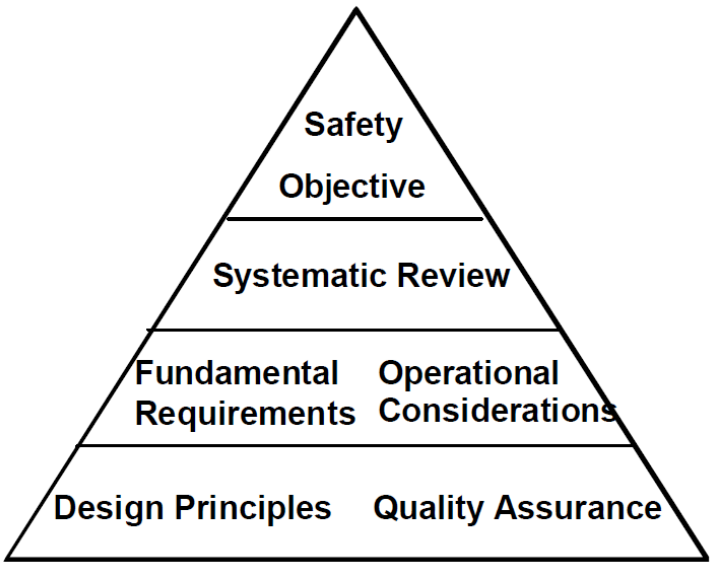

Figure 4-1. Safety Hierarchy. Picture courtesy of (DNV, 2010a)

The structural design, that is commonly used for this industry are divided into two methods; Working Stress Design (WSD) and Load and Resistance Factor Design (LRFD). In general, the difference between WSD and LRFD is that the working stress design focuses only on that

the working stress that results from action loads shall be under a certain limit with a single safety factor which is used take into account the influence of uncertainty. On the other hand, the load and resistance factor design is determined based on various design loads and resistance conditions where the uncertainties are accounted for individually for each different condition based on different safety factor criteria.

For this thesis, the rises are designed based on the Load and Resistance Factor Design (LRFD) method. The selection of this method is due mainly to the fact that the LRFD method represents a more flexible and optimal design with uniform safety level and is considered better than the WSD method. In the following sections, the design criteria of the riser will be presented with focusing on the LRFD method which is generally provided in DNV-OS-F201 (DNV, 2010a).

4.2 Design Principles

The objective of the design system is that the risers should comply with the safety philosophy. For example, all work associated with design, construct, install, operate and maintain the risers shall be carried out in such way that no single failure will lead to life-threatening situations for any person, and no releases of fluid contents will be accepted during operation of the riser system (DNV, 2010a). In order to achieve the design objective, any hazardous impact shall be reduced or eliminated to be as low as reasonably practicable (ALARP Principle).

In absence of a company standard policy regarding human aspects, environment and financial issue, risk assessment may be required to identify the design criteria in terms of safety aspects. A systematic review by using quantitative risk analysis (QRA) may provide sufficient input to select an appropriate safety class in respect to structural failure probability. The choice of safety class should also describe the critical level of the riser system.

DNV provides a classification of safety classes for the riser's design based on the failure consequences. Prior to the design, the risk analysis and assessment by using QRA should be conducted to identify which safety class is required for the risers. Thus, the riser can be designed with different safety requirements based on conditions of the riser system. Table 4-1 presents the classification of safety classes which is revealed in DNV-OS-F201 section C204 (DNV, 2010a).

Table 4-1 Classification of Safety Classes (DNV, 2010a).

Safety Class	Definition
Low	Where failure implies low risk of human injury and minor environmental and economic consequences.
Normal	For conditions where failure implies risk of human injury, significant environmental pollution or very high economic or political consequences.
High	For operating conditions where failure implies high risk of human injury, significant environmental pollution or very high economic or political consequences

The safety class of a riser can also be determined based on the hazard potential of the fluid in the riser, location of the riser that is being installed, and the riser category whether it is production risers or drilling risers (DNV, 2010a). Once the safety class is chosen, the risers system shall apply to the basic design principle according to DNV, as follow;

- The riser system shall satisfy functional and operational requirements as given in the design basis.
- The riser system shall be designed such that an unintended event does not escalate into an accident of significantly greater extent than the original event;
- Permit simple and reliable installation, retrieval, and be robust with respect to use;
- Provide adequate access for inspection, maintenance, replacement and repair;
- The riser joints and components shall be made such that fabrication can be accomplished in accordance with relevant recognized techniques and practice;
- Design of structural details and use of materials shall be done with the objective to minimize the effect wear and tear, corrosion, and erosion;
- The riser mechanical components shall, as far as practicable, be designed "fail safe". Consideration is to be given in the design to possible early detection of failure or redundancy for essential components, which cannot be designed according to this principle;
- The design should facilitate monitoring of its behavior in terms of tension, stresses, angles, vibrations, fatigue cracks, wear, abrasion, corrosion etc.

The fundamental principle of the design method is to verify that factored design load effects do not exceed factored design resistant for any considered limit states. This principle is also implied for Load Resistance Factor Design (LRFD) method. The LRFD method uses four design load effects to be considered in the design, which are:

- Pressure load effects
- Functional load effects
- Environmental load effects
- Accidental load effects

The sum of the applicable load factor effects is going to be compared to the resistance factor, and the design implies a safe design when the resistance factor has larger value compared to the sum of applicable load factor effects.

The general LRFD safety format can be expressed as:

$$S_d(S_P;\gamma_F.S_F;\gamma_E.S_E;\gamma_A.S_A;) \leq \frac{R_K}{\gamma_{SC}.\gamma_m.\gamma_c} \quad (4.1)$$

Where:

S_d = Sum of design load factor

S_P = Pressure Loads

S_F = Load effect from functional load (vector or scalar)

S_E = Load effect from environmental loads (vector or scalar)

S_A = Load effect from accidental loads (vector or scalar)

γ_F = Load effect factor for functional loads (vector or scalar)

γ_E = Load effect factor for environmental loads

γ_A = Load effect factor for accidental loads

R_k = Generalized resistance (vector or scalar)

γ_{SC} = Resistance factor to take into account the safety class

γ_m = Resistance factor to account for material and resistance uncertainties

γ_c = Resistance factor to account for special conditions.

4.3 Design Load

The DNV categorizes the loads and deformations into four groups as follows:

- Pressure (P) loads,
- Functional (F) loads,
- Environmental (E) loads,
- Accidental (A) loads,

The descriptions of the each load groups are presented in the Table 4-2:

Table 4-2 Example of categorizations of loads (DNV, 2010a).

Functional loads (F-loads)	Environmental loads (E-loads)	Pressure loads (P-loads)[6)]
Weigh and buoyancy[5)] of riser, tubing, coatings[5)], marine growth[1)], anodes, buoyancy modules, contents, and attachments. Weight internal fluid. Applied tension for top-tension risers. Installation induced residual loads or pre-stressing. Pre-load of connectors. Applied displacements and guidance loads, including active positioning of support floater. Thermal loads. Soil pressure on buried risers. Differential settlements. Loads from drilling operations. Construction loads and loads caused by tools.	Waves. Internal waves and other effects due to differences in water density. Current. Earthquake[3)]. Ice[2)]. Floater motions induced by wind, waves and current, i.e.: – Mean offset including steady wave. – Drift, wind and current forces. – Wave frequency motions. – Low frequency motions.	External hydrostatic pressure. Water levels. Internal fluid pressure, i.e. : – hydrostatic – static – dynamic[4)] contributions, as relevant

Note:

Accidental loads, both size and frequency, for a specific riser and floater may be defined by a risk analysis.

1. For temporary risers, marine growth can often be neglected due to the limited duration of planned operations.
2. Ice effects shall be taken into account in areas where ice may develop or drift.
3. Earthquake load effects shall be considered in the riser design for regions considered being seismically active.
4. Slugs and pressure surges may introduce global load effects for compliant configurations.
5. Includes also absorbed water.
6. Possible dynamic load effects from P-loads and F-loads shall be treated as E-loads, e.g. slug flow.

4.4 Limit States Design

By using the LRFD method, the DNV recommends four types of limit states that need to be considered in the designs. These are serviceability limit state (SLS), ultimate limit state (ULS), accidental limit state (ALS) and fatigue limit state (FLS). Based on DNV (DNV, 2010a), the general descriptions for these categories are described as follow:

- Serviceability Limit State (SLS): the riser must be able to remain fit during the service period and operate properly. This limit state corresponds to criteria limiting or governing the normal operation (functional use) of the riser.
- Ultimate Limit State (ULS) requires that the riser must remain intact and avoid rupture, but not necessary be able to operate.
- Accidental Limit State (ALS): the riser must be able to remain intact and avoid rupture, but not necessary be able to run the operation (for example, accidental collision, dropped object, explosion, etc.)
- Fatigue Limit State (FLS): the riser must be able to remain fit to operate during service life from accumulated excessive fatigue crack growth or damage under cyclic load.

The SLS, ULS and ALS should express the most probable extreme combined load effect over a specified design time period. For permanent operational conditions, the riser should be designed for maximum value of a 100 years return period (annual exceedence probability of 10^{-2}). The combination of environmental condition typically apply omni-directional for wind, waves and currents in the same return period (i.e. 100 year) to obtain a severe combination of environmental load effects. For the FLS, all relevant cyclic loads that affect the riser shall be considered in the design for the periods of the riser's service life, such as first order wave effects (direct wave loads and associated floater motions), second order floater motions, thermal and pressure induced stress cycles, vortex vibrations, and collisions (DNV, 2010a).

The calculation of the load effects for each design limit states is achieved by the summation of the load effect for each category multiplied by their corresponding load effect factor. For example, the calculation for bending moment and effective tension are described in below formula.

The formula for the bending moment, according to DNV (DNV, 2010a) is listed as;

$$M_d = \gamma_F . M_F + \gamma_E . M_E + \gamma_A . M_A \quad (4.2)$$

Where:

M_F = Bending moment from functional loads

M_E = Mending moment from environmental loads

M_A = Bending moment from accidental loads

The effective tension design for the load effects is listed as;

$$T_{ed} = \gamma_F . T_{eF} + \gamma_E . T_{eE} + \gamma_A . T_{eA} \quad (4.3)$$

Where:

T_{eF} = Effective Tension from functional loads

T_{eE} = Effective Tension from environmental loads

T_{eA} = Effective Tension from accidental loads

Where the effective tension, T_e is given as follow;

$$T_e = T_W - p_i . A_i + p_e . A_e \quad (4.4)$$

Where:

T_W = True wall tension (i.e. axial stress resultant found by integrating axial stress over the cross-section)

P_i = Internal (local) pressure

P_{ie} = External (local) pressure

A_i = Internal cross-sectional area

Every load category has an applicable load factor, and DNV suggests load effect factors for all design load effects according to the design limit states and safety classes. The load effect factors based on the limit states and design loads are shown in Table 4-3.

Table 4-3 Load Effect Factors (DNV, 2010a).

Limit State	F-Load effect	E-load effect	A-load effect
	γ_F	γ_E	γ_A
ULS	1.1	1.3	NA
FLS	1.0	1.0	NA
SLS & ALS	1.0	1.0	1.0
Note: 1. If the functional load effect reduces the combined load effects, γ_F shall be taken as 1/1.1 2. If the environmental load effect reduces the combined load effects, γ_F shall be taken as 1/1.3			

On the other hand, the resistance factors are composed of the safety class factor (γ_{SC}), the material resistance factor (γ_M), and the condition factor (γ_C). DNV (DNV, 2010a) suggests that these factors must be used as follow;

- Safety class factor γ_{SC} (presented in Table 4-4) is selected based on the failure consequences which presented on the safety class (refer to Table 4-1).
- Material resistance factor γ_M (presented in Table 4-5) is selected based on the limit states in order to represent the material uncertainties.
- The condition factor γ_C (presented in Table 4-7) is selected based on the relevant limit states in order to account specified condition explicitly.

Table 4-4 Safety Class Resistance Factors (DNV, 2010a).

Safety class factor, γ_{SC}		
Low	Normal	High
1.04	1.14	1.26

Table 4-5 Material Resistance Factors (DNV, 2010a).

Material resistance factor, γ_M	
ULS & ALS	SLS & FLS
1.15	1.0

4.4.1 Ultimate Limit State

The ultimate limit state (ULS) design states that the risers shall be able to sustain the loads from the maximum load combinations for an annual exceedance probability of 10^{-2}. The risers should be able to operate normally under the ULS design conditions. DNV (DNV, 2010a) proposes the relevant failure modes for the limit states that need to be considered in the design. The typical failure modes for this limit state are;

- Bursting
- Hoop buckling (collapse)
- Propagating buckling
- Gross plastic deformation and local buckling

- Gross plastic deformation, local buckling and hoop buckling
- Unstable fracture and gross plastic deformation
- Liquid tightness
- Global buckling

In addition, the calculation of the wall thickness for normal steel pipe should examine the possibilities that the nominal wall thickness may be reduced. DNV (DNV, 2010a) suggests using a minimum wall thickness (t_1) for bursting and collapse failure modes. These failure modes are normally caused by internal overpressure, therefore the fabrication allowance and corrosion allowance shall be taken into account to calculate the final wall thickness. Unless otherwise noted, for the failure likely to occur due to external extreme load effect, the wall thickness (t_2) is sufficiently calculated by considering the corrosion allowance only. The wall thickness calculations for the riser design are presented in Equations (4.5) and (4.6).

$$t_1 = t_{nom} - t_{fab} - t_{corr} \tag{4.5}$$

$$t_2 = t_{nom} - t_{corr} \tag{4.6}$$

Where:

t_{nom} = Nominal (specified) pipe wall thickness

t_{fab} = Fabrication (manufacture) negative tolerance

t_{corr} = Corrosion/wear/erosion allowance

Bursting

The content fluids in the pipe produce internal pressure which affects the thickness of the pipe. This internal pressure, if the wall-thickness is not sufficient, may cause rupture of the walls due to high pressure. The failure of the pipe mainly due to internal overpressure is called bursting. DNV (DNV, 2010a) provides the formula to investigate the wall thickness requirement of the pipe:

$$(p_{li} - p_e) \leq \frac{p_b(t_1)}{\gamma_{SC} \cdot \gamma_m} \tag{4.7}$$

With:

$$p_{li} = p_{inc} + \rho_i . g . h \tag{4.8}$$

$$p_b(t_1) = \frac{2}{\sqrt{3}} . \frac{2 . t_1}{D - t_1} . \min\left(f_y ; \frac{f_u}{1.15}\right) \tag{4.9}$$

Where:

p_{li} = Local incidental pressure, this is the maximum expected internal pressure with a low annual exceedance probability.

p_e = External pressure

ρ_i = The density of the internal fluid

g = The avcceleration of gravity

$p_b(t_1)$ = The burst resistance

D = Nominal outside diameter

f_y = Yield Stength of material

f_u = Tensile strength of material

In the design practice, normally the incidental surface pressure (p_{li}) is taken 10% higher than the design pressure (p_d) (DNV, 2010a).

$$p_{li} = p_{ld} + 0.1 \cdot p_d \tag{4.10}$$

$$p_{Id} = p_d + \rho_i . g . h \tag{4.11}$$

Where:

p_{Id} = Local internal design pressure

p_d = Design pressure, the maximum surface pressure during normal operations

Based on Equations (4.7) and (4.9), the minimum wall thickness required for a straight pipe without allowance and tolerance is calculated as follow;

$$t_1 = \frac{D}{\frac{4}{\sqrt{3}} \cdot \frac{\min(f_y; \frac{f_u}{1.15})}{\gamma_{SC} \cdot \gamma_m \cdot (p_{li} - p_e)} + 1} \tag{4.12}$$

Hoop Buckling (Collapse)

Additionally, if the external pressure dominates the wall thickness selection of the pipe, then the pipe should be designed to sustain collapse from the external pressure. Together with the internal pressure from the content fluids, DNV (DNV, 2010a) proposes that the pipe should be designed with respect to excessive pressure from outside as well.

$$(p_e - p_{min}) \leq \frac{p_c(t_1)}{\gamma_{SC} \cdot \gamma_m} \tag{4.13}$$

Where:

p_{min} = Minimum internal pressure

$p_c(t_1)$ = The resistance for external pressusre (hoop buckling)

According to DNV-OS-F101 (DNV, 2013), the resistance for external pressure (hoop buckling) can be found from the equation as follows;

$$(p_c(t_1) - p_{el}(t_1)).\left(p_c^2(t_1) - p_p^2(t_1)\right) = p_c(t_1).p_c(t_1).p_p(t_1).f_0.\frac{D}{t_1} \quad (4.14)$$

With:

$$p_{el}(t_1) = \frac{2.E.\left(\frac{D}{t}\right)^3}{1-\vartheta^2} \quad (4.15)$$

$$p_p(t_1) = 2.\frac{t}{D}.f_y.\alpha_{fab} \quad (4.16)$$

$$f_0 = \frac{D_{max} - D_{min}}{D} \quad (4.17)$$

Where:

$p_{el}(t_1)$ = The elastic collapse pressure

$p_p(t_1)$ = Plastic collapse pressure

α_{fab} = Fabrication factor

f_0 = Initial ovality

Propagating Buckling

A propagating buckling will happen when a transversal buckle (local buckling) takes place. The transversal buckle is caused if the external overpressure changes into a longitudinal buckle that propagates along the pipe. The buckle should remain as a local effect. To avoid an extensive buckle in the longitudinal direction, the propagating buckling (collapse) shall be checked. According to DNV (DNV, 2010a), the pipe should be designed with minimum pressure resistance against buckling propagation, as follow:

$$(p_e - p_{min}) \leq \frac{p_{pr}}{\gamma_C.\gamma_m.\gamma_{SC}} \quad (4.18)$$

With:

$$p_{pr} = 35.f_y.\alpha_{fab}.\left(\frac{t_2}{D}\right)^{2.5} \quad (4.19)$$

Where:

γ_C = Condition factor for buckle propagation. The value is equal to 1 if no propagation factor is allowed and 0.9 if buckle is allowed to propagate a short distance.

p_{pr} = The resistance against buckling propagation.

t_2 = The minimum wall-thickness, refer to Equation (4.6)

As seen in the Equation (4.19), the propagation buckle pressure calculates is only based on yield strength of the material and D/t ratio. The stress state of the pipe is not related to the propagation phenomenon. Once a local buckle has been initiated, the pipe buckle is developing longitudinally if the resistance against buckling propagation is less than the hydrostatic pressure.

Combine Loading Criteria

In addition, when the pipe is subjected to a bending moment, effective tension and net internal overpressure; and for the pipe subjected to bending moment, effective tension and net external overpressure, DNV suggests that the pipe shall be designed to satisfy Equation (4.20) and Equation (4.21) respectively (DNV, 2010a).

$$\{\gamma_{SC}.\gamma_m\}\left\{\left(\frac{|M_d|}{M_k}.\sqrt{1-\left(\frac{P_{id}-P_e}{P_b(t_2)}\right)^2}\right)+\left(\frac{T_{ed}}{T_k}\right)^2\right\}+\left(\frac{P_{id}-P_e}{P_b(t_2)}\right)^2 \leq 1 \quad (4.20)$$

$$\{\gamma_{SC}.\gamma_m\}^2\left\{\frac{|M_d|}{M_k}+\left(\frac{T_{ed}}{T_k}\right)^2\right\}^2+\{\gamma_{SC}.\gamma_m\}^2\left(\frac{P_e-P_{min}}{P_c(t_2)}\right)^2 \leq 1 \quad (4.21)$$

With:

$$M_k = f_y.\alpha_c\,(D-t_2)^2.t_2 \quad (4.22)$$

$$t_k = f_y.\alpha_c.\pi.(D-t_2)^2.t_2 \quad (4.23)$$

Where:

M_d = Design bending moment, refer to Equation (4.2)

T_{ed} = Design effective tension, refer to Equation (4.3)

P_{Id} = Local internal design pressure, refer to Equation (4.11)

M_k = Plastic bending moment resistance

T_k = Plastic axial force resistance

$P_c(t_2)$ = Hoop buckling capacity, refer to Equation (4.14) as a function of t_2

The parameter for strain hardening α_c can be calculated according to DNV with value is not to be taken larger than 1.2 (DNV, 2010a).

$$\alpha_c = (1-\beta) + \beta.\frac{f_u}{f_y} \tag{4.21}$$

$$\beta = \begin{cases} (0.4+q_h) & \text{for } D/t_2 < 15 \\ (0.4+q_h)(60-{}^{D}/_{t_2}) & \text{for } 15 < D/t_2 < 60 \\ 0 & \text{for } D/t_2 > 60 \end{cases}$$

$$q_h = \begin{cases} \frac{(P_{Id}-P_e)}{P_b(t_2)}\frac{2}{\sqrt{3}} & \text{For } P_{Id} > P_e \\ 0 & \text{else} \end{cases}$$

4.4.2 Fatigue Limit State

If the risers system is exposed to repeated/cyclic loading in some period of time, this could lead to operational failure of the risers. Every cyclic load that affects the riser should be carefully investigated. If the magnitude and number of the cycles are considered large enough, the corresponding fatigue damage should be calculated from each source of the loading. In the operating condition of the risers, the wave induced load, the low frequency and the vortex induced stresses are the main components which produce cyclic loads on the risers. These components are mainly contributing to failure of the riser due to fatigue.

DNV specifies a dedicated limit state, fatigue limit state (FLS), to check the structure from failure due to the cyclic loads. In order to fulfill the requirements of the FLS, the riser should have sufficient factored fatigue life within the service life of the risers. In general the fatigue life of the risers can be divided into two phases; crack initiation and propagation. A crack in the pipe is very dangerous and it will affect the strength of the riser components. In case of crack initiation happened, the fatigue life of the pipes may be decreased up to 5% from the total fatigue life (DNV, 2010a). According to DNV, the fatigue assessment methods are categorized as follow;

- Method based on S-N curve
- Method based on fatigue crack propagation

The S-N curve method is normally used during the design. The number of cyclic loadings is selected based on S-N curve corresponding to the nominal stress component of the risers. Whereas, fatigue crack propagation calculation is based on an inspection method to estimate fatigue crack growth life. By means of this method, the risers shall be designed and inspected so that maximum expected initial defect size would not grow to a critical size during service life. NDT is applied during fabrication and operation to inspect the fatigue crack growth and thus the fatigue life of the risers can be estimated (DNV, 2010a).

S-N Curve

According to DNV, the criterion that shall be satisfied for the fatigue limit state design by using S-N curve method may be written as follow (DNV, 2010a);

$$D_{fat}.DFF \leq 1.0 \quad (4.21)$$

Where:

D_{fat} = Accumulated fatigue damage (Palmgren-Miner rule)

DFF = Design fatigue factor, refer to Table 4-6

Table 4-6 Design Fatigue Factors (DNV, 2010a).

Safety Class		
Low	Normal	High
3.0	6.0	10.0

For the selection of an appropriate S-N curve and calculation of the stress concentration factor (SCF), DNV-RP-C203 may be used as a guidance to calculate the fatigue damage by using this method (DNV, 2012).

Fatigue Crack Propagation

The DNV provides a formula to estimate fatigue crack growth life. The system shall be designed and inspected to satisfy the following criteria (DNV, 2010a);

$$\frac{N_{tot}}{N_{cg}}.DFF \leq 1.0 \quad (4.21)$$

Where:

N_{tot} = Total number of applied stress cycles during service or to in-service inspection

N_{cg} = Number of stress cycles necessary to increase the defect from the initial to the critical defect size

DFF = Design fatigue factor, refer to Table 4-6

4.4.3 Accidental Limit State

During the service life, the riser may be subjected to abnormal conditions, incorrect operations or unexpected loads. Due to these facts, the accidental limit state (ALS) has been introduced to avoid catastrophic accidents in the risers system. Accidental loads on the risers system typically results from unplanned occurrences, which may be categorized into (not limited to) the following circumstances;

- Fire and explosion
- Impact/collision
- Hook/snag loads
- Failure of the support system, i.e. loss of buoyancy, loss of mooring line, etc.
- Failure due to internal over pressure, i.e. failure of well tubing or packers, well kill, etc.
- Iceberg approaches

The design of accidental loads is classified based on the frequency of the occurrences and the accident effects to the riser system. The main idea is that the riser system should be able to resist relevant functional loads in the extreme condition and avoid fatal failure that may impact human lives, environment and financial aspects. Prior to check the ALS design, the risers should be ensured to satisfy the ultimate limit states design. A service ability limit states (SLS) should be introduced as well as complied to in order to define the operational limitation. The simplified design check with respect to accidental load may be performed as described in Table 4-7 (DNV, 2010a).

Table 4-7 Simplified Design Check for Accidental loads (DNV, 2010a).

<table>
<tr><td rowspan="2">Probability of occurrence</td><td colspan="3">Safety Class</td></tr>
<tr><td>Low</td><td>Normal</td><td>High</td></tr>
<tr><td>$> 10^{-2}$</td><td colspan="3">Accidental loads may be regarded similar to environmental loads and may be evaluated similar to ULS design check</td></tr>
<tr><td>10^{-2} - 10^{-3}</td><td colspan="3">To be evaluated on a case by case basis</td></tr>
<tr><td>10^{-3} - 10^{-4}</td><td>$\gamma_c = 1.0$</td><td>$\gamma_c = 1.0$</td><td>$\gamma_c = 1.0$</td></tr>
<tr><td>10^{-4} - 10^{-5}</td><td rowspan="3" colspan="2">Accidental loads or events may be disregarded</td><td>$\gamma_c = 1.0$</td></tr>
<tr><td>10^{-5} - 10^{-6}</td><td>$\gamma_c = 1.0$</td></tr>
<tr><td>$< 10^{-6}$</td><td></td></tr>
</table>

4.4.4 Serviceability Limit State

The criteria of the serviceability limit state are associated with the ability of the riser system to operate in normal condition with certain limitation. Normally, the operator will specify the requirement in order to fulfil the limit states. In some cases, the riser condition may exceed the serviceability limit state (SLS), and then the engineer must carefully evaluate the case to make sure that the riser will not exceed the ultimate limit state (ULS) and an accidental limit state (ALS) shall be defined in accordance with exceedance of SLS. The exceeding an SLS should be closely monitored by maintenance/inspection routines and by implementation of early warning or fail-safe type system in the design (DNV, 2010a).

In case of company specifications, DNV defines limitations that need to be controlled in the global riser design. The parameters in the SLS are associated with the limitations of deflections, displacements, and rotation or ovalisation of the riser pipe.

Ovalisation limit due to bending

The risers shall be designed to prevent excessive ovalisation in order to prevent local buckling which in turn will initiate buckle propagation. The flattening due to bending together with out-of-roundness tolerance from fabrication of the pipe shall be limited to 3.0% (DNV, 2010a).

$$f_0 = \frac{D_{max} - D_{min}}{D} \leq 0.03 \tag{4.17}$$

Riser Stroke

The term "riser stroke" is referring to the travel of the tensioner. A tensioner maintains constant tension along the top part of the riser in order to limit bending. It should continue to pull as the riser and the floater move vertically relative to each other. In addition to static responses, the dynamic responses of environmental loadings and the set down effects of the floater shall be included in the calculation of the riser stroke. DNV suggests that during the installation phase, the riser system shall be designed to have sufficient stroke so as to avoid damages to riser, components and equipment (DNV, 2010a).

Example of SLS for Production Risers

To summarize, the serviceability limit state (SLS) for production risers with surface trees is presented in Table 4-8.

Table 4-8 Example of SLS for production risers with surface tree (DNV, 2010a).

Component	Function	Reason for SLS	Comment
Riser installation	Running and retrieving the riser	A weather limitation would be set to avoid riser interference	Usually run on guide in close proximity to other risers
Riser Stroke	Limit the frequency of bottom out	The tensioner may be designed for bottom-out	Energy absorption criteria shall be specified
	Limit the design requirements for the jumper from the surface tree to the topside piping	The tensioner may be designed for bottom-out	Energy absorption criteria shall be specified

5. Theoretical Background

5.1 Introduction

This chapter describes the background knowledge that is required for the riser analysis that will be discussed in Chapter 7. The theoretical understanding is required in order to be able to design and analyze the riser in various environmental and design conditions. The load and responses which will be discussed in this chapter are limited to waves, currents, floater motions, response amplitude operator (RAO), hydrodynamic load effects, and interactions between the risers and the soil foundations.

5.2 Waves

There is no single object on the sea surface that does not get affected by wave actions. The main force in generating waves is caused by winds acting on a certain contact area of the water surfaces. The contact area between the water surface and the wind in generating waves is known as the fetch. The waves can be classified into two types based on the location where they are generated, which are wind seas and swells. Wind seas are the wave type that are generated when the wind is acting on a local area, and for the swells, the waves are generated far away and have traveled out from the origin of the generating area where they were developed. In addition to the above, waves can be also generated from the interaction between gravitational attraction of the moon and the sun, which creates the longest water waves on earth known as a wave tide.

The waves are generally described by the main parameters which are wave length, height, periods, water depth and wave directions. The directions refer to the directions from where the waves are propagating. The other wave parameters such as velocities, accelerations, wave forces, wave energy, etc., are theoretically derived from the main parameters.

It is very rare to find an exactly linear (regular) wave in the ocean. Normally, the observation of a wave in the nature attains a nonlinear character which has irregular and random shapes. However, these nonlinear waves can be considered as a sum of many linear waves with different parameters and directions. If a device is used to measure water surfaces elevation (η) in some period of time, the outcome might typically be captured as a random water surface as shown in Figure 5-1. Figure 5-2 proves that the random water surface can be approached as a superposition of a number of linear waves.

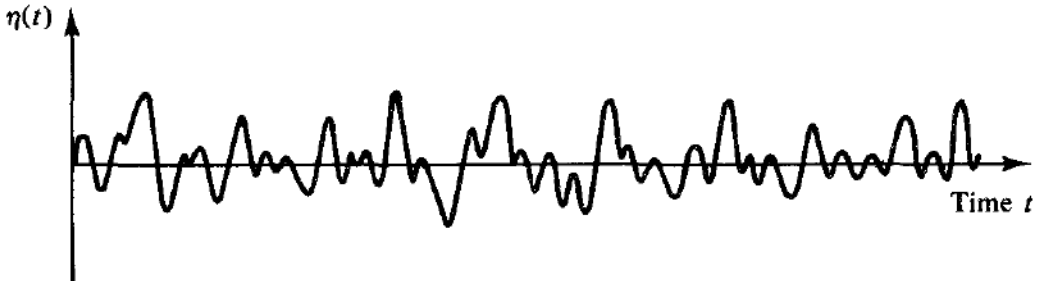

Figure 5-1. Possible Water Surface Observation Results. Picture courtesy of (Dean & Dalrymple, 1984)

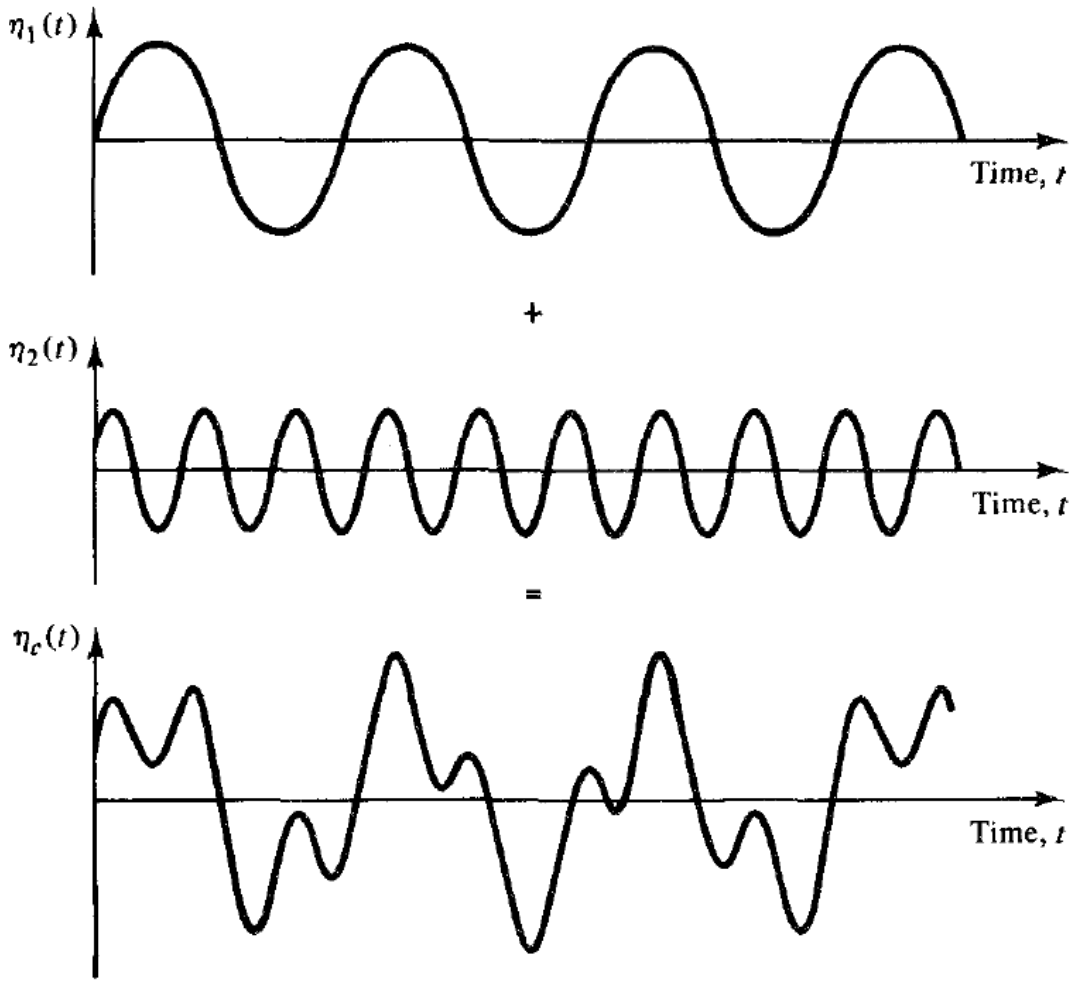

Figure 5-2. Superposition of Waves. Picture courtesy of (Dean & Dalrymple, 1984)

The offshore structures must be able to sustain severe load actions from waves in extreme environmental conditions without major destruction. In order to recognize the impact of the action loads, the waves can be described either by deterministic design wave method or by using a stochastic method applying wave spectra (DNV, 2010b). The deterministic design wave method is used to obtain the extreme force for analysis of the quasi-static response of the structure. This method is represented by a maximum wave height with the corresponding wave period. In order to determine the wave parameters, the statistical approach may be used for this method. Indeed, the deterministic design wave method does not represent the actual phenomenon of the ocean waves where the action effects of the waves may vary in different wave periods as well as wave heights, and thus the parameters should not be limited only to the maximum value of the wave height with the corresponding period. This method is not used in this thesis; hence the explanation about this method is not presented in detail.

Another method to describe the wave load effects is using the stochastic method by applying wave spectra. This method is suitable for a structure that is mainly affected by the dynamic effects, for instance, floating structures. The stochastic method gives result as better

representative of the ocean waves compared to the deterministic wave method. Normally, the stochastic data is presented in a scatter diagram which contains a wide range of significant wave heights and representative peak periods. Omni directional wave spreading tables may be added to specify the annual probability of the wave occurrences at the particular sea-state locations. For the design operating conditions, DNV introduces three hour wave measurements as a standard time for sea-states (DNV, 2010b).

The wave spectrum has the capability to describe the irregularity and the randomness of the ocean waves. Wave measurements are conducted to obtain the real wave data, where every wave event can be characterized by the significant wave height (Hs) and Peak Period (Tp). The term 'significant wave height' refers to the average of the highest one-third waves measured in the indicated time and the term 'peak period' is an inverse of frequency at the time when the spectrum reaches its maximum value.

Nowadays, different theoretical spectrum models such as Pierson-Moskowitz, JONSWAP, Bretschneider, Ochi-Hubble, and Torsethaugen double peaked spectrum are available to suit different types of sea-states. Each spectrum has different characteristics in order to represent typical conditions of the ocean waves. Pierson-Moskowitz (PM) spectrum is used in the area where waves are typically dominated by the wind seas. While, JONSWAP spectrum is an improvement of the PM spectrum by considering the fetch as a limitation of the waves' development. However, if the swells and the wind seas are presented in one sea region, a two-peak spectrum should be used to represent this sea condition. The Ochi-Huble and Torsethaugen spectrums are two-peak spectra that could be used for this particular sea-state (DNV, 2010b).

5.2.1 Wave Spectrum Energy

The wave energy is transported through wave heights and velocities. Two types of wave energy are contained when the waves are traveling which are Kinematic Energy and Potential Energy. These energies are distributed based on different wave lengths or wave frequencies. As mentioned previously, the ocean waves contain random and irregular waves with different wave heights and periods, thus this wave energy is different for every individual wave. With this in mind, the best way to model wave energy is by using the energy spectrum approach.

The basic investigation is always based on wave observation records. Firstly, the sample of random wave records in some time is divided into an equal time intervals (Δt) as shown in Figure 5-3. Then, each periodic function of the individual random wave may be investigated by using Fourier series analysis to obtain each frequency characteristic. According to Journee and Massie (Journee & Massie, 2001), the spontaneous change of wave elevation has a Gaussian distribution and zero mean. Therefore, the wave energy spectrum can be developed from the random waves as a superposition of a series of sinusoidal waves by applying the Fourier series method as will be detailed below.

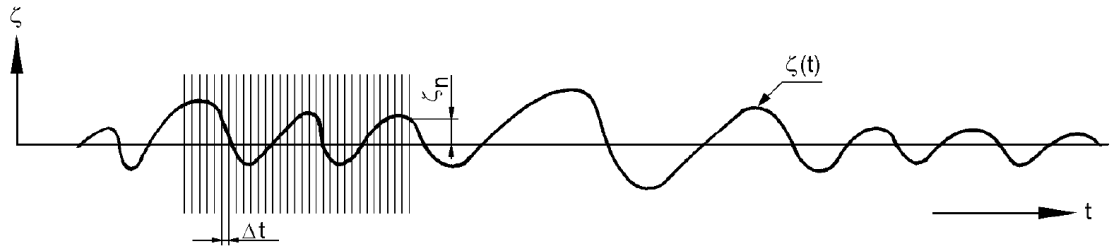

Figure 5-3 Wave Sampling Methods. Picture courtesy of (Journee & Massie, 2001)

As mentioned in Section 5.2, random waves can be seen as a superposition of many sinusoidal waves. In the same manner, the wave elevation may be written as the sum of regular wave components in the frequency domain (Journee & Massie, 2001), as follows:

$$\zeta(t) = \sum_{n=1}^{N} \zeta_{an}.\cos(\omega_n t - k_n \alpha + \varepsilon_n) \tag{5.1}$$

Where:

ζ_{an} = Wave amplitude component (m)

ω_n = Circular frequency component (rad/s)

k_n = Wave number component (rad/m)

ε_n = Random phase angle component (rad)

A sum of infinite data samples measured at interval periods (Δt) (refer to Figure 5-3) can be represented by a Fourier series. The total period of the wave sample can be defined as follows:

$$\tau = N.\Delta t \tag{5.2}$$

If the sample interval (Δt) is considered small enough, then the square average value ($\bar{\zeta}_{an}^2$) of the sample's amplitude can be neglected. The variance of the water surface elevations can be expressed by Equation (5.3).

$$\sigma_\zeta^2 = \frac{1}{N}\sum_{n=1}^{N}(\zeta_{an} - \bar{\zeta}_{an})^2 = \frac{1}{N}\sum_{n=1}^{N}{\zeta_{an}}^2$$

$$= \frac{1}{N.\Delta t}\sum_{n=1}^{N}{\zeta_{an}}^2.\Delta t = \frac{1}{\tau}\sum_{n=1}^{N}{\zeta_{an}}^2.\Delta t$$

$$= \frac{1}{\tau}\int_0^\tau {\zeta_{an}}^2(t)\,dt = \frac{1}{\tau}\int_0^\tau \left\{\sum_{n=1}^{N}\zeta_{an}.\cos(\omega_n t - k_n\alpha + \varepsilon_n)\right\}^2 dt$$

$$\sigma_\zeta^2 = \sum_{n=1}^{N} \frac{1}{2} {\zeta_{an}}^2 \tag{5.3}$$

The variance in above equation is a function of the time period. In another way, the variance can also be expressed by a frequency ($\omega = \frac{2\pi}{\tau}$). So, the wave amplitude (ζ_{an}) can be written as a part of a wave spectrum in accordance with following equation.

$$S_\zeta(\omega_n).\Delta\omega = \sum_{\omega_n}^{\omega_n+\omega} \frac{1}{2} {\zeta_{an}}^2(\omega) \tag{5.4}$$

Where:

$\Delta\omega$ = A frequency interval in the waves spectral density chart (refer to Figure 5-4)

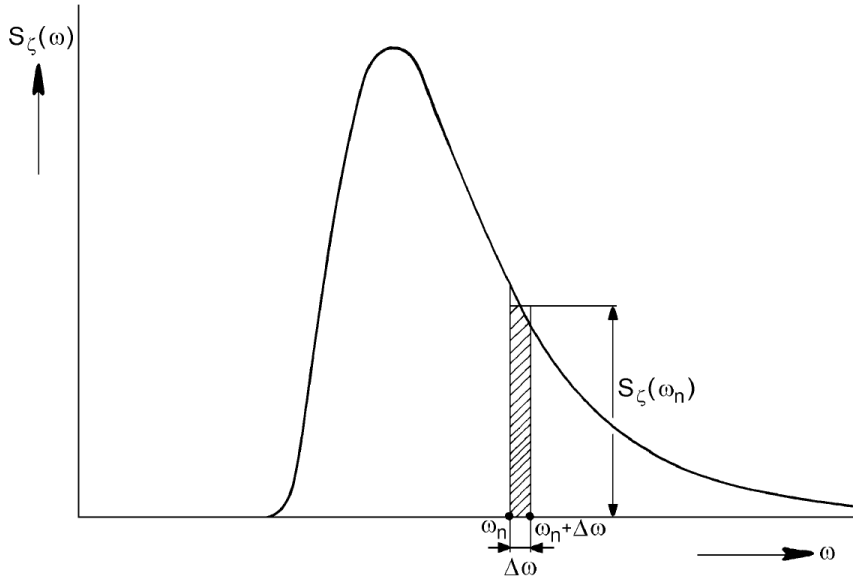

Figure 5-4 Spectral Wave Density. Picture courtesy of (Journee & Massie, 2001)

The Equation (5.4) describes the energy per unit area of the waves in an interval frequency of length $\Delta\omega$ as shown in Figure 5-4. If $\Delta\omega$ is considered as a small value, then the equation of the wave spectrum coordinates becomes:

$$S_\zeta(\omega_n).d\omega = \frac{1}{2} {\zeta_{an}}^2 \tag{5.5}$$

The total wave energy spectrum is equal to the variance of water surface elevations which is shown in Equation (5.3). This term can also be expressed as the total area under the spectral wave density curve.

$$\sigma_\zeta^2 = \int_0^\infty S_\zeta(\omega_n).d\omega \tag{5.6}$$

The statistical method is used to determine other wave parameters by calculating the moments of the area under the spectrum curve. If "n" is nth order moment, hence the general formula of a spectrum moment is written as:

$$m_{n\zeta} = \int_0^\infty \omega^n.S_\zeta(\omega_n).d\omega \tag{5.7}$$

Some important spectral moments are $m_{0\zeta}$, $m_{1\zeta}$, and $m_{2\zeta}$. The zero spectral moment or $m_{0\zeta}$ indicates the variance or the total area under the spectrum curve, $m_{1\zeta}$ is the first order moment (static moment) of this area, and $m_{2\zeta}$ is the second order moment (moment of inertia) of this area. The relationship of these spectrum moments to the wave height and wave period are presented as follows:

$$H_{1/3} = 4.\sqrt{m_{0\zeta}} = significant\ wave\ amplitude \tag{5.8}$$

$$T_z = 2\pi.\sqrt{\frac{m_{0\zeta}}{m_{2\zeta}}} = mean\ zero - crossing\ wave\ period \tag{5.9}$$

5.2.2 Wave Spectrum Models

Pierson-Moskowitz Spectrum (PM)

The PM spectrum was developed in 1964 by Pierson and Moskowitz. This spectrum is suitable for an area where the waves are generated by steady winds for a long time and without fetch limitation. The wave reaches equilibrium with the wind, which is known as fully developed seas (wind seas). The observation was taken in the North Atlantic, when a large area of the North Atlantic was influenced by the steadily wind for a long period of time. Roughly, a long time period is ten-thousand wave periods and a large area is five-thousand wave lengths on each side (Stewart, 2008).

According to DNV (DNV, 2010b), the PM spectrum formula is given by:

$$S_{PM}(\omega) = \frac{5}{16}.H_s^2.\omega_p^4.\omega^{-5}\exp\left\{-\frac{5}{4}.\left(\frac{\omega}{\omega_P}\right)^{-4}\right\} \tag{5.10}$$

Where:

ω_P = Angular spectral peak frequency = $\frac{2\pi}{T_p}$

JONSWAP Spectrum

This spectrum was developed based on the PM spectrum. A research project called Joint Operation North Sea Wave Project (JONSWAP) analyzed a new model of the spectrum when the wind seas are limited to the fetch area. Although, the wave is never fully developed by the wind seas, the wave continues to develop through non-linear interactions between waves for the long period of time (Stewart, 2008). According to DNV (DNV, 2010b), JONSWAP spectrum is formulated as a result of a modification of the PM spectrum formula as presented in the following equation:

$$S_J(\omega) = A_\omega S_{PM}(\omega).\gamma^{exp\left\{-0.5\left(\frac{\omega-\omega_P}{\sigma.\omega_P}\right)^2\right\}} \quad (5.11)$$

Where:

S_{PM} = Pierson-Moskowitz Spectrum

σ = Spectral width parameters

σ = σ_a for $\omega \leq \omega_p$ (for average value, $\sigma_a = 0.07$)

σ = σ_b for $\omega > \omega_p$ (for average value, $\sigma_a = 0.09$)

A_ω = 1 - 0.287 ln (γ) is a normalizing factor

γ = non-dimensional peak shape parameter

γ = 5 for $\frac{T_p}{\sqrt{H_s}} \leq 3.6$

γ = exp (5.75 – 1.15 $\frac{T_p}{\sqrt{H_s}}$) for $3.6 < \frac{T_p}{\sqrt{H_s}} < 5$

γ = 1 for $5 < \frac{T_p}{\sqrt{H_s}}$

5.3 Currents

The open seas have two main components causing hydrodynamic effects; waves and currents. Therefore, when designing offshore structures, load effects from currents should be considered as important as the wave effects. A real time current data may be obtained during an offshore survey campaign at the specific field location. In case insufficient data of current measurements exists, a hindcasting method may be utilized to predict the effect of wave induced current due to wind or a practical approach by generating current models using hydrodynamic software can be used to generate current models. However, the exact measurement of current data is preferred to represent the actual conditions of the current at a designated area as a representative of the total current effects from wind, tide, ocean current circulation, etc.

The currents are not only generated by the wind, DNV has classified six different ocean currents that are mentioned as the following (DNV, 2010b):

- Wind generated currents, when the currents are developed by wind stress and the atmospheric pressure gradient during a storm.
- Tidal current, this current represent regularly flows in accordance with harmonic astronomical motions of the planet objects (moon and sun). The current determines the elevation of the sea level (i.e. HAT and LAT). Characteristics of this current are weak in deep water but strengthen when the water depth decreases.
- Circulation currents are the steady large scale currents which circulate across the oceans (i.e. Gulf Stream in the Atlantic Ocean).
- Solition currents, the current occurs due to different densities in the wave column.
- Loop eddy currents, the current generates when the solition currents penetrates deeply in the water column.
- Long shore current, this current is a result of wave breaking in coastal regions, and it runs parallel to the shore. The current is also known as littoral current.

The current load is important to consider in design of offshore structures, pipelines or risers. Vortex Induced Vibration (VIV) is, furthermore, one of the main design aspects which are mainly caused by current that passes a structural component (normally of cylinder shape). Certain current flow velocities generate an unsteady flow around the cylinder that can lead to excessive oscillations of slender elements. DNV (DNV, 2010b) concludes about the significant load effects of currents acting on pipeline risers, which are described in the following list.

- Large steady excursions and slow drift motions of floating facilities
- Drag and lift forces on the risers
- The risers' vibrations, which are affected by Vortex Induced Vibration (VIV)
- Vortex Induced Motions (VIM), for large volume structures (i.e. floating facilities)
- Changes in wave height and wave period due to interaction between strong currents and waves
- Seabed scouring which may happen on mounted structures at the seabed.

Current data is generally presented by the velocity (in m/s) which is considered as a steady flow as a function of depth. For design purpose, the total current velocity should be taken as the sum of each current component that is relevant for the particular field environment (i.e. wind generated currents, tidal currents, circulation currents, etc.). If the current measurement data is not available, DNV (DNV, 2010b) suggests that the current profile formula should be a simple power law as a function of depth. The current profile formula is presented in the following equation:

$$v_c(z) = v_{c,wind}(z) + v_{c,tide}(z) + v_{c,circ}(z) + \ldots \quad (5.12)$$

With:

$$v_{c,wind}(z) = v_{c,wind}(0)\left(\frac{d+z}{d}\right)^{\alpha} \quad (5.13)$$

$$v_{c,tide}(z) = v_{c,tide}(0)\left(\frac{d_0+z}{d_0}\right)^{\alpha} \quad (5.14)$$

Where:

$v_c(z)$	=	Total current velocity at level z
z	=	Distance from still water level, positive upwards
$v_{c,wind}(0)$	=	Wind-generated current velocity at the still water level
$v_{c,tide}(0)$	=	Tidal current velocity at the still water level
d	=	Water depth to still water level (taken positive)
d_0	=	Reference depth for wind generated current, d_0 = 50 m
α	=	Exponent (typical = 1/7)

5.4 Floater Motions

In the open sea, a rigid body is always affected by combined actions loads from waves, currents, winds, and the inertia volumes of the rigid body itself. The coordinate system should be determined in order to understand the different motion types of the floating structure. The front end of the floater is the bow (+X) and the other end is called the stern (-X). As one looks toward the front end (bow direction), the starboard side (-Y) is in the right hand side, and the port side (+Y) is the opposite side. Furthermore, the convention has decided to classify motions of the floaters by dividing the motions into three perpendicular translation motions and three rotation motions with respect to the central gravity of the floaters. Figure 5-5 gives an illustration of the coordinate system.

The translation motions of the ship's center of gravity (G) in the directions of x, y and z are presented as follows:

- Surge in the longitudinal positive x-direction motion, which is in line with bow direction.
- Sway in the lateral positive y-direction motion, which is in line with port direction.
- Heave in the vertical positive z-direction motion, which is upwards.

The rotational motions of the ship's center of gravity (G) relatively to x, y and z are presented as follows:

- Roll (ϕ) is motion about the x-axis, positive for the right hand turning
- Pitch (θ) is motion about the y-axis, positive for the right hand turning
- Yaw (ψ) is motion about the z-axis, positive for the right hand turning

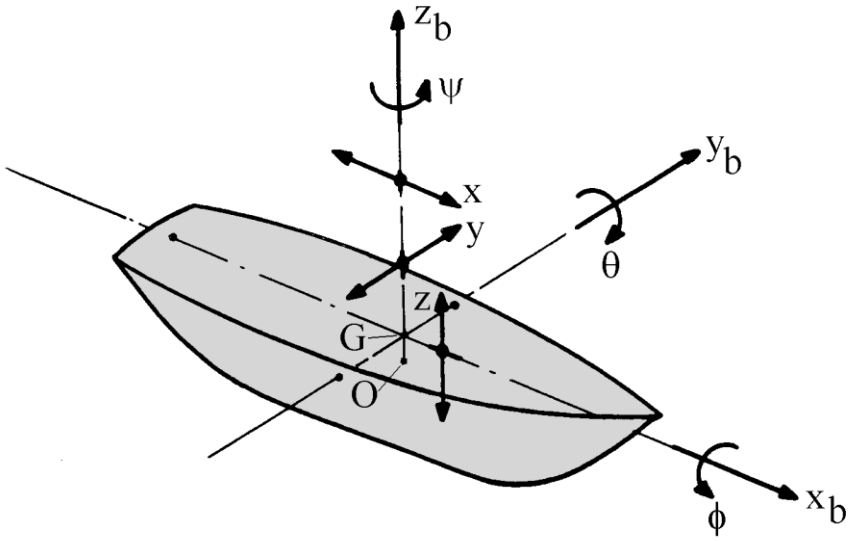

Figure 5-5 Convention of Ship Motion Coordinates. Picture courtesy of (Journee & Massie, 2002)

The loads that affect the floater motions in the open seas are in fact continuous and thus the floater can be analyzed as having a continuum response caused by the external forces. In the steady state condition, the floater motions are defined by a simple motion equation of the three translations and three rotations of the floater's center of gravity. The equations is given as follows (assume that there is no difference in the phase angles).

Surge : $x = x_0 \cos(\omega_0 t)$

Sway : $y = y_0 \cos(\omega_0 t)$

Heave : $z = z_0 \cos(\omega_0 t)$ (5.15)

Roll : $\phi = \phi_0 \cos(\omega_0 t)$

Pitch : $\theta = \theta_0 \cos(\omega_0 t)$

Yaw : $\psi = \psi_0 \cos(\omega_0 t)$

Where:

ω_0 = The frequency characteristic of the floater.

Using the above, it is then possible to calculate the motions in any point on the floater by using the superposition principle, once the motions of the ship's center of gravity is obtained.

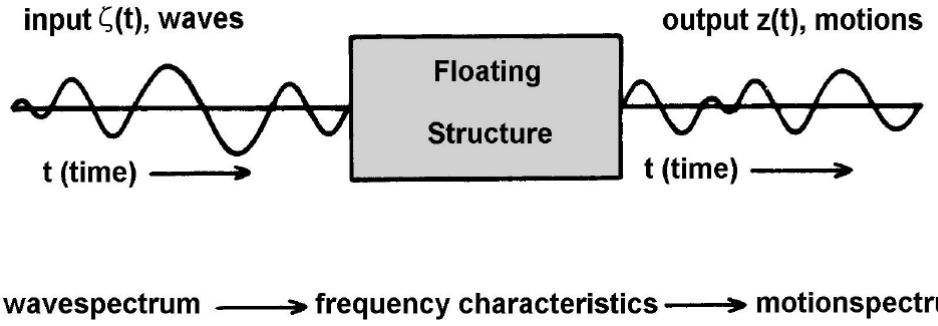

Figure 5-6 Relation between Waves and Floater Motions. Picture courtesy of (Journee & Massie, 2002)

The above figure shows the relationship between wave and floater motions. The diagram, which was established by Journee and Massie, consists of three components; wave input (irregular waves), floating structures, and response motions. The input is random waves which have an energy distribution over the wave frequency that can be formulated by using the wave energy spectrum (refer to Section 5.2.1). The sea waves are acting on the floater which has frequency characteristics that can be found for instances from model experiments or computational modeling. As a result, the output of the system is the motions of the floater. These motions can be described by motion spectrum just as the wave spectrum that causes the motion (Journee & Massie, 2002).

Excessive floater motions may cause a floater offset. Both static and dynamic loadings on the riser are the main sources of the floater offset. The types of floater offset that is considered in the analysis are presented as follows (Nurwanto, 2012):

- Static (nominal) offset: Mean offset due to average wave, wind, and current loads.
- Near offset: the floater is displaced along the plane of the riser towards the riser-seabed connection.
- Far offset: the floater is displaced along the plane of the riser away from the riser-seabed connection.

- Cross offset: the floater is displaced perpendicular to the plane of the riser.

DNV classifies two types of floater motions based on the floater motion periods. The two motion characteristics refer to wave frequency motion which is usually known as Response Amplitude Operator (RAO) and the low frequency motion. The definition of these types of motions is described as follows:

- Wave Frequency (WF) motions: the motions that are a direct consequence of first order wave forces acting on the floater, that may cause the floater moving at periods 3-25 seconds.
- Low Frequency (LF) motion: This motion is a response frequency below the wave frequencies. The response frequency is near surge, sway, and yaw eigen frequencies for the floater (second order wave forces). The LF motion typically has periods in between 30 and 300 seconds.

5.5 Response Amplitude Operator (RAO)

The Response Amplitude operator (RAO) is a dimensionless parameter that can be calculated from the displacement ratio. The RAO is also known as a transfer function which means that the parameter can be used to find the motions characteristic of the floaters (i.e. heave, roll, surge, etc.) from the response to wave forces. The behavior of floaters on the open sea can be calculated by using model tests in the laboratory or through hydrodynamic computational modeling.

Using wave energy spectrum from Equation (5.5), the response spectrum of the floaters, i.e. the heave response can be defined by:

$$S_z(\omega_n).d\omega = \frac{1}{2}{z_a}^2(\omega)$$

$$= \left|\frac{z_a}{\zeta_a}(\omega)\right|^2 . \frac{1}{2}{\zeta_n}^2(\omega)$$

$$= \left|\frac{z_a}{\zeta_a}(\omega)\right|^2 . S_\zeta(\omega_n).d\omega \qquad (5.16)$$

Based on Equation (5.16), the heave response spectrum can be defined as a multiplication of the transfer function (RAO) with the wave energy spectrum.

$$S_z(\omega_n) = \left|\frac{z_a}{\zeta_a}(\omega)\right|^2 . S_\zeta(\omega_n) \qquad (5.17)$$

Where:

$z_a(\omega)$ = Heave amplitude

$\zeta_a(\omega)$ = Wave amplitude

$S_\zeta(\omega)$ = Wave energy spectrum

In general, the natural period of a floating structure can be divided into three categories. Firstly the normal barge that has the largest natural frequency, almost all the wave energy will be transferred into heave motions. In an extreme condition, if an object moves along with the wave displacement then the RAO is equal to 1. Secondly is a ship which has a lower natural frequency than a barge. The amount of wave energy that is converted into response motion is relatively small. And the last is a semi-submersible, which has the smallest natural frequency. The semi-submersible is considered to have excellent motion characteristics, mainly due to small amount of wave energy being transferred to the response motions. Figure 5-7 shows an example of the heave motion characteristics of a container ship as a response to a wave spectrum having significant wave height of 5.0 m and 6.0 s in peak period.

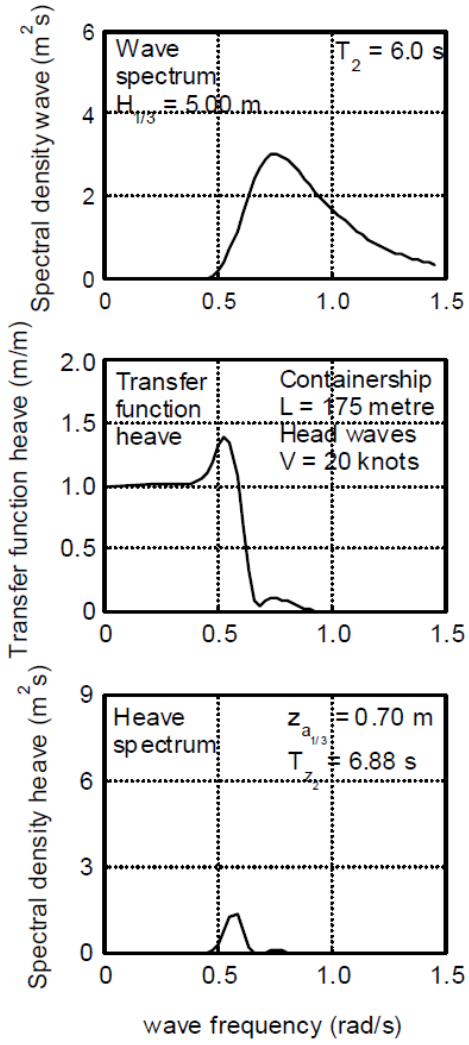

Figure 5-7 Container Ship Heave Responses in the Waves. Picture courtesy of (Journee & Massie, 2002)

5.6 Hydrodynamic Load Effects on a Slender Cylinder

A cylinder is defined as slender when the diameter is relatively small compared to the wave length. The slender cylinder should satisfy the condition $^{D}/_{\lambda} = 0.2$ where D is cylinder diameter and λ is wave length. This condition is satisfied for small diameter cylinders i.e. riser pipes as the main component of concern in this thesis. Furthermore, when the member length is much larger than the diameter of the member, the end-effects can be neglected and thus the total force acting on the cylinder can be calculated as the sum of forces on each cross section (DNV, 2010b).

The wave load effects on the riser can be calculated by the Morison's load equation which consists of two components; an inertia force and a drag force. The inertia term is related to Newton's second law where forces result from accelerations. While the experiments shown that the drag term is proportional to the wave velocity. DNV has proposed suitable Morison's equations for the slender cylinder in normal direction and tangential direction to the wave (DNV, 2010a).

$$f_n = \frac{1}{2}\rho C_D^n D_h |v_n - \dot{r}_n| + \rho \frac{\pi D_b^2}{4} C_M^n \dot{v}_n - \rho \frac{\pi D_b^2}{4}(C_M^n - 1)\ddot{r}_n \tag{5.18}$$

$$f_t = \frac{1}{2}\rho C_D^t D_h |v_t - \dot{r}_t| + \rho \frac{\pi D_b^2}{4} C_M^t \dot{v}_t - \rho \frac{\pi D_b^2}{4}(C_M^t - 1)\ddot{r}_t \tag{5.19}$$

Where:

f_n	=	Force per unit length in normal direction
f_t	=	Force per unit length in tangential direction
ρ	=	Water density
D_b	=	Buoyancy diameter (i.e. equivalent diameter for description of resulting buoyancy on a general riser cross section)
D_h	=	Hydrodynamic diameter
$v_n, \dot{v}_n$	=	Fluid velocity and acceleration in normal direction
$\dot{r}_n, \ddot{r}_n$	=	Structural velocity and acceleration in normal direction
C_D^n, C_M^n	=	Drag and inertia coefficients in normal direction
$v_t, \dot{v}_t$	=	Fluid velocity and acceleration in tangential direction
C_t^n, C_t^n	=	Drag and inertia coefficients in tangential direction

The drag and inertia coefficients in Equations (5.18) and (5.19) can be defined according to several parameters that are listed below.

- Body shape
- Reynolds number Re= UD/v, where U is the free stream velocity, D is the diameter and v is the kinematic viscosity
- Keulegan Carpenter number KC = $U_M T/D$, where UM is the free stream velocity amplitude of the oscillatory flow and T is the period of oscillatory flow and T is the period of oscillation
- The Roughness ratio k/D, where k is the characteristic dimension of the roughness on the body
- Reduced velocity U/f_nD, where f_n us the natural frequency of the riser
- Relative current number Uc/U_M, where Uc is the current velocity and U_M is the velocity of the oscillatory motion.

DNV suggests that an appropriate approach to determine the coefficients based on experimental results. The value of Inertia and Drag coefficients on three-dimensional objects for steady flow can be found in to DNV RP C-205 Appendix D and Appendix E, respectively (DNV, 2010b).

5.7 Soil-Riser Interactions

The catenary riser configuration may suffer critical fatigue loadings and bending moments in the touch down area of the riser with the soils at the seafloor. In-plane loads will probably occur due to heave motions of the floater, while out-plane motions may be caused by lateral loads from currents as well as waves. In case of repetition loads on the risers, modeling of soil properties should be as precise as possible to represent the actual condition of the soils in order to obtain accurate prediction of fatigue damage. A sensitivity study is required to identify uncertainty parameters (i.e. soil properties) for fatigue analysis in the touch down area. The pipe-soil interaction is commonly specified as a linear spring (elastic soil stiffness) (Bai & Bai, 2010). However, in this thesis, the soil is modeled by using the friction coefficient (sliding resistance).

6. Design Basis

6.1 Introduction

The purpose of this chapter is to provide design data and methodology that is applicable for the analysis of uncoupled riser configurations. It has been decided that two types of selected uncouple risers will be analyzed in respect of riser performances during operating conditions. The aim of this research project has therefore been to compare and study a field proven technology and a new development technology of uncoupled risers in terms of robustness in the deep water field. SLOR as the field proven uncoupled riser configuration has widely been installed in several oil field locations and has achieved a tremendous success. However, the major problem of this configuration is an expensive cost of the bottom assembly. Due mainly to this problem, COBRA is developed as a new uncoupled riser configuration that is to be proven in the field to provide a solution and avoid the expensive bottom assembly.

A finite element method is utilized in the computer modeling for this thesis. The method is able to handle non-linear effects from large deformations and deflections of slender structures from the original shape. The reader shall refer to Chapter 5 for the detail information of theoretical backgrounds that is relevant for this thesis work (i.e. waves, currents, floatation motions, etc.). In practice, the analysis model will be presented in the Orcflex Software (Version 9.7a), a marine dynamic program developed by Orcina Inc. which has capacity to perform static and dynamic analysis of risers (Orcina, 2013).

6.2 Analysis Methodology

According to Chapter 4, the structural design of risers should be based on the Limit Resistance Factor Design (LRFD) as defined in DNV-OS-F201 (DNV, 2010a). All riser components shall be designed with higher safety than the acceptable design limitations, which will ensure that the riser can withstand and operate as intended across the production period of the oil and gas fields. Moreover, the riser shall also be designed in a manner such that it has a down time period as low as possible.

In the operating conditions, the risers should satisfy minimum design requirement of global strength analysis and time domain fatigue analysis. The additional requirements may apply for a specific condition, for instance, during maximum floater drift offset, minimum geometry of a disconnected riser in case of iceberg approach, etc. In that case, the additional requirements are given in Chapter 8.

The major objective in performing the global strength analysis is to determine the overall structural characteristics of the riser configurations. Furthermore, throughout the analysis, the riser system may be confirmed safe to operate, and the structural components are adequately designed in accordance to the appropriate loading effects from static as well as dynamic loadings.

To gain better understanding of loading effects on the risers, DNV discusses the relevant global response quantities as an output result from global riser analysis. Based on that, the

structural responses are divided into four categories (DNV, 2010a), which are specified as follow:

- Cross-sectional forces, e.g. effective tension, bending moments, torsional moment
- Global riser deflections, e.g. curvature, elongation, angular orientation
- Global riser position, e.g. co-ordinates, translations, clearance, TDP position, etc.
- Support forces at termination to rigid structures (reaction force and moments)

Generally, the global strength analysis consists of two stages; static analysis and dynamic analysis. The main difference between these two analyses is indicated in the behavior of the loading that affect the risers. The static analysis only applies a maximum load value as static loadings. Meanwhile, the dynamic analysis applies a load that is varied in time as an addition to the static loading.

6.2.1 Static Analysis

A static analysis is always performed prior to the global analysis. This analysis is required to define the starting point for the further analysis such as the dynamic analysis. The main aim of this analysis is to assess the static loadings on each riser component and establish the equilibrium for the riser configurations. The static loading that applies on the riser can be derived from the volume forces on riser pipes and the designated external forces.

The static equilibrium for riser pipes in the water is affected by the weights of the riser, the hydrostatic loadings (hydrostatic pressure and buoyancy), and the fluid contents. According to Barltop (Baltrop, 1998), the static equilibrium calculation can be simplified based on the effective tension and the effective weight. Figure 6-1 shows the equilibrium conditions of a curved pipe under the volume forces. Based on that, the formula for the effective tension and the effective weight can be expressed by:

$$W_{eff} = \gamma_s A_s + \gamma_i A_i - \gamma_o A_o \quad (6.1)$$

$$T_{eff} = T_i + P_o A_0 - P_i A_i - \rho_i U_i^2 A_i \quad (6.2)$$

Where:

γ	=	Weight density
A	=	Area
P	=	Pressure
ρ	=	Mass density

U	=	Flow velocity
i	=	Subscripts for ‘internal’
o	=	Subscripts for ‘external’
s	=	Subscripts for ‘structural’

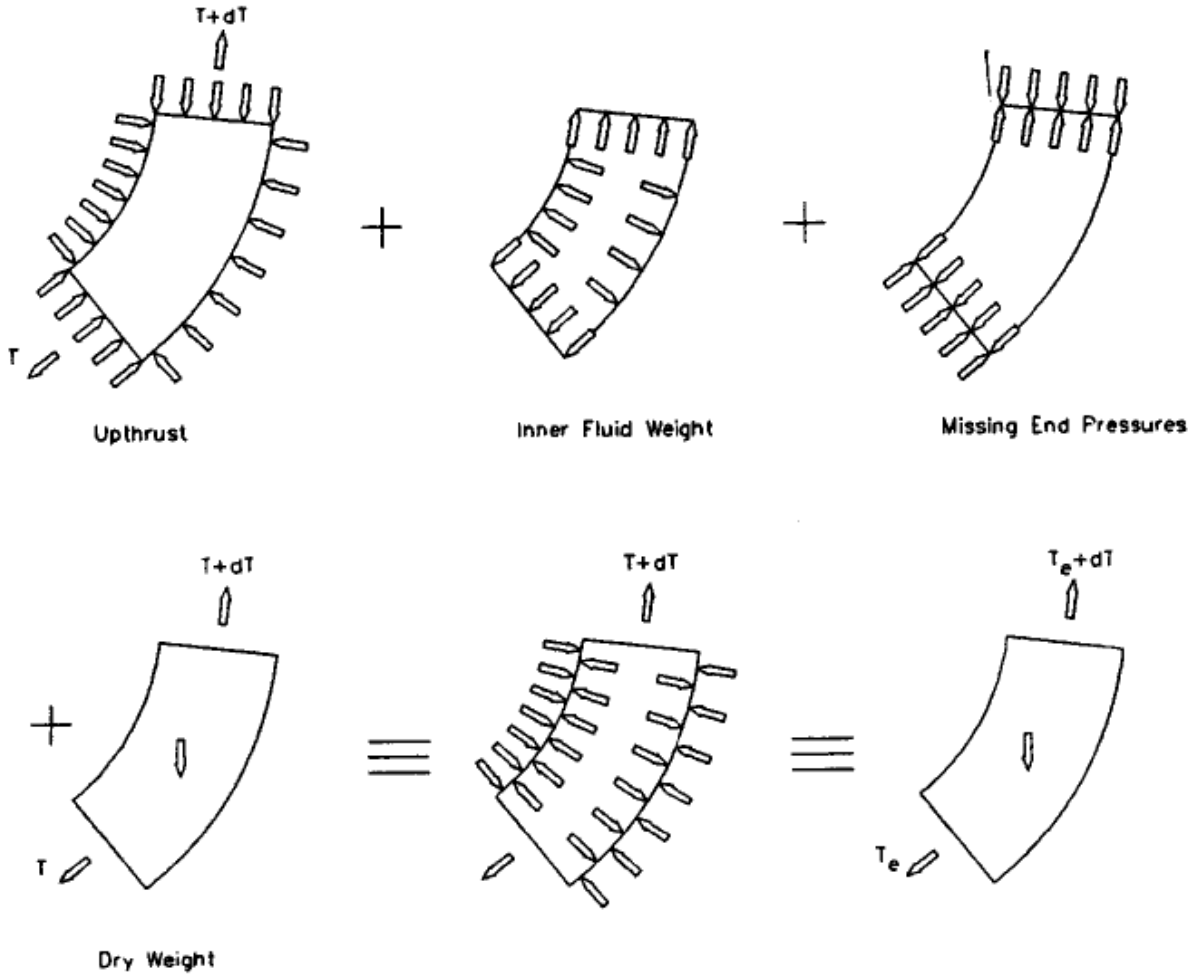

Figure 6-1 Static Equilibrium of Risers. Picture courtesy of (Baltrop, 1998)

The riser’s equilibrium is certainly affected by the size of external forces. The possible static external forces acting on the riser are tensioner forces, pulling forces and current forces. These forces act on the riser according to the design stages, for instance; tensioner forces and pulling forces are the forces that only exist in the installation stage. Therefore, this thesis only considers the current forces for the static loading which is applicable during the operating conditions. The total current forces on the risers may be compared to the effective tension forces in order to identify the current effects, whether it has significant impact on the risers or not.

6.2.2 Dynamic Analysis

The global dynamic analysis is mainly performed based on the wave frequency (WF) floater motion and direct waves as an addition to current loadings. The WF floater motions are represented by RAOs (the vessel's transfer functions). In addition, for this thesis, the low frequency (LF) floater motions are implemented as fixed floater offsets (i.e. static offset, near offset, far offset, and cross offset) as the floater does not dynamically responds to LF floater motions. Otherwise, DNV suggest the combination of WF and LF floater motions should be considered in the analysis if the floater is sensitive to LF excitation (DNV, 2010a).

The first step of a dynamic analysis is to calculate the natural frequency of the riser pipes in different mode shapes. The natural frequency, or also called the 'eigen frequency', is important to investigate in order to avoid resonance effects. Once the 'eigen frequency' of the risers has similar value as the vortex sheading frequency excessive vibrations of the riser may occur. If there is no assessment to prevent the resonances, the cyclic load due to pipe vibrations may lead to fatigue damage on the pipe structures.

The combination of floater, riser and mooring system creates a complex dynamic system response. Furthermore, the interaction between riser configurations and environmental loadings produce nonlinearities in the riser system. To deal with these problems, the dynamic finite element (FE) method is commonly used to describe the nonlinearities by using frequency domain analysis and time domain analysis as follows:

- Frequency Domain Analysis, the analysis assumes that stiffness, damping, inertia and external forces have linear behavior at static equilibrium conditions. A stochastic linearization is also required for combining irregular wave and current analysis. According to Chapter 5.2.1, the irregular wave analysis in frequency domain will always give a gaussian distribution in the response spectrum and therefore is not recommended to use frequency domain analysis for extreme conditions (DNV, 2010a).

- Nonlinear Time Domain Analysis, the analysis is using Newton-Rapshon method for step by step numerical integration of the incremental dynamic equations. This analysis has a nonlinear approach which will give sufficient result for all nonlinear effects. Consequently, there is a possibility to have a non-gausian response by this analysis method (DNV, 2010a).

6.3 Design Parameters

6.3.1 Environmental Data

Water Depth

Three water depths have been selected for the comparison study in this thesis work, which are 400m, 1000m and 1500m with a constant sea water density of 1025 kg/m^3.

Waves

The wave data that is used for this thesis is considered as a typical environmental condition in the Norwegian Sea. The data is collected with 3 hours sample intervals in between the period of 1958 and 2008.

A number of researchers have reported that the Norwegian Sea is considered as fetch limited area, thus the modified JOSWAP spectrum is the most suitable spectrum to model the irregular waves. Table 6-1 shows the maximum value of annual significant wave height data (H_s) with corresponding wave spectral peak period (T_p). The data is presented for an annual probability exceedance of 10^{-1} (10-year) and 10^{-2} (100-year).

Table 6-1 Wave data

Wave Characteristics	10-year data	100-year data
Significant wave height, H_s (m)	14.6	17.0
Corresponding spectral wave peak period, T_p (s)	17.5	18.8

For Ultimate Limit Stress (ULS) conditions, the annual probability exceedance of 10^{-2} shall be used in design of risers.

Current

The current data follows a typical current profile in the Norwegian Sea in accordance with Norsok N-003. For modeling purpose, the current load direction is assumed to be parallel with the riser's lay direction to obtain the worst case scenario for static loadings. The most extreme current speed for all directions is presented in Table 6-2 as function of depth. The duration of the extreme event is 10 minutes with an annual probability exceedance of 10^{-1} (10-year) and 10^{-2} (100-year).

Table 6-2 Current Profiles

No	Water Depth (m)	10-year data (cm/s)	100-year data (cm/s)
1	10	165	185
2	50	126	140

No	Water Depth (m)	10-year data (cm/s)	100-year data (cm/s)
3	100	125	140
4	200	109	120
5	300	83	90
6	400	74	80
7	500	73	80
8	600	60	65
9	800	60	65
10	1000	55	60
11	1200	55	60
12	3m above sea bottom	46	50

According to DNV standard, the riser design in ULS conditions should use the current profile with the annual probability of 10^{-2} (DNV, 2010a). The extreme current profile in 1500 m water depth that is used for the design is the presented in Figure 6-2.

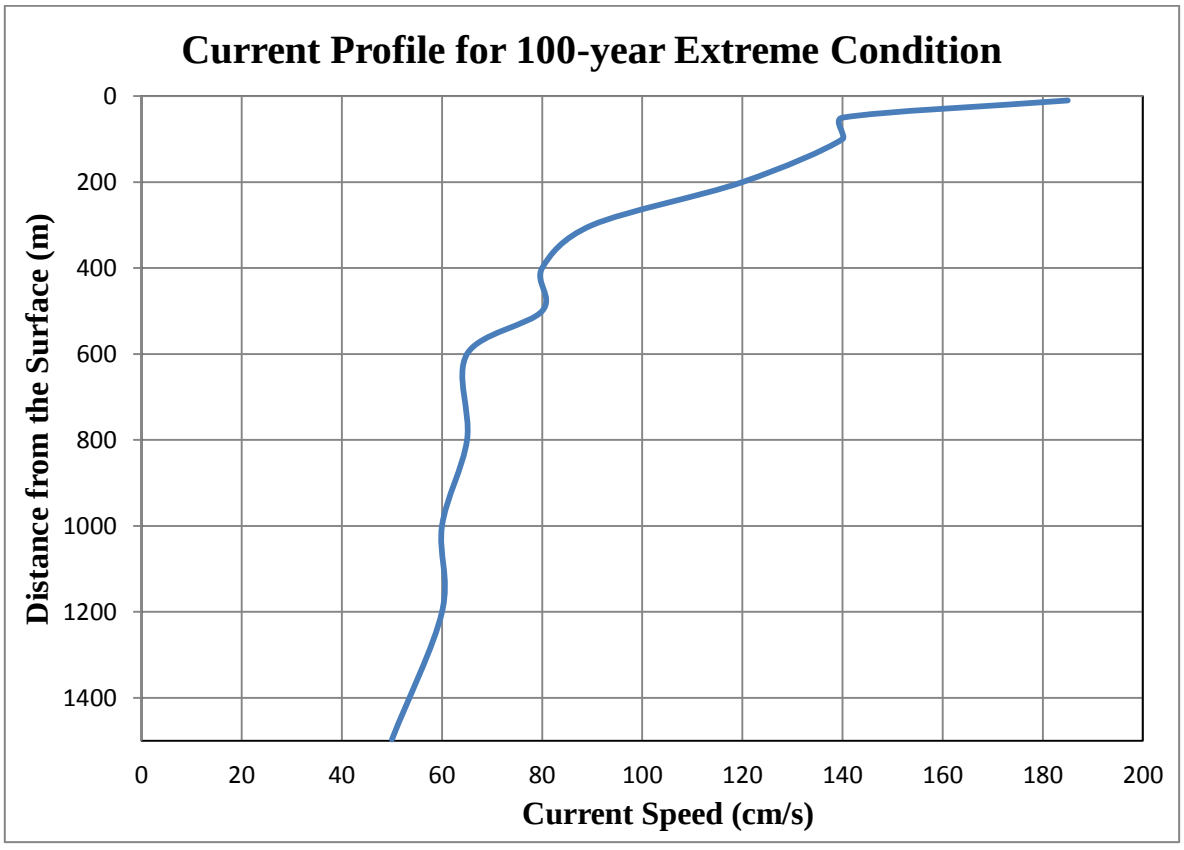

Figure 6-2 Current Profile with Annual Probability of 10^{-2}

Marine Growth

Norsok N-003 suggests taking into account a marine growth factor for all submerged structures. It has been specified in the standard that the mass density of marine growths in air as 13000 N/m^3 (NORSOK, 2007). If scheduled maintenance to clean the submerged structures is not planned, the marine growth thickness may be taken according to Table 6-3. The thickness of marine growths is assumed to be constant surrounding the pipe surface and the water depth is measured from mean water level.

Table 6-3 Thickness of Marine Growth (NORSOK, 2007)

Water Depth (m)	Marine Growth Thickness (mm)
+2 to -40	60
Under -40 up to -300	30

In this thesis work, the marine growth is only applicable for the flexible jumper. In the upper section, a 60mm marine growth thickness is applied until the elevation -40 m, then a 30 mm marine growth thickness is considered up to elevation -300 m for the middle section, and in the last section, the flexible jumper is considered free from the marine growth. For the steel riser, the surface coating prevents the attachment of marine growth on the pipe. Moreover, the steel riser elevation is maintained below -300 m of water depths, thus the marine growth thickness criterion is not applicable for the steel riser.

Hydrodynamic Coefficients

In order to obtain accurate hydrodynamic load effects on the riser pipes, the hydrodynamic coefficient shall be appropriately chosen according to several parameters that are listed in Section 5.6. The hydrodynamic coefficients that have been utilized in this thesis work are presented in Table 6-4.

Table 6-4 Hydrodynamic coefficients

Coefficient Types	Flexible Jumper	Steel Riser
Drag Coefficient, CD	0.80	1.10
Added Mass Coefficient, CM	1.00	1.00

The hydrodynamic forces in normal direction may be neglected due to the slender cylinder has relatively small diameter compared to the length of pipes.

Soil-riser interaction

As mentioned in the previous chapter, the soil-riser interactions are modeled as sliding resistance by specifying friction coefficients of the soils. Following soil parameters have been used for this thesis work.

- Lateral friction Coefficient : 0.50
- Axial friction Coefficient : 0.30
- Horizontal lateral/axial soil stiffness : 200 kN/m^2
- Vertical soil stiffness : 50 kN/m^2

6.3.2 Vessel Data

A ship-shaped FPSO vessel is used as surface facility in this thesis. The riser is tied back to the FPSO throughout an internal turret system. A default response amplitude operator (RAO) from the Orcaflex software is used to represent motion characteristics of the FPSO. The selected RAO is considered as the most conservative transfer function which has been modeled for FPSOs up to date.

For the purpose of analysis, a fixed offset is applied to model the low frequency (LF) motions. Table 6-5 shows three different positions which are considered in the analysis, for instances; normal position, near offset position, far offset position. The offset is considerably low due mainly to a taut mooring is deployed for the FPSO anchor system. If the catenary mooring configuration is used, the distance of vessel offsets need to be kept below 8% of water depths (Seymour, Zhang, & Wibner, 2003).

Table 6-5 Vessel Offset

Type Analysis		Vessel Offset (m)
Static Analysis	Near Position	- 80
	Normal Position	0
	Far Position	+ 80
Dynamic Analysis	Near Position	- 80
	Normal Position	0
	Far Position	+ 80

6.3.3 Riser and Flexible Jumper Data

Based on the process design basis, a 10” inner diameter pipe is required to transport hydrocarbon fluids from the sea bed to the surface facility during operational conditions. This minimum inside diameter is recommended for the steel risers as well as the flexible jumper. For the flexible jumper, the limitations of allowable tension and minimum bending radius shall be carefully evaluated. Moreover, for steel risers, the minimum required wall thickness should be designed according to DNV-OS-F201 (DNV, 2010a) and DNV-OS-F101 (DNV, 2013). The wall thickness calculations check can be found in Appendix A.

The design basis of the flexible jumper and the riser are presented in Tables 6-6 and 6-7, respectively.

Table 6-6 Flexible Jumper Data

Parameter	Value	Unit
Design Pressure	500	bar
Content Density (Oil)	8000	kg/m^3
Internal Diameter	254	mm
Outside Diameter	424	mm
Mass Density	4640	kg/m^3
Minimum Bending Radius (MBR)	5000	mm

Table 6-7 Steel Riser Data

Parameter	Value	Unit
Riser material is Carbon Steel, Grade X65		
Design Pressure	500	bar
Content Density (Oil)	800	kg/m^3
Internal Diameter	254	mm
Outside Diameter	306	mm
Young Modulus	207000	MPa
Thickness Protective Coating	76.2	mm
Density of The Coating	700	kg/m^3
Safety Class	Consider High	
Corrosion Allowance	3	mm

In order to prevent excessive stress concentration in the connection point, the steel riser has to be equipped with a 10 m tapered stress joint section with maximum wall thickness of 2.5". As mention earlier, this section has high specification requirements to accommodate long term fatigue loading and high bending loads. The tapered stress joint is located at the bottom connection point of the buoyancy module and an additional stress joint for the SLOR is located on the top of the offtake spool at the foundation assembly.

6.3.4 Content Loads

The content load should be considered to accommodate the weight of the hydrocarbon fluids in the pipes. The fluid is assumed as oil base with density of 800 kg/m^3 with corresponding internal design pressure of 500 Bar.

6.3.5 Buoyancy Module Data

Drawing on an extensive range of sources, the usage of a subsurface buoy in the uncoupled riser configurations is very important to decouple the floater motions. The buoyancy module is required to provide an intermediate connection point between the flexible jumper and the steel riser. Therefore, the buoyancy module should be properly designed during the engineering design stages. In this thesis, two types of buoyancy module are prepared according to the buoyancy requirements for each riser configuration.

In general, the buoyancy module is encompassed of a long slender cylinder with a number of compartments and bulkheads as a separator. Table 6-8 provides data for the buoyancy module for the SLOR and the COBRA concepts.

Table 6-8 Buoyancy Module Data

Parameter (unit)	SLOR	COBRA
Outer Diameter (m)	7.0	7.0
Length (m)	20.0	18.0
Weight in air (kN)	2321.04	2088.93
Displacement (kN)	7736.78	6963.11
Weight in water (kN)	-5415.75	-4874.17

A sensitivity study is performed to achieve the ideal configuration of buoyancy module geometries by locating the buoyancy module in different positions at sufficient water depth away from the wave zone. The optimum design of the buoyancy modules can be achieved by designing a module that has minimum buoyancy forces.

6.3.6 Mooring Line Data for COBRA

The buoyancy module in the COBRA configuration has to be tethered down to the seabed. According to Karunakaran & Baarholm (Karunakaran & Baarholm, 2013), two mooring lines are required to maintain the buoyancy module in the designated position. The mooring line is connected underneath the buoyancy module to the anchor point at the seabed. To optimize the moorings functionality, the mooring line should be maintained as straight as possible in which clearance between the mooring lines has to be equal on both connection points; at the anchor point and the buoy point.

The mooring line properties are provided in Table 6-9.

Table 6-9 Mooring Line Data

Parameter	Value	Unit
Outer Diameter	135	mm
Mass in air	13	kg/m
Axial Stiffness	400	MN
Torsional Stiffness	80	$kN.m^2$

6.4 Model Overview

The thesis uses the Orcaflex software to model the riser in a 3D finite element model as well as to simulate the hydrodynamic effects on the riser according to the environmental design conditions. The buoyancy module is modeled as a 6D buoy element which is a rigid body with 6 degrees of freedom (3 translational and 3 rotational). The risers (steel and flexible jumper) and the anchor moorings are modeled as line elements. Each line element can be divided into a number of equal segments which is made up of two co-axial telescoping rods and connected by axial and torsional springs + dampers (Orcina, 2013). Moreover, a FPSO vessel model is used as a surface facility where the riser is tied back. The FPSO has motion characteristics (RAO) that are taken from a typical motion characteristic of an Orcaflex's Vessel.

The riser configurations consist of three main elements; a flexible jumper, a buoyancy module, and a steel riser. The flexible jumper is connected to the bottom of the turret which is located in the FPSO at elevation -18.5 m below the mean sea level (MSL). Another end of the flexible jumper is hanging on the upper part of a buoyancy module. The last section of the riser is the steel riser. The steel riser is connected at the bottom part of the buoyancy module to the seabed. Two different configurations of steel risers are studied in this thesis, which are the top tensioned riser for a SLOR configuration, and the catenary riser for a COBRA configuration. In addition, the COBRA configuration has one set of mooring lines which is attached from the bottom parts of the buoyancy module and tethered down to the sea bed.

In the initial condition of the SLOR and COBRA riser configurations, the buoyancy module is located at a water depth of 300 m with horizontal offset of 350 m from the center line of the vessel. The riser's lay direction is arranged in conjunction with wave and current directions in order to obtain the worst load combination scenario which will affect the riser configurations. Two sets of riser arrangements are modeled and located in opposite direction. By using this arrangement, the riser components could be checked and controlled in one Orcaflex's model due to vessel offset. Figure 6-3 and Figure 6-4 present the initial condition of the riser configuration for SLOR and COBRA respectively.

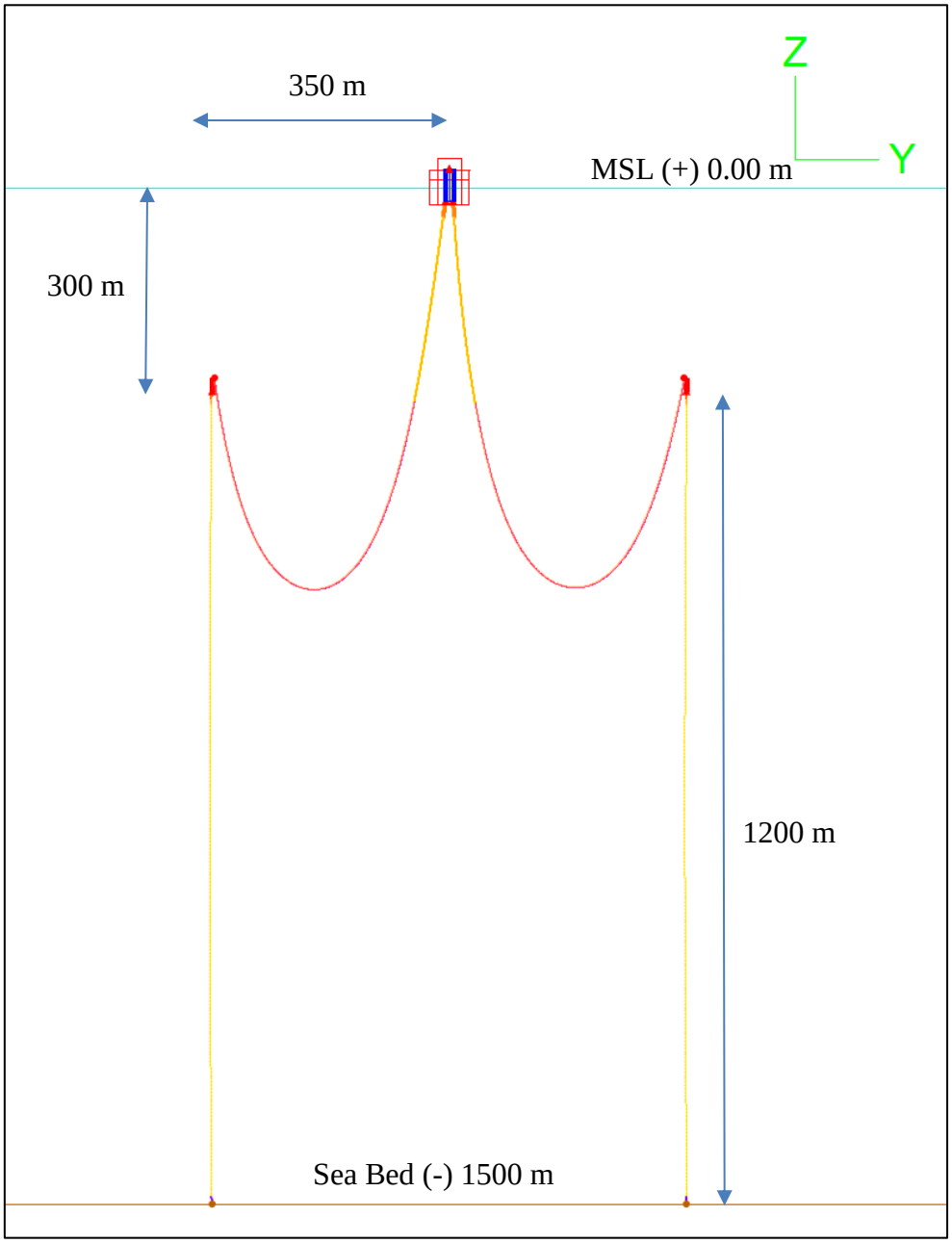

Figure 6-3 Initial Static Condition of the SLOR Configuration

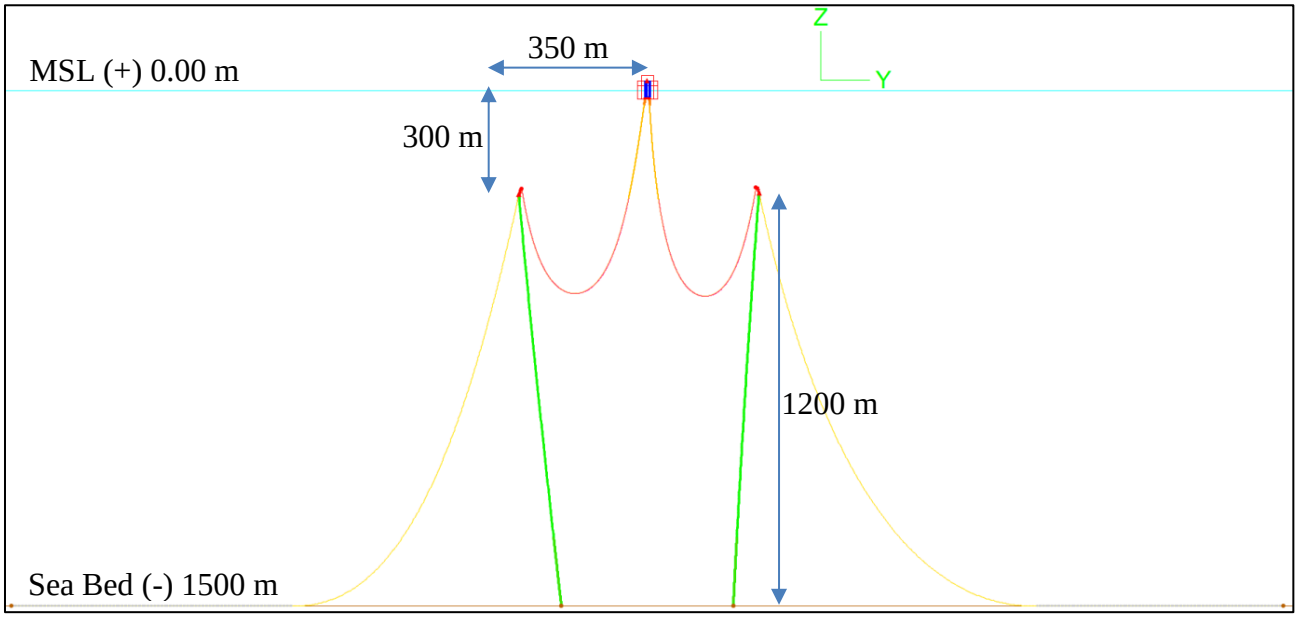

Figure 6-4 Initial Static Condition of the COBRA Configuration

6.5 Analysis Concept

The thesis work consists of two study parts; base case study and accidental study due to iceberg approach. For the base case study, three different water depths are selected in order to observe the effects of hydrodynamic forces on the riser configurations. The risers shall be designed to comply with the requirement of the ultimate limit state (ULS). The ULS analysis is considering the combination of hydrodynamic forces due to wave frequency (WF) motion and fixed vessel offsets due to low frequency (LF) motion. The detail analysis result is presented in Chapter 7.

The purpose of the accidental study is to check the riser performances in the event of an iceberg approach in accordance with the accidental limit state (ALS). The main concern of this thesis is to examine the ability of the uncoupled riser configurations to avoid the iceberg collision by implementing the vessel's drift off from the initial position. Bearing that in mind, the riser initial configurations for this study are prepared to accommodate the possibility that the vessel may drift off to all directions. Two different water depths are selected to examine the maximum distance of a vessel could drift off during the accidental event. Based on earlier chapter, two solutions have been considered to avoid iceberg collision, either by using drift off or a disconnectable turret. Chapter 8 presents the proposed solution in case of an iceberg approach and the results of this analysis.

The work diagram for this thesis is presented in Figure 6-5.

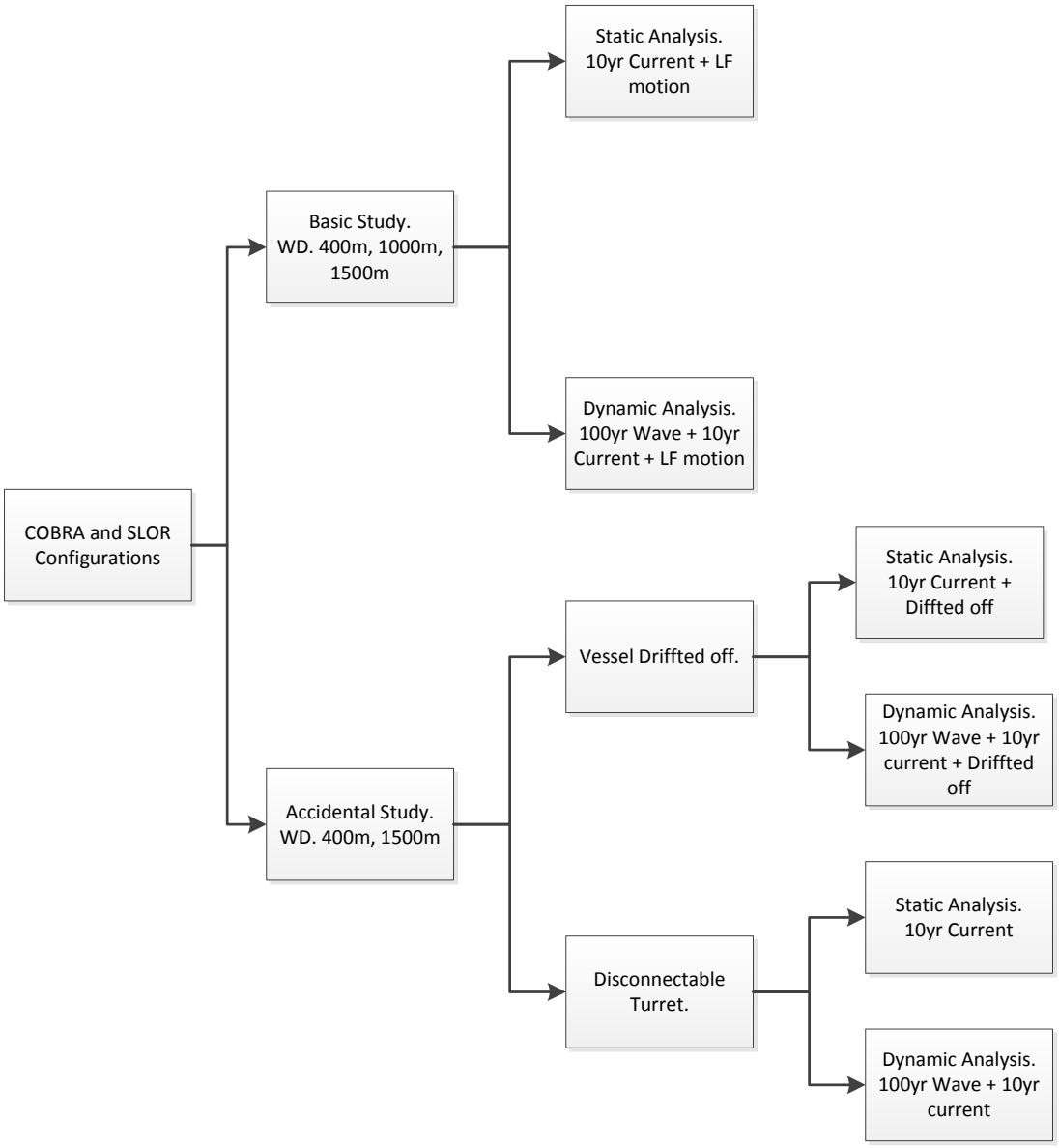

Figure 6-5 Thesis Work Diagram

6.6 Acceptance Criteria

The analysis result shall be checked and compared to a specific limitation given in design codes and specifications that are used during the design stages. The limitations shall encompass different aspects from the riser design criteria up to the vessel capacity. By fulfilling the design limitations, the riser configurations could meet the design requirement and operate as intended during operating conditions. The following paragraphs refer to the acceptance criteria that should be considered for this thesis.

Flexible Jumper

- Minimum Bending Radius (MBR)

  The bending load is critical for a flexible jumper pipe since this pipes is categorizes as a long slender cylinder. 'Minimum Bending Radius (MBR)' of pipes refers to the minimum radius that pipe can be bended without damaging the pipe's structure. The bending capacity is related to the mechanical properties of the pipes. The flexible jumper has very low bending radius that is achieved by composite wall construction made of a number of spiral laid steel and thermoplastic layers with high stiffness.

  In this thesis, MBR of the flexible jumper is given as 5 m. The bending radius of a flexible jumper should not less than the specified MBR's value for all design conditions. Normally, the MBR's value can be found in the product specifications that are issued by the manufacturer of flexible jumpers.

- Compression Load

  In the conservative approach, the flexible jumpers shall remain in tension at all the times. Thus, no compression load is permissible on flexible jumpers.

Vessel

- Departure Angle of a Flexible Jumper

  The minimum horizontal load on the 'riser guide tube' can be achieved by limiting the departure angle of the flexible jumpers on the vessel. The departure angle is measured relative to the vertical axis. In this thesis, the departure angle of flexible jumpers shall not exceed 12.5 degrees.

Steel Riser

- Buckling Utilization Factor

  According to the design requirement, the maximum buckling utilization factor shall be less than 1.0 for every limit state design (ULS and ALS).

7. COBRA and SLOR Analysis

7.1 Introduction

In Chapter 7 the results of the base case study for COBRA and SLOR configurations in three different water depths are reported. As described in Chapter 5, ultimate limit strength analysis is performed on the riser configuration based on ultimate limit state (ULS) requirements. The analysis of the risers is divided into two categories; static analysis and dynamic analysis. The static analysis is firstly performed to establish the static equilibrium of the riser configurations and is followed by the dynamic analysis that is used to simulate the motions of the vessel for different wave frequencies (WF). The design parameters and design limitations are mainly referred to in DNV OS F201(DNV, 2010a).

This chapter consists of three main analyses; steel riser wall thickness analysis, static response analysis (ULS), and dynamic response analysis (ULS). Prior to commencing the global analysis, the riser wall thickness should be calculated to obtain the minimum required wall thickness. The calculation check for wall thickness design is presented in Section 7.2. In order to obtain the structure's equilibrium, the static response analysis shall be performed as a first step prior to the global analysis. The result of the static analysis is presented in Section 7.4. After obtaining the static equilibrium, the risers proceed to the dynamic response analysis, and Section 7.5 will present the summary results of the dynamic response of the riser configurations. To summarize, Section 7.6 presents the discussion for COBRA and SLOR analysis for the base case conditions.

7.2 Wall Thickness Design

The minimum required wall thickness is determined in accordance with ultimate limit state (ULS) design. The riser pipe design shall be designed to satisfy the design conditions as mentioned in Section 4.4.1. All pipes cross sections shall adequately resist net internal over-pressure from fluid contents and operating pressure. In addition to that, the pipe is designed to withstand the net external overpressure from hydrostatic pressure. The pipes may also be designed to satisfy minimum wall thickness requirements to resist buckling propagation. The appropriate parameters shall be selected according to DNV OS F201 (DNV, 2010a), such as load effect factors, safety class resistance factor and material resistance factor which are listed in Table 4-3, Table 4-4 and Table 4-5 respectively.

Based on the process design basis, an internal pipe diameter of 10 inches is required to transport hydrocarbon fluids from the sea-bed to the surface facility. In this thesis, the carbon steel material grade X65 is used for the steel riser. The riser holds content with 800 kg/m3 content density and with a 500 bar design pressure. For conservative design, a maximum water depth of 1500 m is used to calculate hydrostatic pressure on the pipe. To check the adequacy of wall thickness, the steel pipe is designed according to DNV OS F201 (DNV, 2010a) and DNV OS F101 (DNV, 2013). Table 7-1 provides the unity check results for the 306 mm OD x 26 mm WT steel pipe in 1500 m water depth.

Table 7-1 Unity Check Factor for 306 mm OD x 26 mm WT Steel Pipes in 1500 m Water Depth

Burst (Operating Condition)	Burst (Test Condition)	Collapse	Propagating Buckling
0.78	0.62	0.46	0.78

Table 7-1 presents the results obtained from the calculation of minimum wall thickness that is required for the uncoupled riser configuration. From the results in the table above, it is clearly seen that the unity check (UC) values for all load conditions are less than 1, which indicates that 26 mm WT of pipes is adequate to resist the internal and external net overpressures. In addition, the pipe wall thickness is sufficient to avoid propagating buckling along the pipes.

Detailed calculations of wall thickness design are presented in Appendix A.

7.3 ULS Analysis Cases

This chapter mainly focuses on the strength analysis of the SLOR and COBRA configurations. The risers are compared and studied in three different water depths (i.e. 400 m, 1000 m, and 1500 m) to examine the effect of hydrodynamic forces on the risers. According to ULS criteria two types of vessel motions (i.e. low frequency motions and wave frequency motions) shall be considered in the analysis. Therefore, an 80 m offset is applied to accommodate the low frequency (LF) motions on the vessel. The environmental loads of 100-year waves and 10-year currents are considered as the worst load combination case that shall be used for environmental loading analysis of the risers.

Table 7-2 presents 18 load cases that have to be checked for ultimate limit state (ULS) analysis of the SLOR and COBRA configurations.

Table 7-2 ULS Analysis Cases

Load Comb No	Riser Configuration	Water Depth	Environmental Condition	Vessel Offset
1	SLOR	400	100-year waves + 10-year currents	Near Offset, Waves + Currents.
2				Near Offset, Waves + Currents.
3				Near Offset, Waves + Currents.
4		1000		Near Offset, Waves + Currents.
5				Near Offset, Waves + Currents.
6				Near Offset, Waves + Currents.
7		1500		Near Offset, Waves + Currents.
8				Near Offset, Waves + Currents.
9				Near Offset, Waves + Currents.
10	COBRA	400	100-year waves + 10-year currents	Near Offset, Waves + Currents.
11				Near Offset, Waves + Currents.
12				Near Offset, Waves + Currents.
13		1000		Near Offset, Waves + Currents.
14				Near Offset, Waves + Currents.
15				Near Offset, Waves + Currents.
16		1500		Near Offset, Waves + Currents.
17				Near Offset, Waves + Currents.
18				Far Offset, Waves + Currents.

7.4 Static Response (ULS)

The initial static equilibrium should be achieved by the riser configurations prior to proceeding to the dynamic analysis. The riser's equilibrium for the static response can be obtained by applying the static loadings for instance; riser's self-weight, fluid contents, hydrostatic loads, buoyancy effects, and current loads. In order to accommodate three different water depths, the different riser configurations are established to best suit a particular

environmental condition. Section 7.4 presents the initial static equilibrium riser configurations for the three different water depths.

SLOR Configurations

The riser is configured by a flexible jumper, a buoyancy module and a steel riser. In the SLOR configuration, the steel riser section is arranged as a top tensioned riser. The steel riser has three section in total, which comprise two sections of the 10 m tapered stress joints that are located at the bottom of the buoyancy module and on top of the foundation assembly, and in between, a steel riser with material grade X56 is fitted as the longest section.

The SLOR configurations have a distinct arrangement for each water depth. For the intact condition in the 1000 m and 1500 m water depth cases, the buoyancy module is located at 300 m water depth and shifted 350 m from the centerline of the vessel. Meanwhile, in the 400 m water depth, the buoyancy module is located at 200 m water depth and shifted 200 m from the centerline of the vessel. The SLOR configuration is arranged to accommodate the minimum departure angle on the vessel and the minimum flexible jumper length to limit the minimum bending radius (MBR) as described in Section 6.6.

The general arrangement of the SLOR configurations for three different water depths in intact condition is presented in Table 7-3.

Table 7-3 SLOR Configuration in Intact Condition

Parameters	Water Depth		
	400 m	1000 m	1500 m
Flexible jumper length (m)	575	950	1000
Steel riser length (m)	200	700	1200
Buoyancy location (m)[1]	200	300	300
Buoyancy shift (m)[2]	200	350	350

Notes:
[1)] Location is measured from a vertical distance relative to MSL.
[2)] Shifting is measured from a horizontal distance relative to the centerline of the vessel.

As shown in the table above, the flexible jumper length is adjusted to obtain maximum floater offset and minimum departure angle at the vessel. Moreover, the steel riser length is set according to the buoyancy location.

COBRA Configurations

The COBRA riser configurations consist of a flexible jumper, a buoyancy module, a steel riser and two mooring lines. Only one tapered stress joint is utilized for the COBRA configurations, which is located at the bottom of the buoyancy module. According to Section

7.3, this riser configuration is also analyzed for three different water depths. To compare with the SLOR configurations, the COBRA configurations are constructed with identical arrangement for each water depth, except the steel riser configurations. In the COBRA configurations, the steel riser sections are arranged as steel catenary risers.

The general arrangements of the COBRA configurations for three different water depths in intact condition are presented in Table 7-4.

Table 7-4 COBRA Configuration in Intact Condition

Parameters	Water Depth		
	400 m	1000 m	1500 m
Flexible jumper length (m)	575	950	1000
Steel riser length (m)	470	1520	2270
Buoyancy location (m)[1]	200	300	300
Buoyancy shift (m)[2]	200	350	350
Mooring length (m)[3]	200	700	1200

Notes:
[1)] Location is measured from a vertical distance relative to MSL.
[2)] Shifting is measured from a horizontal distance relative to the centerline of the vessel.
[3)] Mooring length is measured for each line.

As presented in Table 7-4, an identical uncoupled riser arrangement, which is used for the SLOR configuration, is established for the COBRA configuration. The steel riser section is arranged as a steel catenary riser in such a way that minimum tension is achieved at the connection to the buoyancy module. Therefore, the length of the steel riser varies based on vertical distance between the buoyancy modules and the seabed.

In general, for the COBRA configurations, the steel riser has two main sections which comprise 10 m of tapered stress joint, located on the bottom of the buoyancy module, and a steel riser with material grade X56, which is installed for the rest of the section. As mentioned in Section 2.3.2, two mooring lines are tethered down to the seabed in order to maintain the buoyancy module in the designated position. The mooring lines shall be maintained as straight (vertical) as possible with the minimum tension working on those lines. As a consequence, the mooring length is determined in accordance with the buoyancy location.

In the following sections, the comparison of SLOR and COBRA configuration results is presented for three different water depths. For each section, the flexible jumper, and steel riser are compared to identify the most suitable uncoupled riser configuration in accordance with the design acceptance criteria (refer to Section 6.6). In addition, Section 7.4.4 presents the mooring line results for the COBRA configuration.

7.4.1 Uncoupled Riser Configurations in Water Depth of 400 m

This section presents the results of the static response analysis for the SLOR and the COBRA configurations in 400 m water depth. According to Section 7.4, the riser arrangements for SLOR and COBRA in intact conditions are shown in Figure 7-1 and Figure 7-2 respectively.

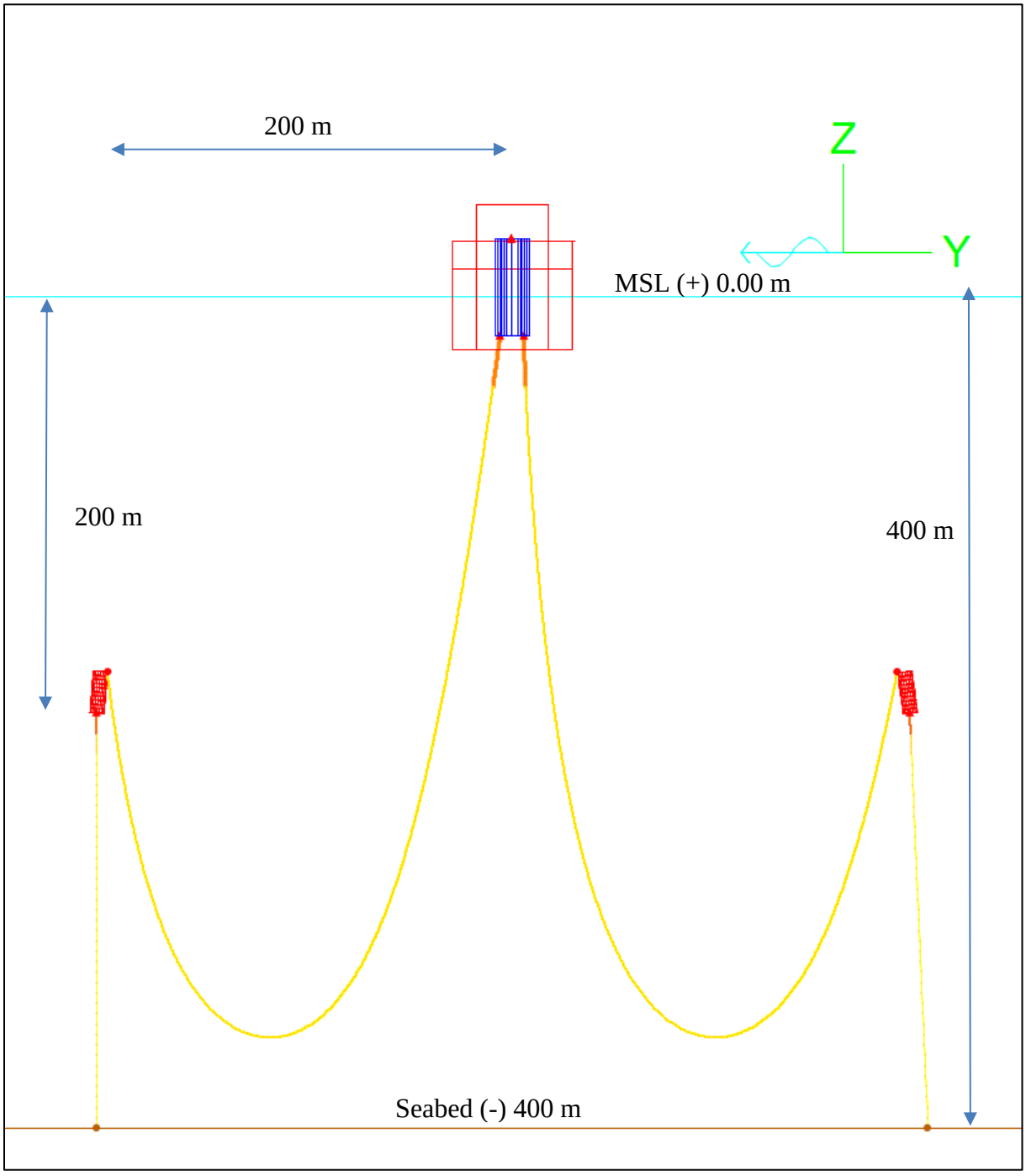

Figure 7-1 SLOR Arrangement at 400 m Water Depth

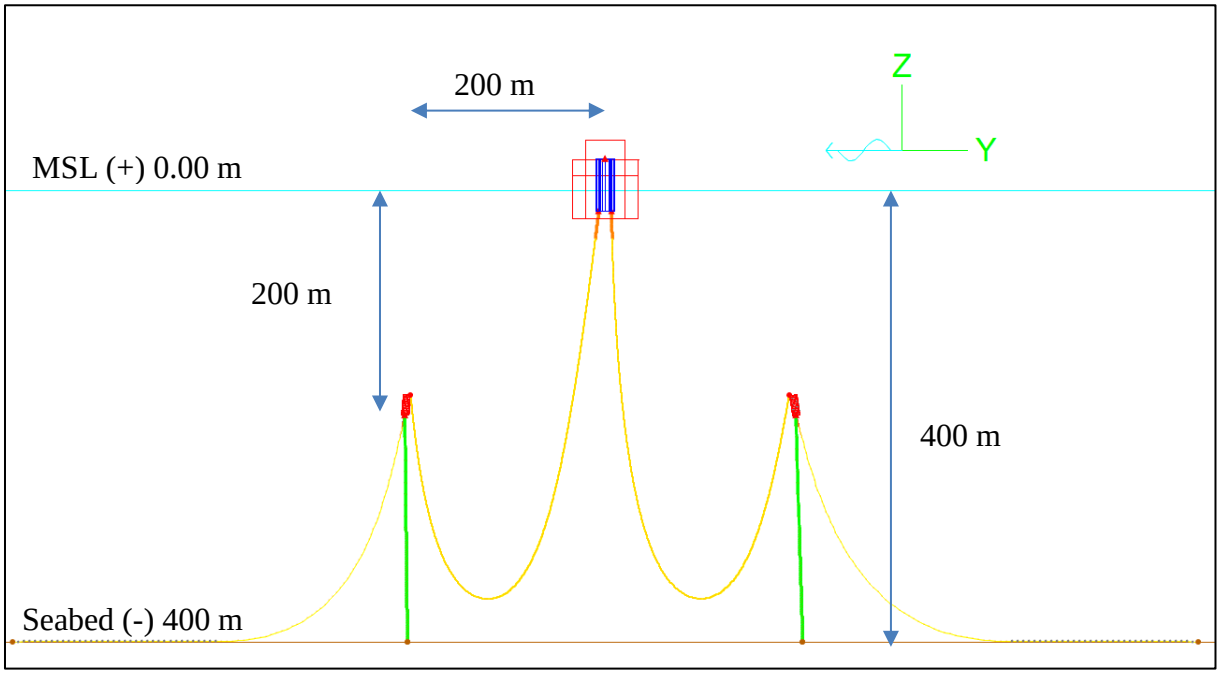

Figure 7-2 COBRA Arrangement at 400 m Water Depth

Flexible Jumper

The flexible jumper is used to connect the steel riser section from the buoyancy module to the surface facility. For the riser arrangements in 400 m water depth, the buoyancy module is located in a water depth of 200 m. To be conservative, the marine growth effect is applied to all cross sections of the flexible jumper based on Table 6-3. According to marine growth effects, the flexible jumper is divided into two sections; for the first section (to 40 m water depth) a 60 mm thickness of marine growth is used, and a 30 mm thickness of marine growth is applied for the last section. In order to maintain the departure angle at less than 12.5^0, 575 m length of flexible jumpers is installed in this configuration.

The design limitation for the flexible jumper is the requirement to maintain the jumper in the tensioned condition at all time. Table 7-5 presents the results of static responses for the uncoupled riser configurations in 400 m water depth with 80 m vessel offset.

Table 7-5 Static Response on Flexible Jumper (400 m WD)

Parameter	COBRA			SLOR		
	Near Y	Intact	Far Y	Near Y	Intact	Far Y
Angle at vessel (deg)[1]	1.29	7.02	10.24	0.72	7.87	11.32
Angle at buoy (deg)[1]	5.27	9.48	11.75	6.35	6.99	13.99
Maximum tension at vessel (kN)	1193.72	1198.46	1205.53	1192.81	1199.05	1208.75
Maximum tension at buoy (kN)	664.76	669.00	675.91	667.38	673.05	682.53
Minimum bending radius (m)	11.58	27.38	48.41	15.54	33.14	56.51

Note:

[1)] The angle is measured relative to the vertical axis.

The results in Table 7-5 show that for the flexible jumper the design limitations under the static loads are satisfied. This can be seen as no compression load occurs along the flexible jumpers. A minimum bending radius of 11.58 m in the COBRA configuration is found at the near vessel position which is acceptable according to the acceptance criteria (refer to Section 6.6). Furthermore, the angle value corresponds with the tension value; a higher angle value results in higher tension loads. This is applicable for the connections both at the vessel as well as at the buoy. In consequence, the tension load shall be carefully controlled because the tension load at the vessel may affect the hang-off capacity of the turrets, while at the buoyancy module, a high tension load on the flexible jumper connection will increase the bending moment on the steel riser which is located at the bottom part of the buoyancy module.

Preliminary results conclude that the tension load on the COBRA's flexible jumper is slightly lower compared to the SLOR's jumper. The maximum departure angle on the vessel is also slightly lower in the COBRA configuration compared to SLOR, which creates a lower tension load on the jumper and a lower horizontal load on the 'riser guide tube'.

Steel Riser

In the uncoupled riser configurations, the steel riser is attached from the bottom parts of the buoyancy module to the seabed. The tapered stress joint is installed on the steel riser sections in order to reduce high bending load. The steel riser is also completed with an external insulation which is applied on the riser to prevent the attachment of marine growth.

Two different steel riser arrangements are used in this thesis; the catenary arrangement for the COBRA configurations and the top-tensioned arrangement for the SLOR configurations. In the COBRA configurations, the steel riser is hanging from the bottom part of the buoyancy module and layback in sufficient distance. The layback distance is measured from the buoyancy module position to the touchdown point. As the water depth increases, at longer layback distance is required to accommodate the higher tension load on the riser.

For the SLOR configurations, the steel riser is constructed in such a manner that the riser shall be maintained in a straight position. To achieve that position, the steel riser is tensioned from the top by utilizing a massive buoyancy module. Consequently, the greatest amount of buoyancy force is required to straighten the steel riser for the SLOR configurations. Due to this concern, the required buoyancy force for the SLOR configurations is relatively larger than that of the COBRA configurations. Thus, the buoyancy module's dimension for the SLOR configurations is relatively bigger than the COBRA configurations as can be seen in Table 6-8.

Table 7-6 presents the static response on the steel risers for both configurations. It is expected that the maximum tension of the steel risers in the SLOR configurations is much greater than in the COBRA configurations.

Table 7-6 Static Response on Steel Risers (400 m WD)

Parameter	COBRA			SLOR		
	Near Y	Intact	Far Y	Near Y	Intact	Far Y
Angle at buoy (deg)[1]	3.47	2.45	1.87	1.56	2.21	1.32
Maximum tension at buoy (kN)	311.39	317.42	271.87	4748.43	4754.73	4761.20
Minimum tension at seabed (kN)	71.76	21.38	30.07	4533.36	4516.12	4522.63

Note:

[1)] The angle is measured relative to the buoy.

It can be seen in Table 7-6 that a maximum angle at the buoy of 3.47^0 in the COBRA configurations is found during the near vessel conditions. The results of tension loads in the steel risers agree with the expectation, in which the SLOR configurations have greater tension forces compared to the COBRA configurations. The maximum tension force observed at the buoy is 4761.20 kN in the SLOR figurations during the far vessel position. Interestingly, the tension forces for the SLOR configuration remain constant in all vessel conditions. Therefore, in respect of the tension forces, the vessel offset may not have a significant impact on the steel riser behavior.

In accordance with the present results, it is concluded that the behavior of steel risers is completely different for each configuration. Moreover, the results of this study indicate that current loads may have significant impact on the steel risers compared to the low frequency (LF) vessel motions.

7.4.2 Uncoupled Riser Configurations in Water Depth of 1000 m

This section discusses the results of the static response for the SLOR and the COBRA configurations in 1000 m water depth. As described in Section 7.4, the initial riser arrangements for SLOR and COBRA in 1000 m water depth are presented in Figure 7-3 and Figure 7-4 respectively.

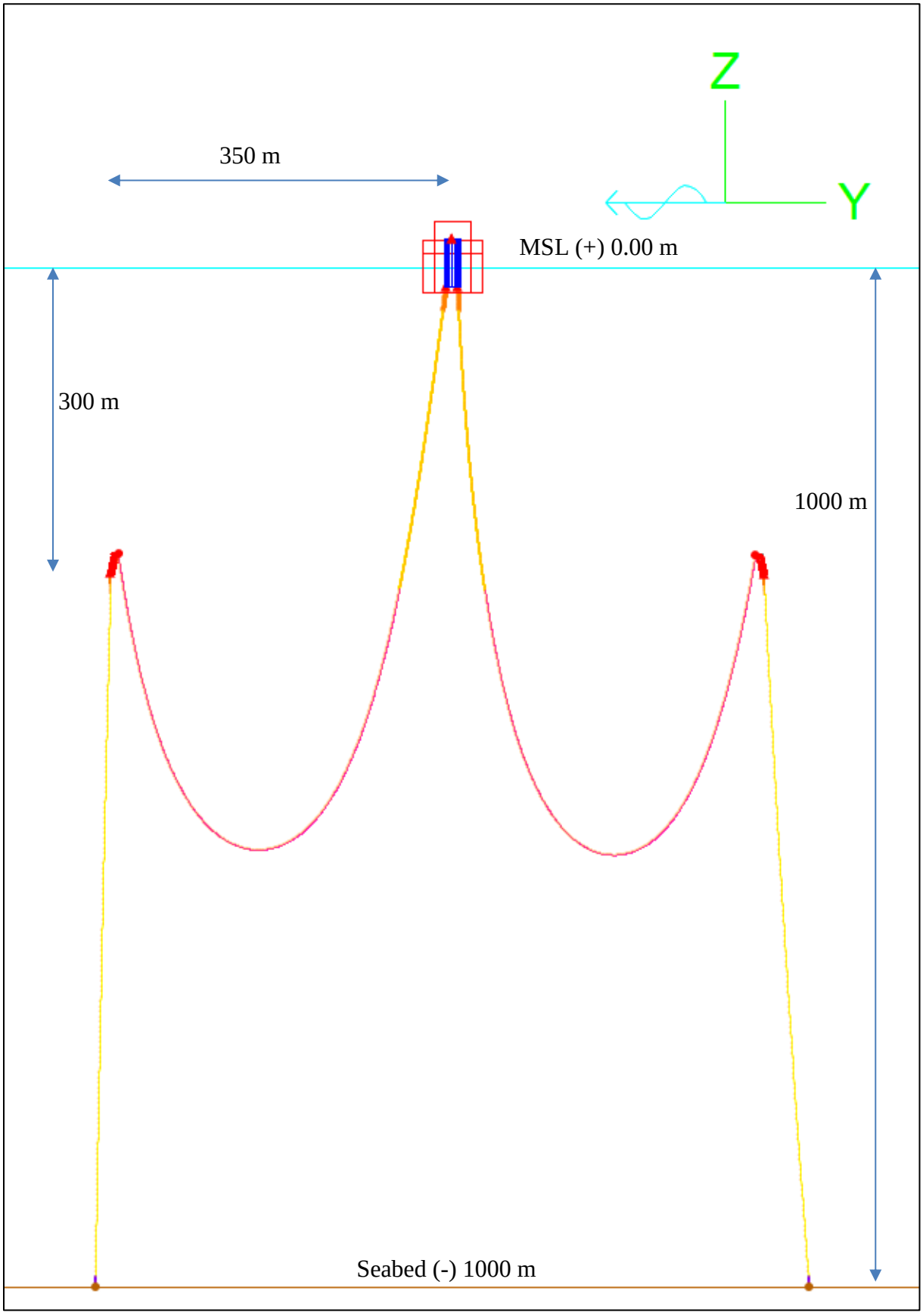

Figure 7-3 SLOR Arrangement at 1000 m Water Depth

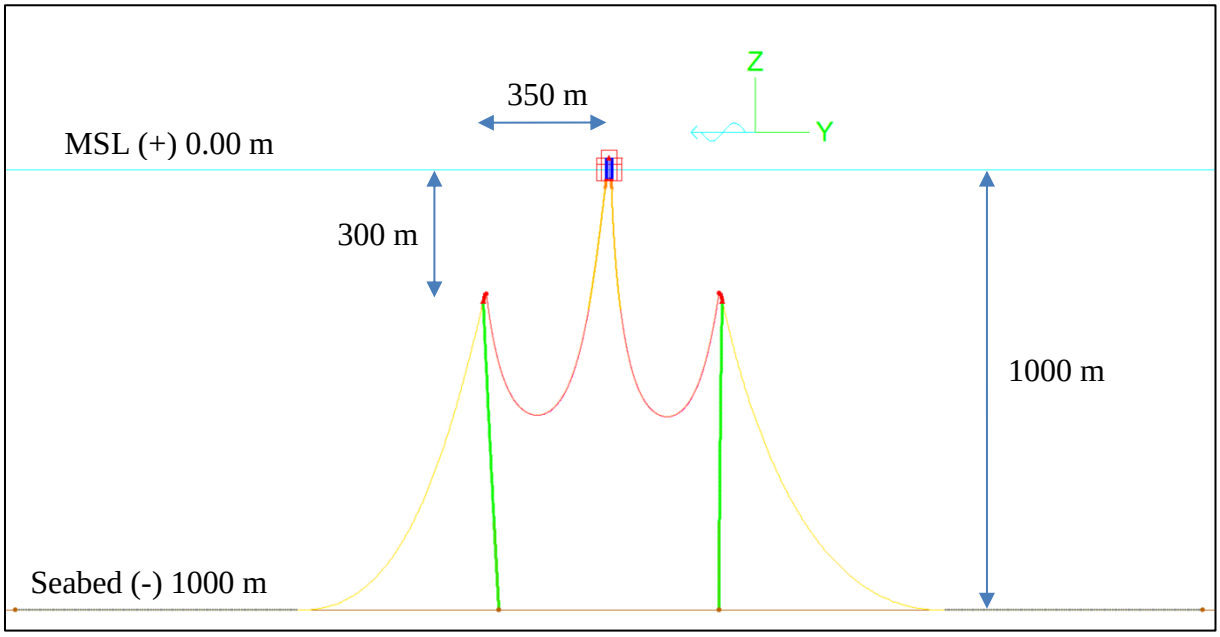

Figure 7-4 COBRA Arrangement at 1000 m Water Depth

Flexible Jumper

The uncoupled riser arrangements in 1000 m water depth are described in Table 7-3 and Table 7-4. According to Section 6.3.1, the marine growth effects should be applied to the flexible jumpers up to water depth of 300 m. By these means, the flexible jumper has to be divided into three different sections; for the first section, a 60 mm thickness of marine growths is considered up to 40 m water depth, then a 30 mm thickness of marine growth is considered for the second section up to 300 m water depth and finally, no marine growth should be applied for the last section, which has a water depth greater than 300 m.

The minimum design for the flexible jumper shall comply with the acceptance criteria which are described in Section 6.6. To maintain the departure angle at less than 12.5^0, the flexible jumper shall be installed with the minimum length of 950 m. Table 7-7 compares the results of static responses between the SLOR and the COBRA configurations in 1000 m water depth with 80 m vessel offset.

Table 7-7 Static Response on Flexible Jumpers (1000 m WD)

Parameter	COBRA			SLOR		
	Near Y	Intact	Far Y	Near Y	Intact	Far Y
Angle at vessel (deg)[1]	0.13	6.66	8.46	1.00	7.45	9.29
Angle at buoy (deg)[1]	5.89	8.62	10.51	7.07	9.81	11.82
Maximum tension at vessel (kN)	1843.79	1848.31	1855.08	1925.24	1931.94	1938.75
Maximum tension at buoy (kN)	990.80	995.19	1000.83	1068.41	1073.10	1082.45
Minimum bending radius (m)	25.85	41.72	64.51	35.35	52.48	77.26

Note:

[1)] The angle is measured relative to the vertical axis.

The results in Table 7-7 show that there is no compression load on the flexible jumper. An acceptable minimum bending radius of 28.85 m is observed in the COBRA configurations in the near vessel position. Moreover, a maximum departure angle of 9.29^0 in the SLOR configurations indicates that the riser arrangements are feasible for static conditions. In general, the behavior of flexible jumpers is mainly affected by the vessel offset which is also recognized in riser configuration for 400 m WD (refer to Section 7.4.1).

In comparison, the COBRA configurations have slightly better results than the SLOR configurations in terms of tension loads and departure angles. The departure angle on the vessel for the COBRA configuration is generally lower than that of the SLOR, which creates a lower tension load on the jumper and a lower horizontal load on the 'riser guide tube'. Although the minimum bending radius is found critical in the COBRA configuration, the value is far above acceptable limit (refer to Section 6.6). There are similarities between the present results and those described in Section 7.4.1.

Steel Riser

The steel risers of the SLOR and the COBRA configurations in 1000 m WD are similar to the riser arrangements that are used in the riser configurations of 400 m WD (refer to Section 7.4.1). The steel sections and materials in the SLOR and the COBRA configurations are arranged in accordance with Section 7.4. Due to these arrangements, the SLOR configurations tend to have a larger amount of tension force than the COBRA configurations. The static responses identified in these riser configurations are summarized in Table 7-8.

Table 7-8 Static Response on Steel Risers (1000 m WD)

Parameter	COBRA			SLOR		
	Near Y	Intact	Far Y	Near Y	Intact	Far Y
Angle at buoy (deg)[1]	4.14	3.41	1.86	2.17	2.83	2.49
Maximum Tension at buoy(kN)	1069.36	1085.52	992.90	4352.11	4360.88	4367.58
Minimum Tension at Seabed (kN)	251.98	267.47	178.68	3537.28	3545.17	3577.41

Note:

[1)] The angle is measured relative to the buoy.

As shown in Table 7-8, the maximum angle observed at the buoy for the COBRA configurations is 4.14^0 in the near vessel condition. In the COBRA configurations, the maximum angle at the buoy increases when the distance from the vessel to the buoyancy module decreases. These results seem possible due to the fact that the highest vertical forces on the jumper are produced in the near vessel position. These forces will pull the buoyancy modules towards horizontal positions.

Form Table 7-8, we can also see that the tension forces in the SLOR configurations are generally greater than in the steel risers of the COBRA configurations. For each riser configuration, the tension forces in the steel risers remain constant, with the tension force for the COBRA configurations being approximately 105 MT and for the SLOR configurations,

approximately 444 MT. This demonstrates that the vessel offset does not have a significant impact on the steel riser arrangements. The present findings seem to be consistent with the result of the steel riser responses for the risers' configuration in 400 m water depth.

These results are consistent with those of riser configurations for 400 m water depth. These findings, while preliminary, suggest that low frequency (LF) motions do not significantly affect the steel riser behavior for both uncoupled riser configurations. This is mainly due to the usage of the buoyancy module which has decoupled the effects of vessel offsets.

7.4.3 Uncoupled Riser Configurations in Water Depth of 1500 m

In this section, the static response for the SLOR and the COBRA configurations in 1500 m water depth is presented. The detailed riser arrangements data for SLOR and COBRA can be found in Section 7.4. Figure 7-5 and Figure 7-6 show the riser arrangements in intact condition for the COBRA and the SLOR configurations respectively.

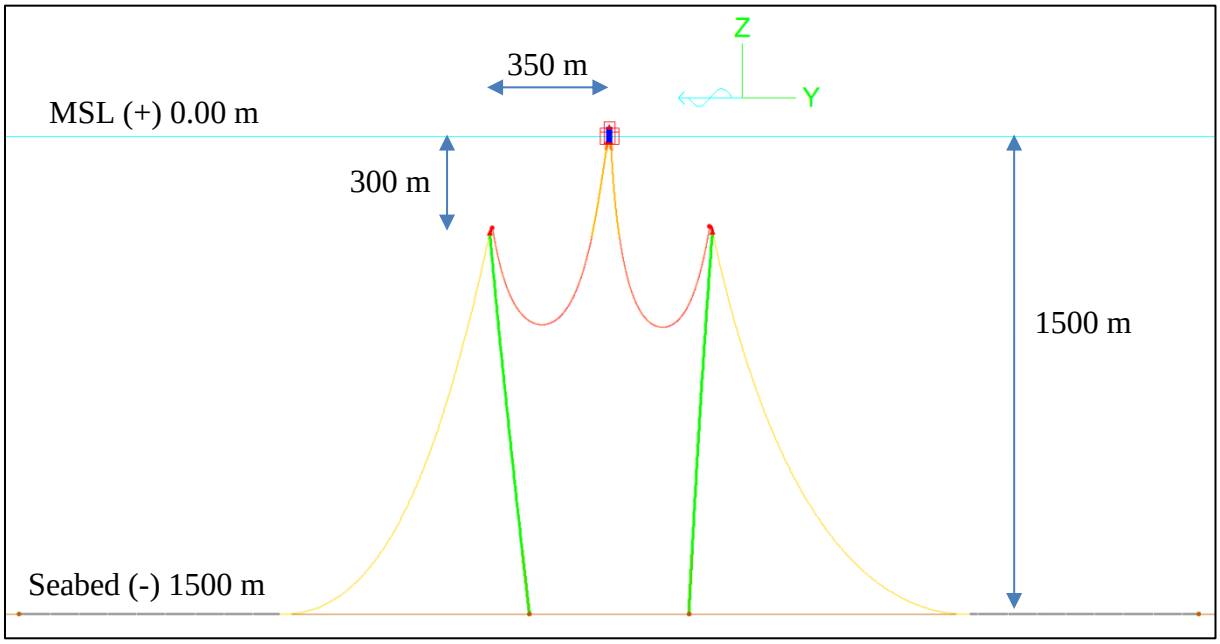

Figure 7-5 COBRA Arrangement at 1500 m Water Depth

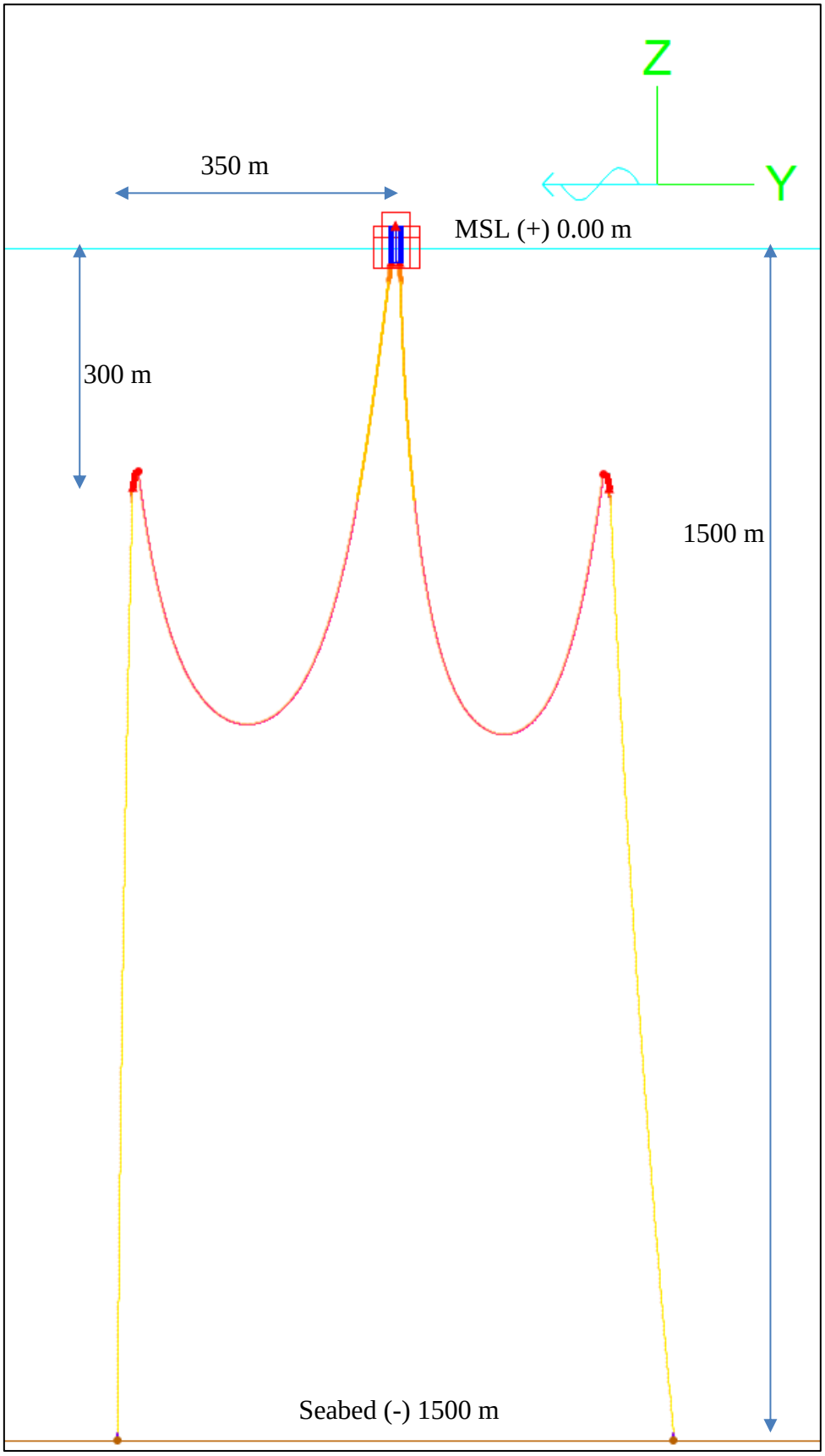

Figure 7-6 SLOR Arrangement at 1500 m Water Depth

Flexible Jumper

The flexible jumpers in 1500 m water depth are 1000 m in length. Each flexible jumper has three sections which are divided according to marine growth effects (refer to Section 6.3.1). The division of the flexible jumpers is similar to that of the flexible jumpers that are used in 1000 m water depth. As described in Section 7.4.2, the first section is used to consider a 60 mm thickness of marine growth up to 40 m water depth, then a 30 mm thickness of marine growth is considered for the second section up to water depth of 300 m and, finally, no marine growth shall be applied for the last section which has water depth greater than 300 m.

Table 7-9 provides the summary results of static responses for uncoupled riser configurations in 1500 m water depth by considering an 80 m vessel offset.

Table 7-9 Static Response on Flexible Jumpers (1500 m WD)

Parameter	COBRA			SLOR		
	Near Y	Intact	Far Y	Near Y	Intact	Far Y
Angle at vessel (deg)[1]	1.27	7.98	9.66	0.24	6.98	8.46
Angle at buoy (deg)[1]	7.24	9.69	12.33	5.57	7.68	9.98
Maximum tension at vessel (kN)	2006.11	2017.76	2025.21	2002.25	2007.44	2012.32
Maximum tension at buoy (kN)	1143.85	1145.78	1157.41	1142.19	1144.23	1155.76
Minimum bending radius (m)	39.14	55.60	85.65	28.03	42.07	71.08

Note:

[1)] The angle is measured relative to the vertical axis.

The results in Table 7-9 show that a maximum departure angle of 9.66^0 in the COBRA configurations is observed during the far vessel position. In accordance with the maximum departure angle, a maximum tension at the vessel of 2025.21 kN is also observed in COBRA configuration during the far vessel position. In addition, the minimum bending radius of 28.03 m is found in the SLOR configuration for the near vessel position.

According to the previous findings, it is also noticed that identical behavior of the flexible jumpers is observed in the water depth of 1500 m. In each type of the riser configuration, there is a positive correlation between the departure angle and the maximum tension of the flexible jumpers. The tension load on the flexible jumper increases when the departure angle increases. Moreover, the correlation can also be found for the minimum bending radius of the flexible jumper; a lower departure angle value results in a lower bending radius. This indicates that the vessel motions have significant impact on the flexible jumper behavior as also mentioned in Sections 7.4.1 and 7.4.2.

Steel Riser

Similar steel riser arrangements of the SLOR and the COBRA configurations in water depths of 400 m and 1000 m are also installed in the water depth of 1500 m. The riser arrangements and materials, which are used for the steel risers, are described in Section 7.4.

As explained previously, the steel riser in the COBRA configurations is installed as a steel catenary riser; meanwhile, for the SLOR configurations the steel riser is installed as a top-tensioned riser. Mainly as a result of these, the SLOR configuration tends to have a larger amount of tension force in steel risers than the COBRA configuration. The results of the static responses for the steel risers are presented in Table 7-10.

Table 7-10 Static Response on Steel Risers (1500 m WD)

Parameter	COBRA			SLOR		
	Near Y	Intact	Far Y	Near Y	Intact	Far Y
Angle at buoy (deg)[1]	4.69	3.54	2.72	1.93	2.48	2.25
Maximum tension at buoy (kN)	1788.09	1815.01	1668.98	4274.78	4282.96	4288.20
Minimum tension at seabed (kN)	384.07	443.15	284.61	2922.54	2903.58	2934.46

Note:

[1)] The angle is measured relative to the buoy.

As expected, the maximum top tension force observed in the SLOR configurations is 4288.2 kN in the far vessel position. This finding may be explained by the fact that, in the SLOR configurations, a high tension force is required to straighten the steel riser. On the other hand, a maximum tension force of 1815.01 kN in the COBRA configurations is found in the vessel's intact condition.

As described in Table 7-10, for each riser configuration, the discrepancy between the tension loads for all conditions is considered small. These findings suggest that the vessel motions are already absorbed by the arrangement of the flexible jumper and the buoyancy module. By utilizing the uncoupled riser arrangements, the motion above the buoyancy modules does not have a significant impact on the steel risers. These results agree with the findings of other studies which are presented in Section 7.4.1 and 7.4.2.

Based on these results, the static response analysis has found that the low frequency (LF) motions, which are modeled as a vessel offset, do not significantly contribute to the steel riser performance for both uncoupled riser configurations. This is mainly due to the usage of a flexible jumper and a buoyancy module that are decoupled the effect of vessel offsets.

7.4.4 Mooring Line of COBRA Configurations

The mooring line is only used in the COBRA riser configurations in order to maintain the location of the buoyancy module as intended. The mooring line is tied in to the bottom part of buoyancy modules and tethered down to the sea bed. In this study, at the similar buoyancy module is used for three different water depths. Thus, it is expected that the tension forces on the mooring line will vary according to the water depth. The general description of the mooring line can be found in Section 2.3.2 while the details of mooring line configurations are described in Section 7.4.

The results obtained from the static response of the mooring lines for three different water depths are described in Table 7-11.

Table 7-11 Static Response on Mooring Line

Parameter	COBRA		
	Near Y	Intact	Far Y
Water Depth of 400 m			
Maximum Mooring Tension (kN)	1949.49	1978.22	1976.64
Water Depth of 1000 m			
Maximum Mooring Tension (kN)	1417.77	1474.53	1466.98
Water Depth of 1500 m			
Maximum Mooring Tension (kN)	992.43	1080.55	1066.29

Table 7-11 illustrates the maximum tension force in each of the mooring lines from three different water depths. It can be observed that the maximum tension load for each water depth occurs during intact conditions, which are 1978.2 kN, 1474.5 kN, and 1080.55 kN for water depth of 400 m, 1000 m and 1500 m respectively. According to the table above, the mooring lines in each water depth have consistent tension forces for all vessel positions. These results provide further support for the hypothesis that the arrangement of the buoyancy module with the flexible jumper is capable to decouple the low frequency (LF) motions.

As expected, there is an opposite correlation between water depth and tension force on the mooring line. The mooring load decreases when the water depth increases. A possible explanation for this might be that in this thesis, the design of the buoyancy modules is identical for all water depths.

7.5 Dynamic Response (ULS)

Further analysis of the dynamic responses is performed on the riser configurations after the equilibrium condition is established by using the static analysis. The nonlinear time domain analysis in irregular waves is presented as a dynamic loading on the risers. The combination of 100-year waves and 10-year currents is introduced as the worst combination case of environmental loadings. These environmental loadings together with the vessel motions for different wave frequencies (WF) are used to simulate the dynamic responses on the riser configurations. The riser analysis procedures shall follow the requirements according to the ultimate limit state (ULS) design by applying the load combinations for the uncoupled riser configurations which can be seen in Table 7-2.

According to DNV OS F201 (DNV, 2010a), for operating conditions, three-hour storm loads shall be applied to the riser with the 100-year annual exceedance probability to fulfill the criteria of the ultimate limit state (ULS). In practice, the riser models should be analyzed for three-hour storm duration as well to represent the real environmental conditions on the simulation models. A 0.02-second time step is considered in the analysis to simulate the three-

hour storm durations with less time simulation. By using this method, the riser is expected to capture the worst dynamic response of three-hour storm duration in less simulation time.

This study set out to determine the dynamic responses from the static equilibrium riser configurations. Therefore, the similar riser configurations in the static responses are used for this analysis as an initial condition which can be found in Section 7.4. The following sections present the results of dynamic responses for the SLOR and the COBRA configurations in three different water depths. Each section consists of two subsections, in which the results of the flexible jumpers and the steel risers will be discussed. In addition, Section 7.5.4 is dedicated to present dynamic results of mooring lines for the COBRA configuration in all water depths.

7.5.1 Uncoupled Riser Configurations in Water Depth of 400 m

The uncouple riser arrangements for the COBRA and the SLOR configurations in 400 m water depth are described in Section 7.4.1. Furthermore, the dynamic response for the flexible jumper and the steel riser are presented in the following paragraphs.

Flexible Jumper

In the global analysis, the flexible jumper shall fulfill the acceptance criteria. As described in Section 6.6, no compression load is allowed in the flexible jumpers, and the minimum bending radius (MBR) shall be not less than 5.00 m. In respect of turret designs, the lower tension load may be achieved by limiting the departure angle on the vessel to 12.5^0.

The dynamic responses in the flexible jumper may diverge to a certain degree. This is mainly due to the fact that the Norwegian Sea has a harsh environmental condition, with the Hs possibly reaching up to 18.8 m for a 100-year return period. Consequently, high wave frequency (WF) on the vessel motions may occur and be expected to be absorbed by the flexible jumpers. In addition, Table 7-12 summarizes the dynamic analysis results of the flexible jumpers in 400 m WD.

Table 7-12 Dynamic Response on Flexible Jumpers (400 m WD)

Parameter	COBRA			SLOR		
	Near Y	Intact	Far Y	Near Y	Intact	Far Y
Angle at vessel (deg)[1]	8.14	12.89	15.59	7.53	13.73	16.71
Angle at buoy (deg)[1]	7.38	12.08	13.24	8.57	13.65	15.49
Minimum bending radius (m)	10.07	22.47	41.92	13.67	27.82	48.81
Maximum water depth (m)[2]	382.55	367.67	349.20	378.07	362.08	342.29
Minimum tension (kN)	28.42	58.69	101.87	38.38	70.99	116.30
Maximum tension at vessel (kN)	1479.31	1468.50	1509.24	1474.80	1468.21	1519.82
Maximum tension at buoy (kN)	683.50	708.39	721.98	690.25	718.00	736.24

Notes:
[1)] The angle is measured relative to vertical axis and taken from the max. angle value of the responses.
[2)] The distance is measured from Mean Sea Level (MSL).

The results in Table 7-12 show that there is no compression load observed on the flexible jumper. Moreover, a minimum bending radius of 10.07 m in the COBRA configurations is found during the near vessel position which is satisfactory according to the acceptance criteria. However, a maximum departure angle of 16.71^0 in the SLOR configurations and 15.59^0 in the COBRA configurations indicates that the flexible jumper arrangements do not comply with the acceptance criteria of the maximum departure angle (refer to Section 6.6). The observed angles in the vessel are relatively high due to the enormous amount of hydrodynamic force in the severe environmental conditions significantly affecting the behavior of the flexible jumpers. A solution to solve the unacceptable design limitation is suggested in Section 7.6.

In dynamic analysis, the maximum tension is observed to identify the effect of wave frequency (WF) motions have a significant impact on the flexible jumpers. Indeed, WF motions on the flexible jumper in comparison to the static analysis results. The comparison between static and dynamic responses for maximum tension force at the vessel is presented in Figure 7-7.

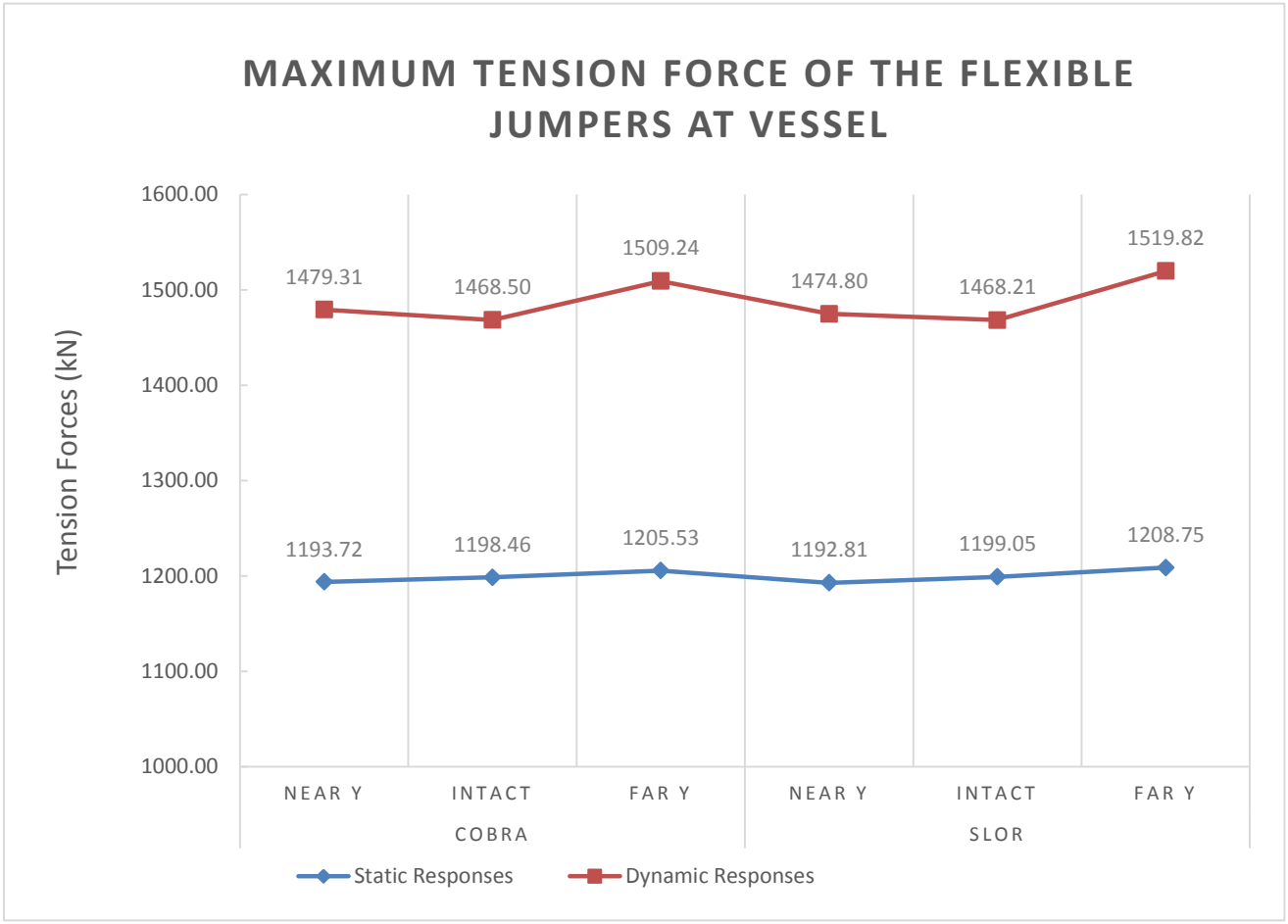

Figure 7-7 Static and Dynamic Tension Forces of Flexible Jumpers at Vessels

From the results in Figure 7-7, it is apparent that the wave frequency (WF) motions have a great influence on the maximum tension of the flexible jumpers at the vessel. The tension forces in the dynamic responses are significantly higher than the tension forces in the static responses. As can be seen from the chart above, for each riser configuration, the tension force reaches its maximum value in the far vessel position which is 1509.24 kN and 1519.82 kN for the COBRA and SLOR configurations respectively. These results indicate that the WF motions have a significant impact on the tension forces in addition to the low frequency (LF) motions.

According to Section 2.3.1, the flexible jumper is utilized to reduce the floater motions on the buoy. It is expected that the motions can be decoupled at the buoyancy module. Thus, only minimum dynamic motions are being transferred to the lower parts of the riser configurations. Figure 7-8 compares the results of the maximum tension force at the buoy obtained from the static responses and the dynamic responses in all vessel positions.

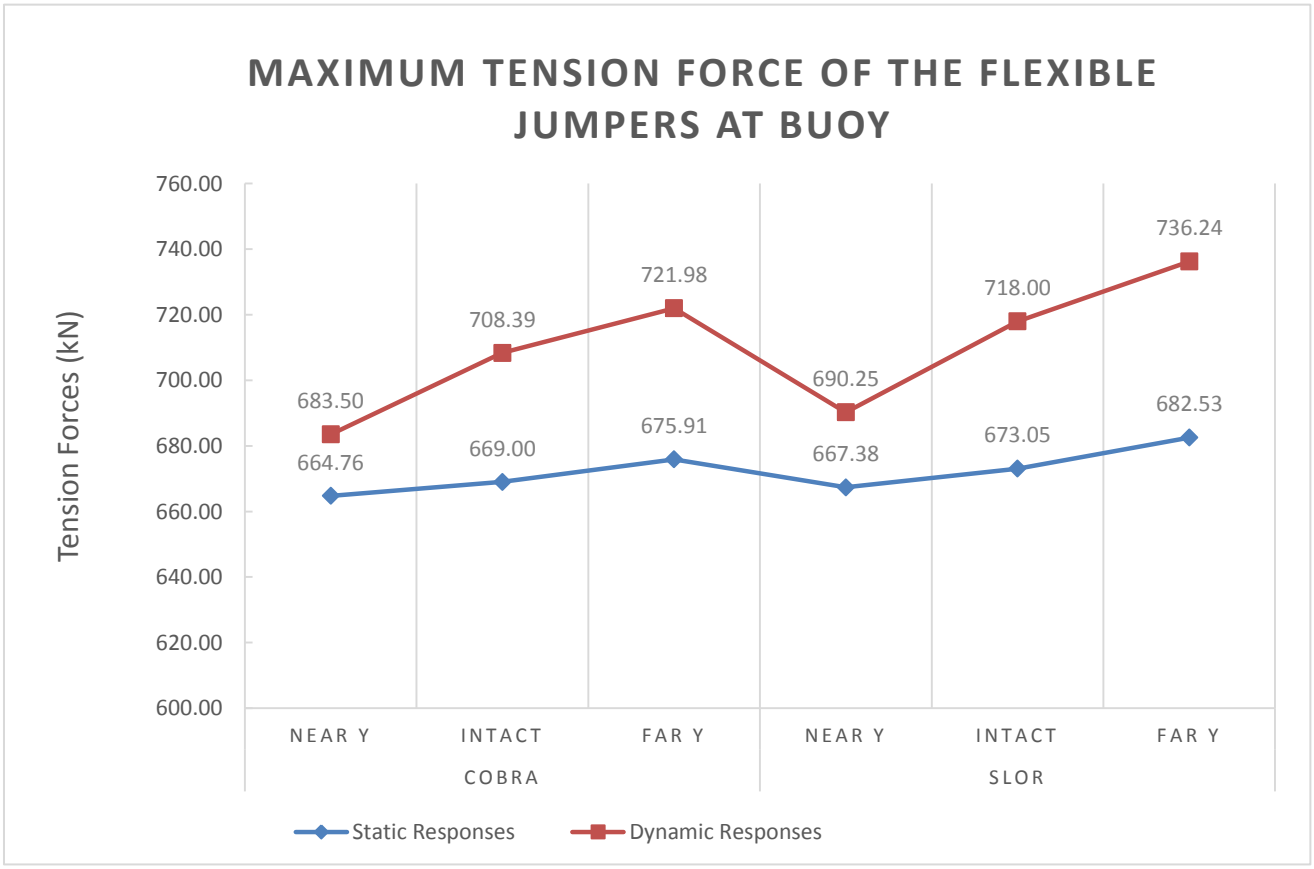

Figure 7-8 Static and Dynamic Tension Forces of Flexible Jumpers at Buoys

From Figure 7-8, it can be observed that the maximum dynamic tension force of the flexible jumper at the buoy is 736.24 kN corresponding to a maximum static tension force of 682.53 kN. As expected, Figure 7-8 reveals that there has been a marked drop in the level of dynamic effect at the buoy in comparison to the dynamic effect at the vessel in respect of tension forces. The results from Figure 7-8 can be compared with the results from Figure 7-7, which show that the WF effects at the buoy are significantly reduced, compared to the WF effects at

the vessel. Numerically, the maximum escalation tension forces due to the WF effects drop from 311.08 kN at the vessel to 52.70 kN at the buoy.

Together these results provide important insights, showing that the WF effects of the vessel motions contribute significantly to the flexible riser behavior, in addition to the LF effects of the vessel motions. Interestingly, the dynamic effects at the sub-surface buoy, which is located in 200 m water depth, are lower compared to the dynamic effects at the vessel. The departure angles for both configurations are not acceptable in accordance with the design acceptance criteria. Hence, the solution to solve this problem shall be suggested in Section 6.6.

Steel Riser

For the arrangement of steel risers for the SLOR and the COBRA configurations in 400 m water depth, refer to Section 7.4.1. Due mainly to these riser arrangements, it is reasonable that the dynamic responses are distinct, especially in respect of tension forces.

The previous findings of the static responses in the steel riser can be found in Section 7.4. The findings suggest that the arrangements of a flexible jumper and a buoyancy module are able to decouple the LF effects of the vessel motions. In the dynamic analysis, the riser responses that come from the WF effects can be observed. Table 7-13 presents the results obtained from the dynamic analysis of the COBRA and the SLOR configurations.

Table 7-13 Dynamic Response on Steel Risers (400 m WD)

Parameter	COBRA			SLOR		
	Near Y	Intact	Far Y	Near Y	Intact	Far Y
Angle at buoy (deg)[1]	4.48	5.00	3.48	2.41	3.08	1.81
Maximum tension at buoy (kN)	328.41	335.53	277.51	4879.63	4899.18	4901.19
Minimum tension at seabed (kN)	63.26	3.28	11.37	4390.35	4356.08	4386.01
von Mises stress at buoy (Mpa)	149.71	149.72	149.69	168.29	168.43	168.44
von Mises stress on steel riser (Mpa)	121.41	121.44	120.43	127.51	127.55	127.50
von Mises stress at seabed (Mpa)	137.25	155.91	148.31	126.95	127.00	126.89
Maximum buckling UF at buoy	0.05	0.05	0.05	0.10	0.10	0.10
Maximum buckling UF at steel riser	0.67	0.79	0.76	0.05	0.05	0.05
Maximum buckling UF at seabed	0.24	0.30	0.28	0.04	0.04	0.04

Note:
[1)] The angle is measured relative to the buoy and taken from the max. angle value of the responses.

As shown in Table 7-13, the results obtained from the dynamic analysis of the steel risers indicate that the steel risers for both configurations have sufficient strength to sustain all load conditions. The maximum buckling utilization factor (UF) observed in the COBRA configurations is 0.79 in the intact vessel position. This is mainly caused by high bending stress near 'Touch Down Point'. In contrast, the buckling UF for the SLOR configurations is

very low due to the fact that the top tensioned riser arrangements produce low bending stress in the shallower water depth.

Furthermore, the maximum von Mises stress is observed in different locations for each configuration. The COBRA configurations have a maximum stress of 155.91 MPa, found at the 'Touch Down Point', while the SLOR configurations have a maximum stress of 168.44 MPa, found at the buoy connection point. In general, for each riser configuration, there are no significant differences in respect of the von Mises stresses in all vessel positions.

In accordance with the static results in Section 7.4.1, the present results demonstrate that the tension forces in the steel riser for the SLOR configurations are much higher than in the steel riser in the COBRA configurations. The maximum tension force in each configuration is 335.53 kN and 4901.19 kN for the COBRA and the SLOR configurations, respectively.

In order to examine the behavior of the steel risers at the buoy, the steel riser angles at the buoy for the static and the dynamic responses are compared in Figure 7-9.

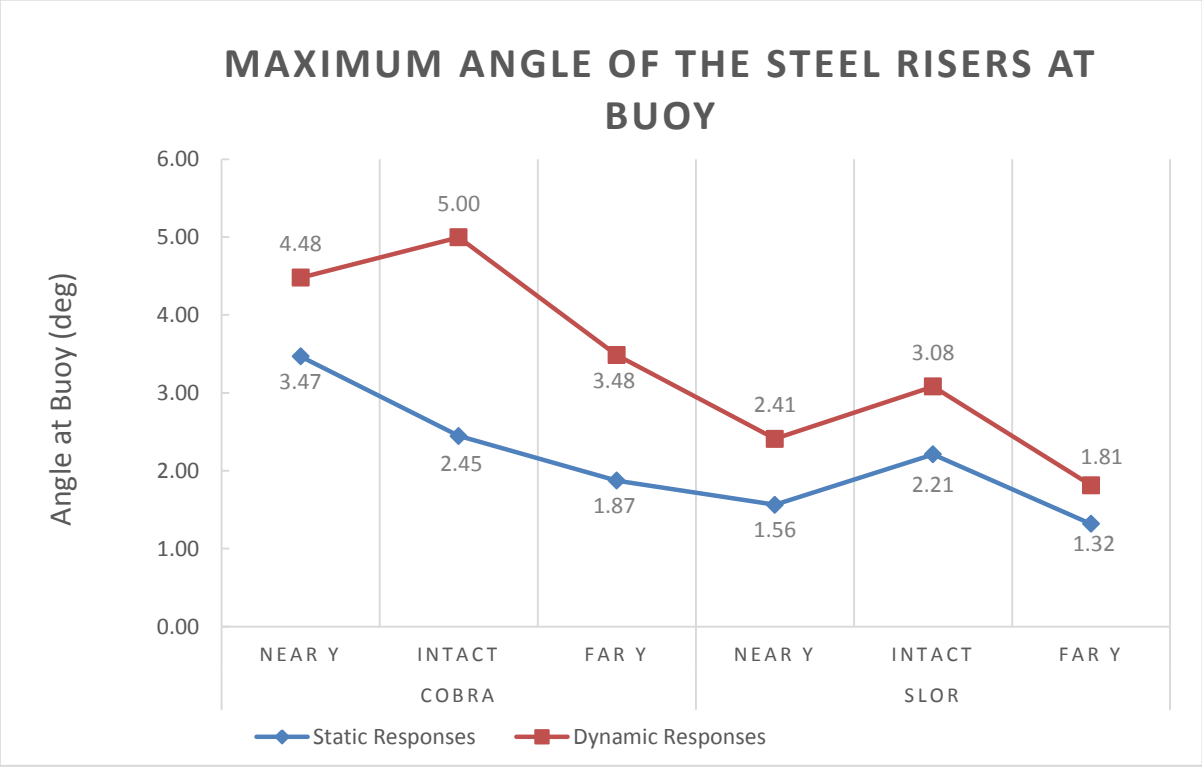

Figure 7-9 Static and Dynamic Response of Steel Riser Angles at Buoys

From the chart, it is clear that there is a small discrepancy between the static steel riser angles and the dynamic steel riser angle occurring at the buoy. The maximum deviation angle from the static to the dynamic response at the COBRA configurations is 2.55^0 during the vessel's intact condition. These small deviations prove that the vessel motions (i.e. LF and WF motions) are uncoupled by using the combination of flexible jumper with buoyancy module.

The comparison of the static and dynamic tension forces at the buoy for the COBRA and the SLOR configurations is presented in Figure 7-10, with the comparison of the tension forces at the bottom point illustrated in Figure 7-11.

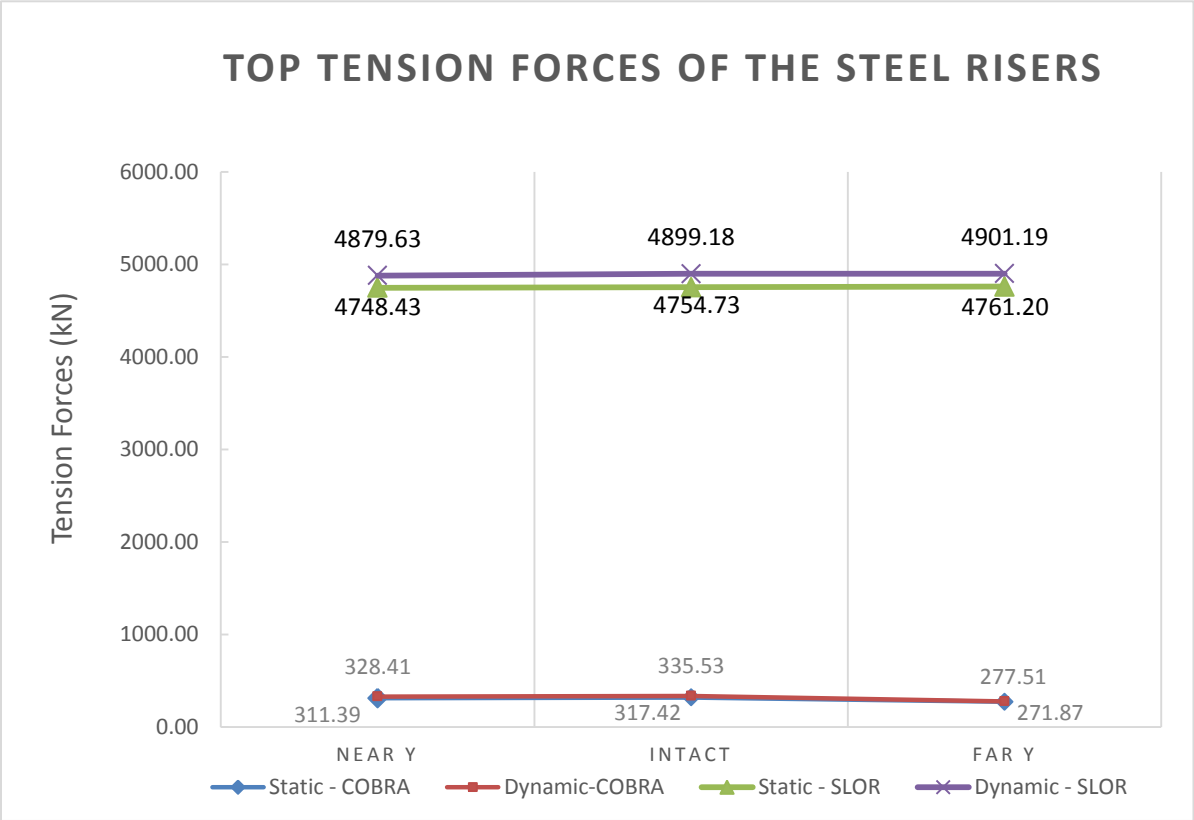

Figure 7-10 Static and Dynamic Response of Top Tension Forces

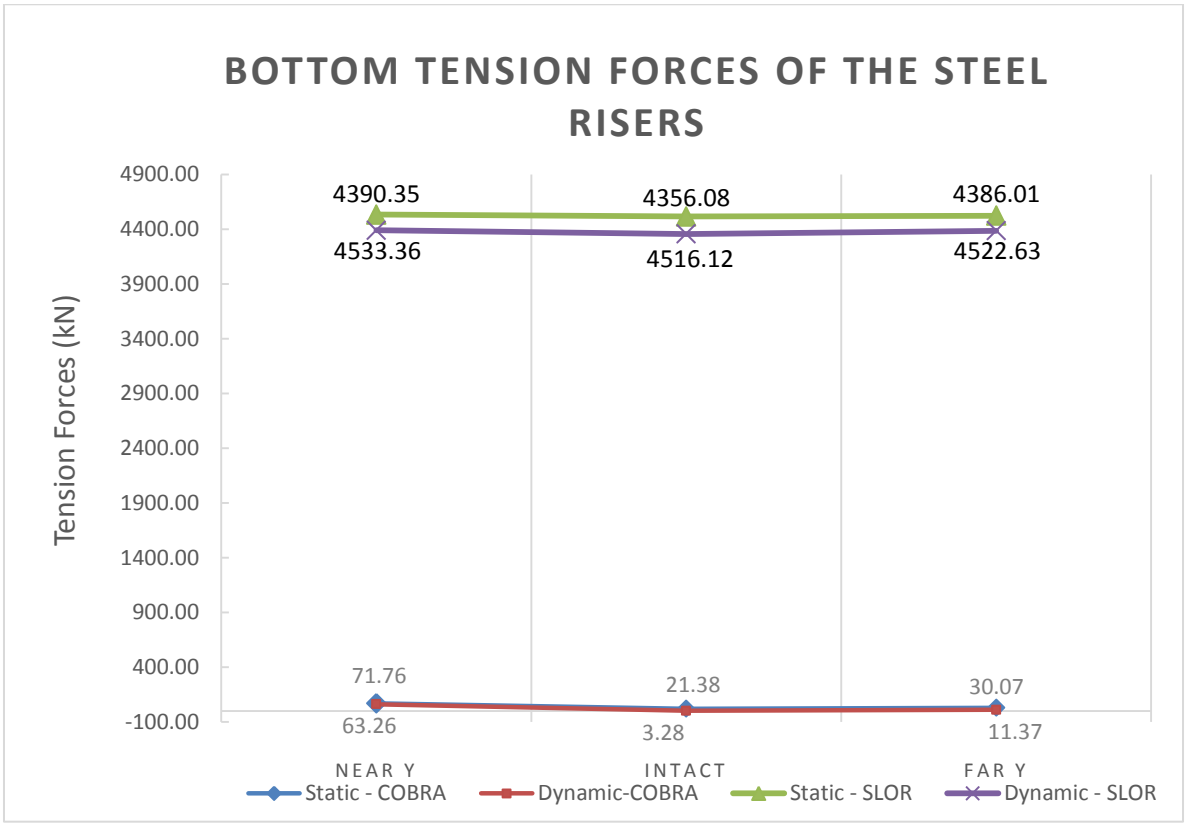

Figure 7-11 Static and Dynamic Response of Bottom Tension Forces

As shown in Figure 7-10 and Figure 7-11, the tension force discrepancies between the static and the dynamic responses in the steel risers are relatively small. Therefore, it can be concluded that the vessel motions do not contribute significant effects to the lower parts of the riser configurations, especially at 'Touch Down Point' for the COBRA configurations.

Overall, the results in this section prove that the uncoupled riser configurations have the ability to reduce the effects of wave frequency (WF) as well as lower frequency (LF) in the steel riser sections. The comparison results between SLOR and COBRA configurations suggest that the SLOR configuration in 400 m water depth tends to have better riser responses in respect of the von Mises Stress and the Buckling UF ratio (refer to Table 7-13). The next section, therefore, moves on to discuss the Uncoupled Riser Configurations in 1000 m water depth.

7.5.2 Uncoupled Riser Configurations in Water Depth of 1000 m

The uncoupled riser arrangements for the COBRA and SLOR in 1000 m water depth are described in detail in Section 7.4.2. Furthermore, the dynamic responses for the flexible jumper and the steel riser are presented in the following paragraphs.

Flexible Jumper

The similar acceptance criteria of flexible jumpers (refer to Section 6.6), which are presented in Section 7.5.1, are also applicable for this section. The complete arrangement of the flexible jumpers in 1000 m water depth for the SLOR and the COBRA configurations can be found in Section 7.3. The results obtained from the dynamic analysis of flexible jumpers are presented in Table 7-14.

Table 7-14 Dynamic Response on Flexible Jumpers (1000 m WD)

Parameter	COBRA			SLOR		
	Near Y	Intact	Far Y	Near Y	Intact	Far Y
Angle at vessel (deg)[1]	5.77	11.75	13.17	4.91	12.46	13.90
Angle at buoy (deg)[1]	6.62	9.48	10.82	7.77	10.59	12.13
Minimum bending radius (m)	24.13	38.11	54.09	33.27	48.26	65.68
Maximum water depth (m)[2]	580.89	566.23	546.43	597.60	582.52	560.68
Minimum tension (kN)	62.74	100.91	140.51	85.87	127.07	167.95
Maximum tension at vessel (kN)	2283.55	2268.76	2305.37	2381.89	2371.93	2415.96
Maximum tension at buoy (kN)	1026.14	1047.95	1058.85	1110.81	1133.66	1147.48

Notes:
[1)] The angle is measured relative to the vertical axis and taken from max. angle value of the responses.
[2)] The distance is measured from Mean Sea Level (MSL).

The results of this study show that the minimum bending radius (MBR) and minimum tension loads of the flexible jumpers are above the acceptable limits (refer to Section 6.6). This draws attention to the fact that the bending radius corresponds with the tension load for each riser configuration. The bending radius and tension force reach a minimum value in the near vessel position. From Table 7-14, the results show that the minimum bending radius in the COBRA configurations is 24.13 m, corresponding with a minimum tension force of 62.74 kN.

The departure angles for both riser configurations do not comply with the minimum requirement during the far vessel position (refer to Section 6.6). The maximum angle value of 13.90^0 in the SLOR configurations is observed. In order to satisfy the minimum design requirements, the solution for the unacceptable departure angle is presented in Section 7.6.

To determine the effect of the floater motions in the flexible jumpers, the comparison of tension forces between the static and the dynamic results shall be presented in detail. By these means, the following figures show the comparison results of maximum tension forces at the vessel and subsurface buoy.

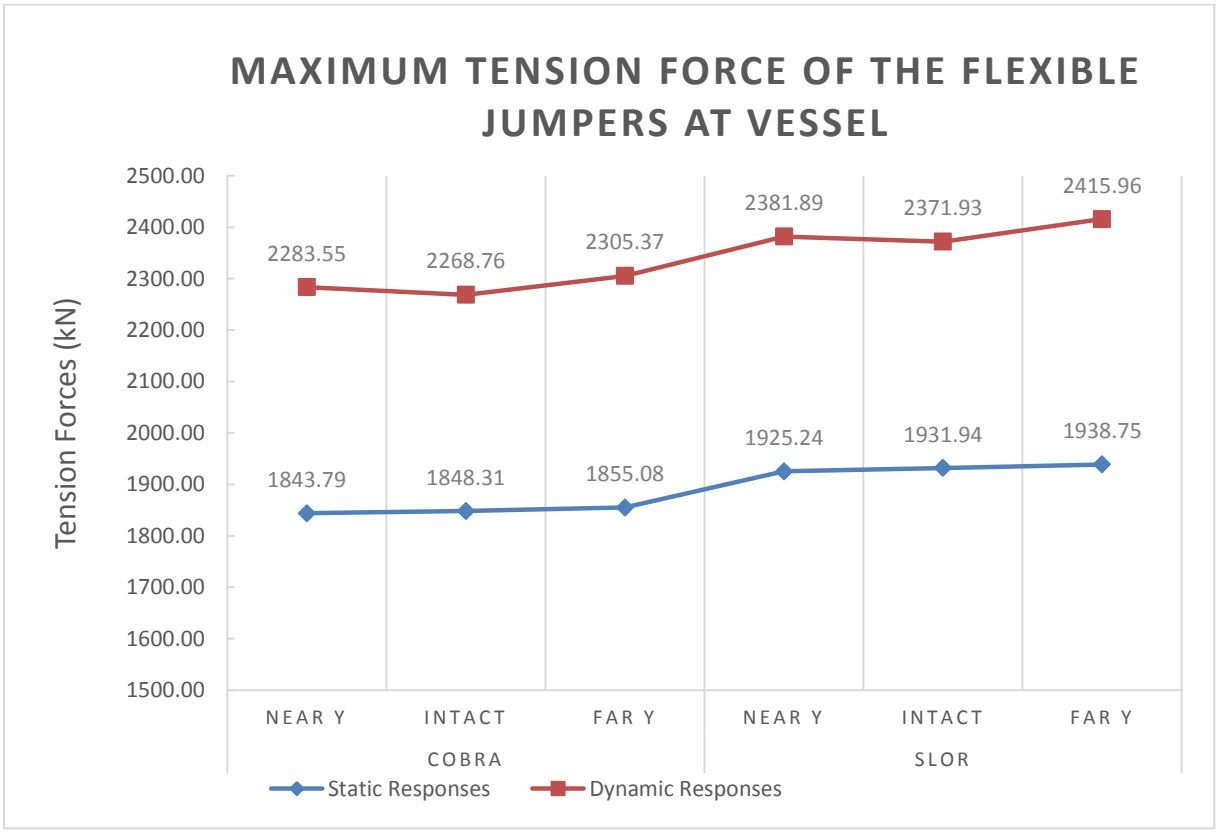

Figure 7-12 Static and Dynamic Response of Flexible Jumpers at Vessels

It can be seen in Figure 7-12 that these results are consistent with those of the riser configuration in 400 m water depth. The results show that the effects of the WF motions are significant at the sea surface. The escalation rate of the tension rate in the dynamic responses is around 24% higher than in the static responses. The highest tension force for all conditions at the vessel is 2415.96 kN for the SLOR configurations in the vessel intact position. The tension forces in the current study are relatively higher than the tension force for the flexible jumper in 400 m water depth. This could be happening due to the longer segment that is used for the flexible jumper in 1000 m water depth.

Figure 7-13 presents the comparison between the dynamic and the static tension at the buoy in order to examine the dynamic responses at the buoy. According to Section 7.5.1, the dynamic floater motions are effectively reduced by the using flexible jumper as a connection between the buoyancy module and the surface facility. Figure 7-13 describes the dynamic effect at the buoy for the riser configurations in 1000 m water depth.

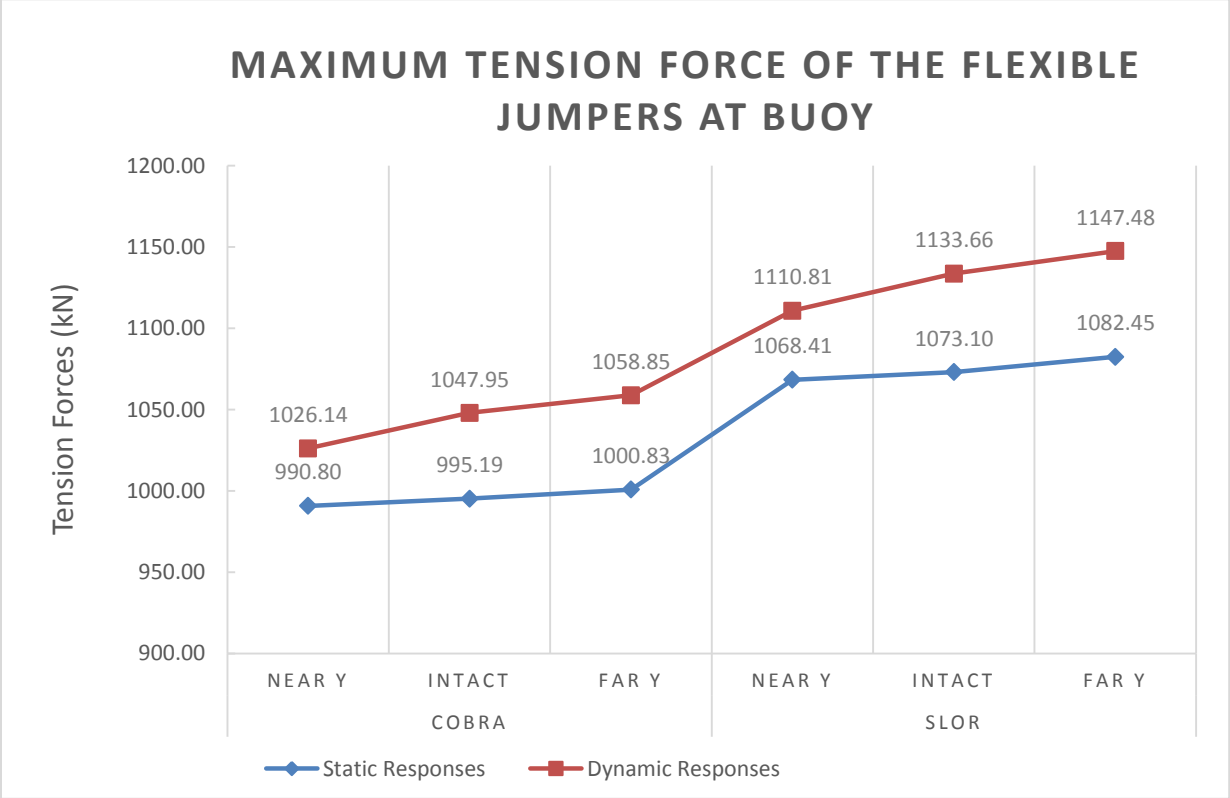

Figure 7-13 Static and Dynamic Response of Flexible Jumpers at Buoys

According to Figure 7-13, it can be seen that the maximum tension force of 1147.48 kN in the SLOR configuration is observed in the far vessel position. The escalation tension forces due to the dynamic effects at the buoy are relatively smaller compared to the escalation tension forces at the vessel. The findings of the current study are consistent with the dynamic results in Section 7.5.1. On average, the escalation tension rates at the buoy is just over 6%, which is significantly smaller than the 24% escalation tension rates at the vessel.

Overall, a similar response to that of the riser configuration for 400 m water depth is produced. The dynamic effects of the flexible jumpers decrease significantly in the buoy which is located in 300 m water depth. These results match those observed in earlier studies (refer to Section 7.5.1).

Steel Riser

The static equilibrium in the steel risers for the SLOR and the COBRA configurations in 1000 m water depth is presented in Section 7.4.2. In this study, the vessel motions for different wave frequencies (WF) in the risers are observed.

The dynamic analysis for this section has a similar procedure to that which is used in Section 7.5.1. According to the acceptance criteria (refer to Section 6.6), the steel risers should have an acceptable buckling utilization factor in ULS condition which is not more than 1.00. The

results of dynamic responses for steel risers in 1000 m water depth are summarized in Table 7-15.

Table 7-15 Dynamic Response on Steel Risers (1000 m WD)

Parameter	COBRA			SLOR		
	Near Y	Intact	Far Y	Near Y	Intact	Far Y
Angle at buoy (deg)[1]	4.49	3.75	2.45	2.45	3.12	2.70
Maximum tension at buoy (kN)	1080.20	1099.28	1004.38	4420.34	4439.95	4445.47
Minimum tension at seabed (kN)	258.35	157.18	173.51	3455.39	3454.93	3457.91
von Mises stress at buoy (Mpa)	147.49	147.52	147.35	162.25	162.39	162.43
von Mises stress on steel riser (Mpa)	118.11	118.14	117.89	123.67	123.73	123.64
von Mises stress at seabed (Mpa)	120.18	124.16	122.98	298.76	299.19	299.33
Maximum buckling UF at buoy	0.05	0.05	0.05	0.09	0.09	0.09
Maximum buckling UF at steel riser	0.33	0.44	0.41	0.38	0.39	0.39
Maximum buckling UF at seabed	0.15	0.18	0.17	0.21	0.22	0.21

Note:
[1)] The angle is measured relative to the buoy and taken from the max. angle value of the responses.

In general, the dynamic results from Table 7-15 show that the steel riser configurations satisfy the design acceptance criteria in accordance with Section 6.6. From the data in Table 7-15, it can be observed that the maximum buckling utilization factor (UF) is 0.44 for the COBRA configurations in the intact vessel position. The von Mises stress reaches a maximum value of 299.19 MPa for the SLOR configurations at the bottom connection point. It can be seen in the table above that the von Mises stress corresponds with the angle value; a higher declination angle at the buoy results in higher stresses at the bottom connection point.

Due mainly to the different arrangement of the steel riser configurations in COBRA and SLOR, the distinct maximum tension forces are observed from Table 7-15. The maximum tension force for each riser configuration is 1099.28 kN for the COBRA configuration and 4445.47 kN for the SLOR configuration. In order to examine the dynamic effects on the steel risers, the tension forces comparison between static and dynamic responses at the buoy and at the bottom point are presented in Table 7-14 and Table 7-15, respectively.

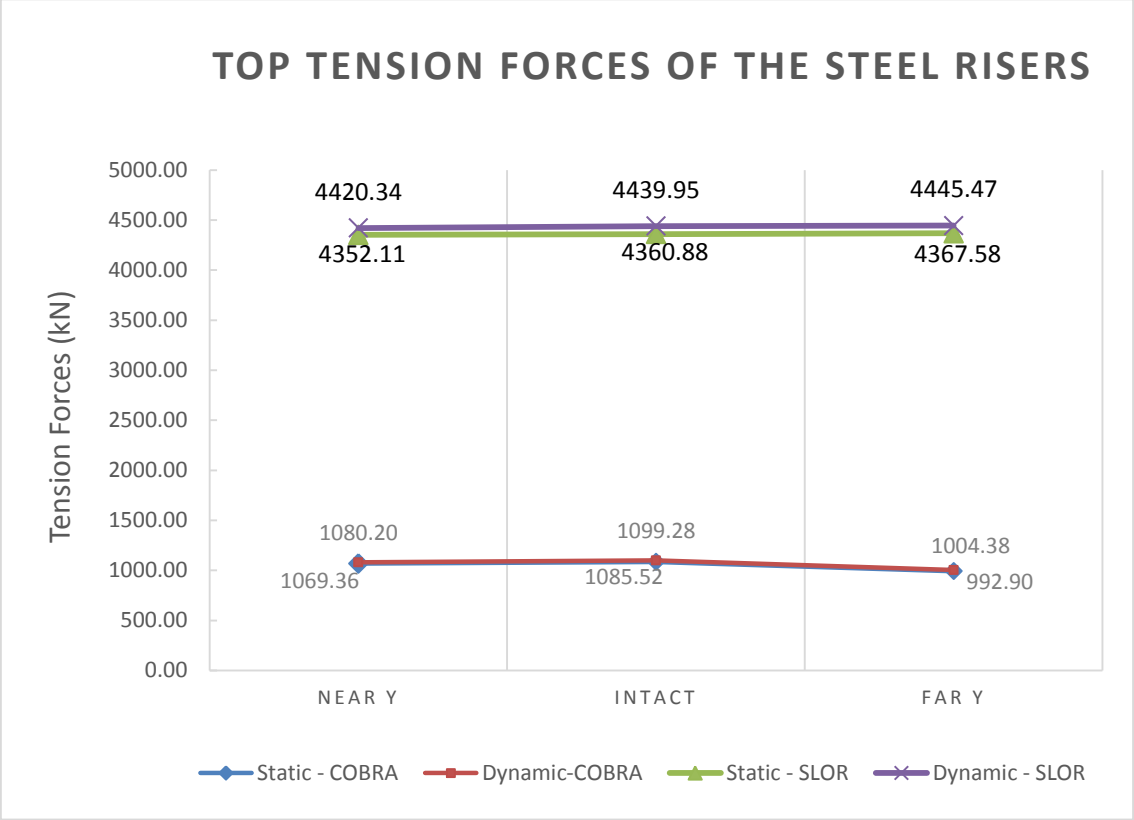

Figure 7-14 Static and Dynamic Response of Top Tension Forces

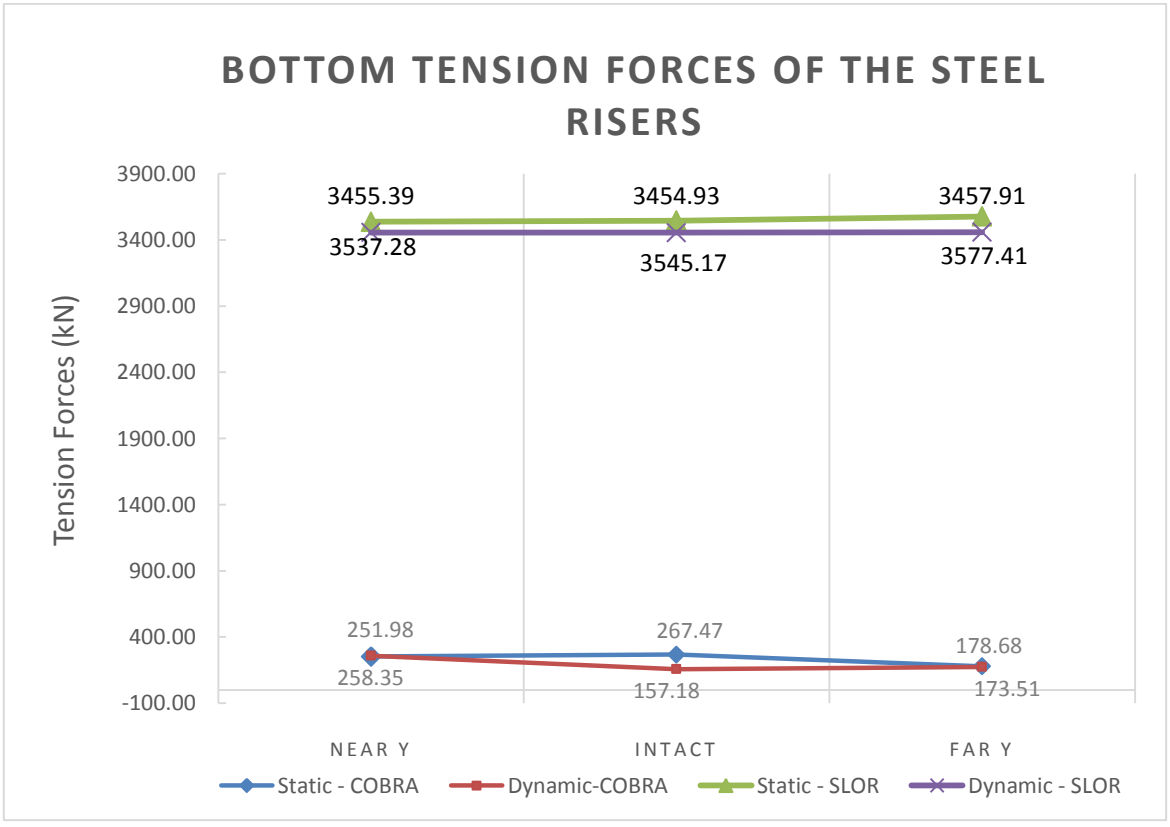

Figure 7-15 Static and Dynamic Response of Bottom Tension Forces

The identical results from the previous study of the steel risers are shown in Table 7-14 and Table 7-15. It can be observed that there are small discrepancies between the static and the dynamic results of the tension forces in the steel risers. It can thus be suggested that the lower part of riser configurations is not affected by the floater motions. These findings support the previous results which are presented in Section 7.5.1.

Furthermore, the buoyancy module behavior can be observed by comparing the steel riser angle at the buoy in static and dynamic responses which is presented in Figure 7-16.

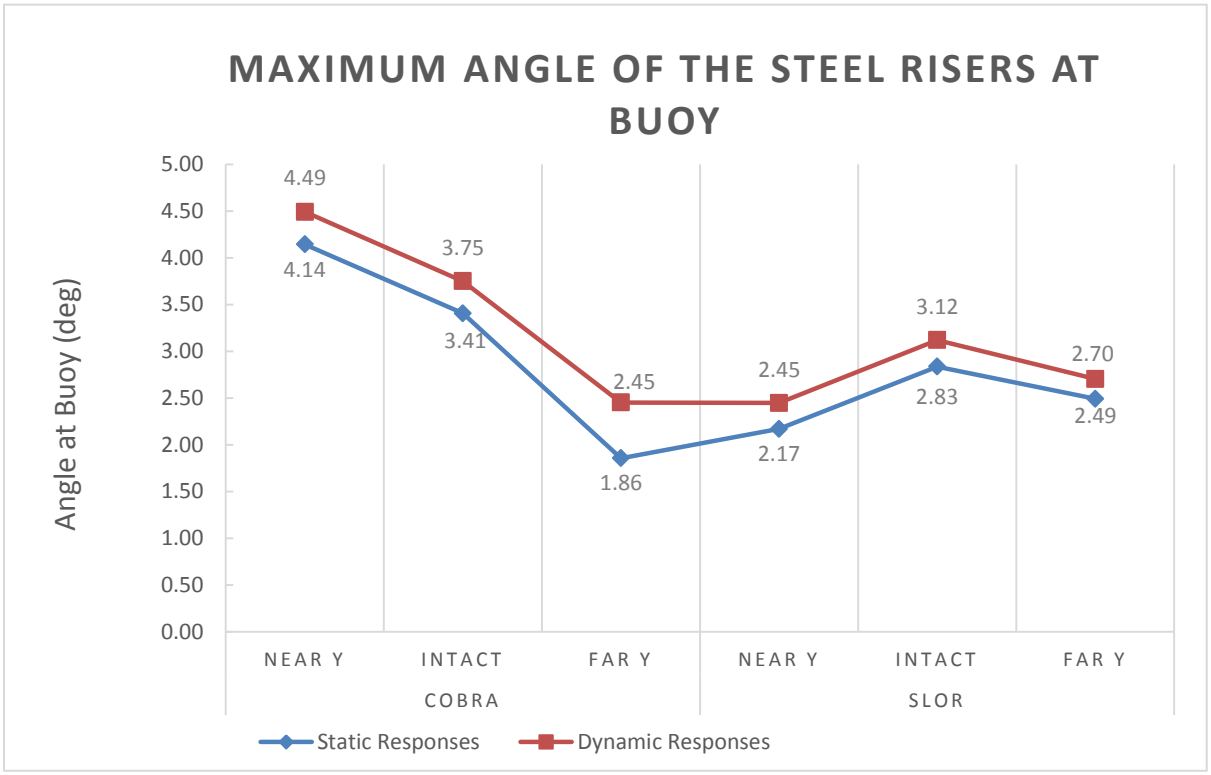

Figure 7-16 Static and Dynamic Response of Steel Riser Angles at Buoys

As can be seen in Figure 7-9, the graph illustrates similar riser behavior to the previous riser configurations which are described in Section 7.5.1. For the uncoupled riser configurations in 1000 m water depth, the buoyancy modules are located in 300 m water depth. As described in Table 7-3 and Table 7-4, the buoyancy module location for the riser configurations in 1000 m water depth is situated deeper than the riser configurations in 400 m water depth. From this fact, we can see that the results from the current studies show lower value of the escalating angles (i.e. 0.60^0) in comparison to the riser configurations in 400 m water depth (i.e. 2.55^0). This study confirms that the hydrodynamic effect is reduced when the water depth increases.

In summary, the current result is in agreement with the uncouple riser configurations in 400 m water depth results. The results prove that the uncoupled riser configurations are suitable to decouple the vessel motions which are caused by harsh environmental conditions. Moreover, the finding from the present study suggests that the buoyancy module may be located in deeper water depths to reduce the hydrodynamic effect from the sea surface.

Overall, both riser configurations have sufficient capacity to perform during operating conditions. However, the steel riser responses for SLOR configurations in the bottom connection should be monitored with caution because the large declination angle may lead to failure. This could happen when the von Mises stress exceeds the permissible stress in the connection point.

7.5.3 Uncoupled Riser Configurations in Water Depth of 1500 m

The description of the COBRA and SLOR configurations for 1500 m water depth can be found in Section 7.3. This section is considered as further analysis of the previous study in Section 7.4.3. Furthermore, this section is divided into two sub-sections in order to discuss the dynamic responses for the flexible jumpers and the steel risers.

Flexible Jumper

For the flexible jumper arrangements in 1500 m water depth, refer to Section 7.4.3. Similar acceptance criteria for the flexible jumper are also applied for these riser configurations (COBRA and SLOR) in accordance with Section 6.6. Table 7-16 presents in detail the dynamic responses of the flexible jumpers in 1500 m water depth.

Table 7-16 Dynamic Response on Flexible Jumpers (1500 m WD)

Parameter	COBRA			SLOR		
	Near Y	Intact	Far Y	Near Y	Intact	Far Y
Angle at vessel (deg)[1]	4.59	12.89	14.19	5.51	11.94	13.05
Angle at buoy (deg)[1]	7.89	10.33	12.66	6.10	8.27	10.26
Minimum bending radius (m)	36.84	52.75	73.17	26.33	39.55	59.52
Maximum water depth (m)[2]	620.02	604.94	580.32	629.95	617.45	590.37
Minimum tension (kN)	93.93	140.20	186.52	68.21	106.10	156.11
Maximum tension at vessel (kN)	2481.45	2475.91	2526.10	2482.23	2465.18	2501.97
Maximum tension at buoy (kN)	1198.62	1223.40	1246.97	1177.86	1196.14	1215.53

Notes:
[1)] The angle is measured relative to vertical axis and taken from the max. angle value of the responses.
[2)] The distance is measured from Mean Sea Level (MSL).

The analysis results in Table 7-16 show that the flexible jumpers have sufficient strength to sustain the design loads according to ultimate limit state (ULS) design. No compression load is observed on the flexible jumpers. A minimum tension load of 68.21 kN in the SLOR configurations is found in the near vessel position. Furthermore, the minimum bending radius of the flexible jumpers for both riser configurations is within the allowable limit (refer to Section 6.6). However, the departure angles of flexible jumpers are observed to be more than the acceptable limitation which is 12.5^0. Similar conditions are described in the previous sections where the maximum departure angle is always observed in the far vessel position. The maximum value could reach up to 14.19^0 for the COBRA configurations and 13.05^0 for

the SLOR configurations. In Section 7.6 a suggestion is provided as a proposed solution to solve the unacceptable departure angles at the vessel.

From the data in Table 7-9 and Table 7-16, the comparison of the tension forces between the static and the dynamic responses is presented in Figure 7-17. By plotting the maximum tension forces, the wave frequency (WF) effects on the flexible jumper can be observed.

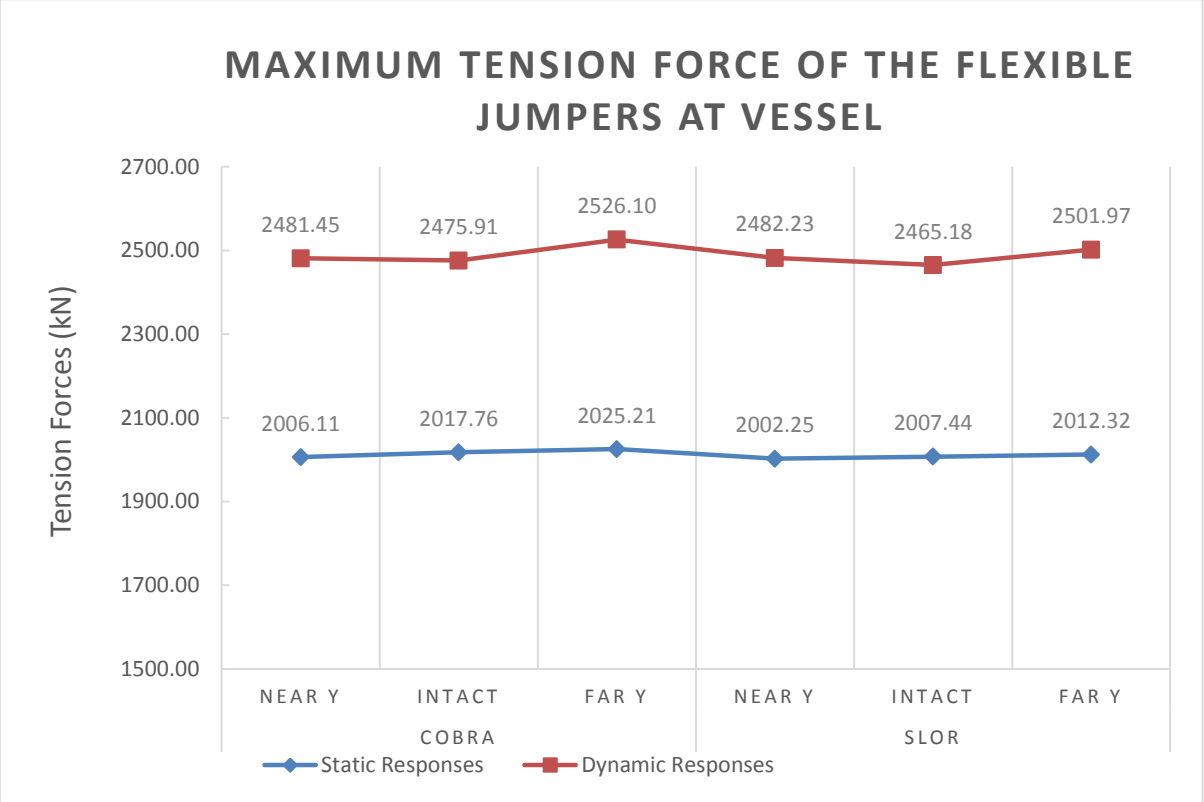

Figure 7-17 Static and Dynamic Response of Flexible Jumpers at Vessels

The result from Figure 7-17 can be compared with the results in Figure 7-12 which show that an identical trend is observed in the dynamic response of the flexible jumpers at the vessel. Although, the maximum tension force in the current study (i.e. 2526.10 kN) is slightly higher than in the previous study (i.e 2415.96 kN), this is mainly due to the fact that a longer section of the flexible jumpers is required for the riser configurations in 1500 m water depth (refer to Section 7.3). Interestingly, the escalation rate of tension forces in the dynamic response is around 24% higher than in the static response. These results match those observed in the earlier study (refer to Section 7.5.2).

Figure 7-17 illustrates the substantial effects of WF motions at the sea surface. According to Section 2.3.1, the flexible jumper is expected to be useful in absorbing the excessive motions in the floater. To prove that, Figure 7-18 describes the comparison between dynamic and static tension at the buoy in order to examine the dynamic effects on the buoy.

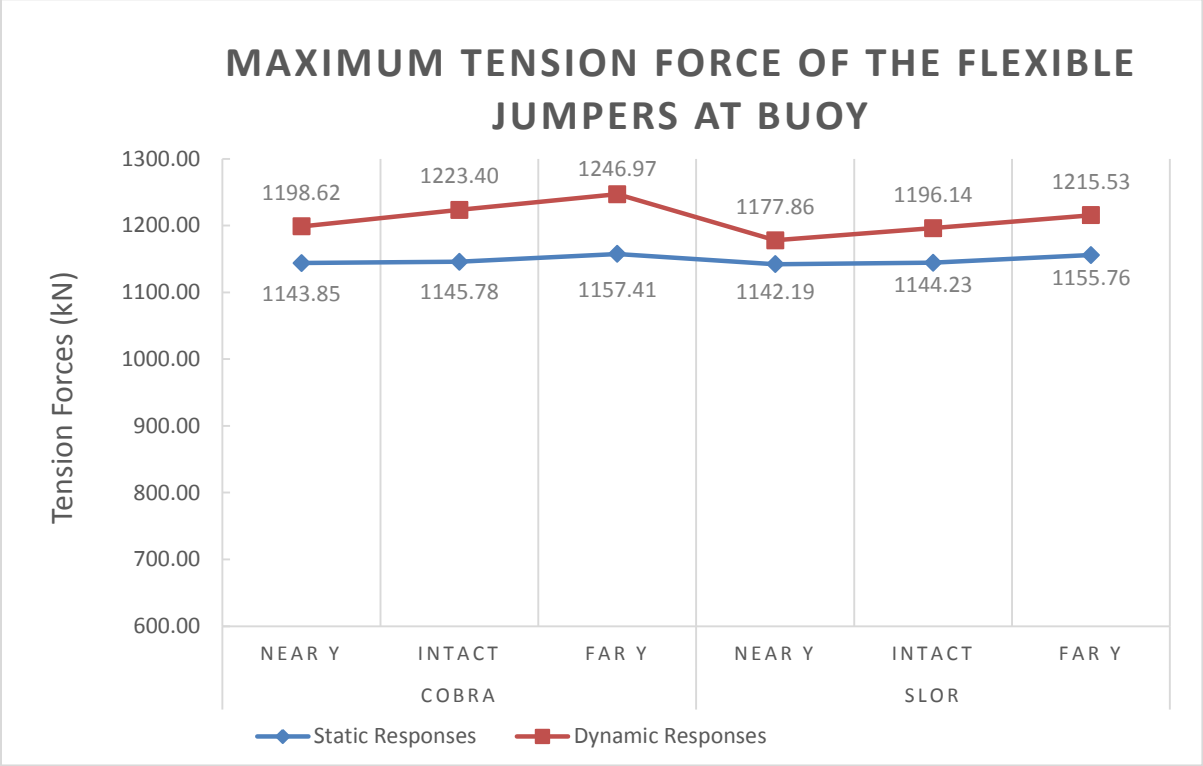

Figure 7-18 Static and Dynamic Response of Flexible Jumpers at Buoys

As shown in Figure 7-13, the results obtained from the dynamic responses show that low escalation forces occur at the buoy due to the WF effects. These results agree with the findings of other studies, in which the escalation tension rate reduces at the buoy in comparison with the tension rate at the vessel. On average, the escalation tension rate of 7.7% is found at the subsurface buoy connection which is significantly smaller than the escalation tension rates of 24% at the vessel connection.

In summary, as expected, the flexible jumper does an excellent job of absorbing the WF effects from the sea surface. Thus, a minimum amount of load affects the buoyancy module, which is located in 300 m water depth. It can be noticed that the escalation tension forces are slightly higher in the current study than the tension forces for the riser configuration in 1000 m water depth. This is mainly due to the installation of a longer section of flexible jumper for riser configuration in 1500 m water depth.

Steel Riser

This section presents the dynamic analysis for the SLOR and COBRA configuration in 1500 m water depth. Static equilibrium has been achieved in the static analysis, which is described in Section 7.4.3, and the riser arrangements in 1500 m water depth have also been explained. The minimum design criteria shall be in accordance with the acceptance criteria which are described in Section 6.6. Furthermore, the dynamic analysis results of steel risers are summarized in Table 7-17.

Table 7-17 Dynamic Response on Steel Risers (1500 m WD)

Parameter	COBRA			SLOR		
	Near Y	Intact	Far Y	Near Y	Intact	Far Y
Angle at buoy (deg)[1]	4.98	4.28	3.27	2.19	2.75	2.47
Maximum tension at buoy (kN)	1821.90	1860.48	1712.88	4341.03	4361.49	4364.50
Minimum tension at seabed (kN)	405.76	251.31	274.61	2824.00	2815.83	2820.89
von Mises stress at buoy (Mpa)	149.28	149.40	148.95	161.71	161.86	161.88
von Mises stress on steel riser (Mpa)	118.74	118.80	118.43	123.45	123.49	123.43
von Mises stress at seabed (Mpa)	115.58	117.93	117.51	279.39	279.77	279.84
Maximum buckling UF at buoy	0.06	0.06	0.06	0.08	0.08	0.08
Maximum buckling UF at steel riser	0.24	0.33	0.31	0.32	0.32	0.32
Maximum buckling UF at seabed	0.12	0.15	0.14	0.18	0.18	0.18

Note:
[1)] The angle is measured relative to the buoy and taken from the max. angle value of the responses.

As can be seen from Table 7-17, the steel riser arrangements in 1500 m water depth have sufficient strength to resist the dynamic loads. It can be seen that the maximum buckling utilization factor (UF) is 0.33 for the COBRA configurations in the intact vessel position. For the COBRA configurations, this buckling UF is the lowest value among the previous studies. It is possible to conclude that the longer lay back distance in deep water may reduce the bending radius of the riser around 'Touch Down Point'. This will eventually result in low bending stress. The maximum von Mises Stress, which is 279.84 MPa, can be observed in the SLOR configurations. Interestingly, the stress values of the current study are slightly lower than the previous studies and the angle values at the buoy are also lower than in the previous studies. The results show that the von Mises stress corresponds with the angle value at the buoy (refer to Table 7-15).

The following figures present the comparison between the static and dynamic responses of the tension forces at the buoy and at the bottom point.

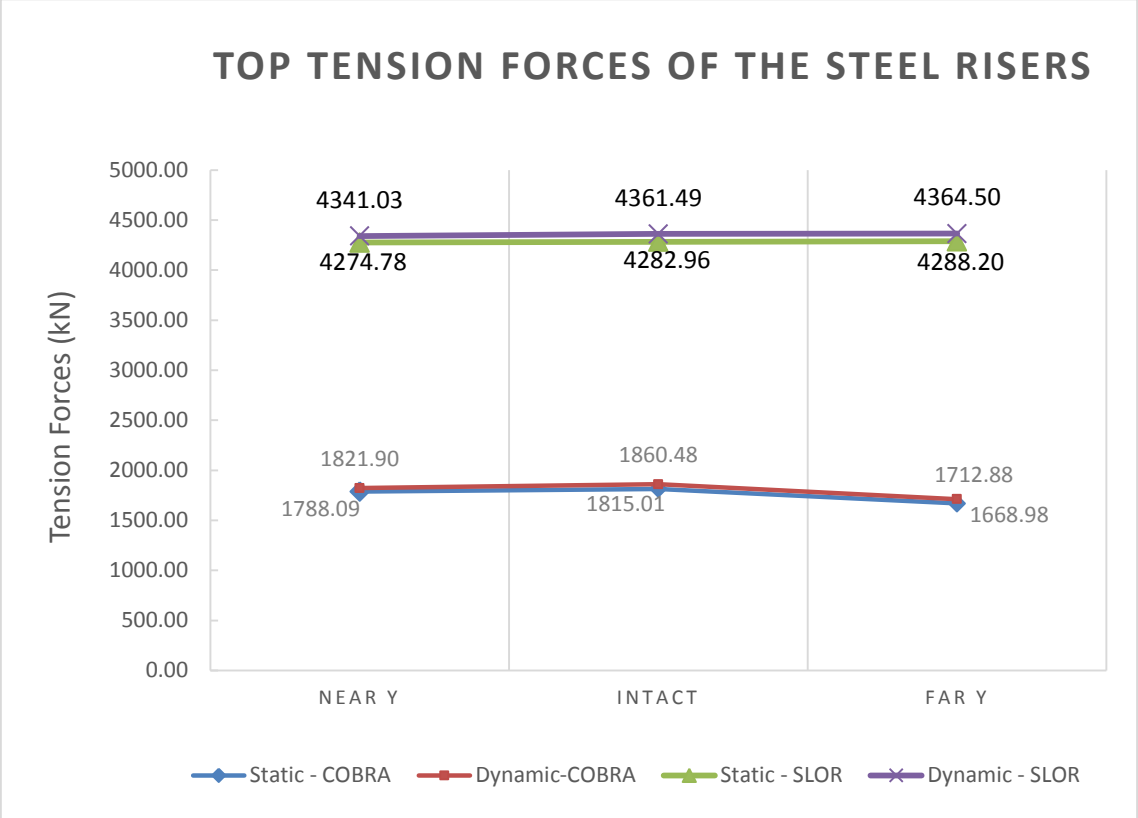

Figure 7-19 Static and Dynamic Response of Top Tension Forces

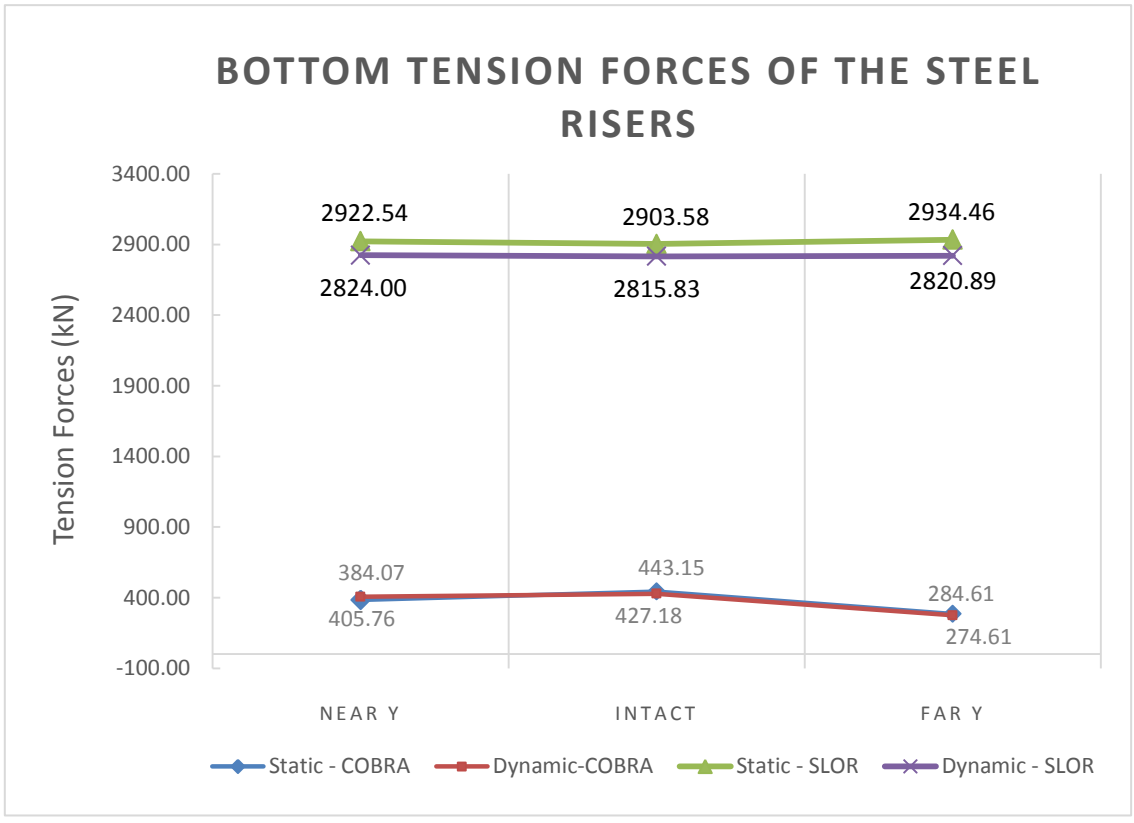

Figure 7-20 Static and Dynamic Response of Bottom Tension Forces

As can be seen in Figure 7-19 and Figure 7-20, these results are consistent with those of other studies and suggest that the effects of the dynamic responses in the tension forces are relatively insignificant. This can be observed by calculating the difference between the static tension forces and the dynamic tension forces. The same finding can also be observed in the riser configuration in 400 m and 1000 m water depth (refer to Section 7.5.1 and 7.5.2).

In order to provide further support for the hypothesis, the buoyancy motion behaviors in the static and the dynamic responses are compared in Figure 7-21.

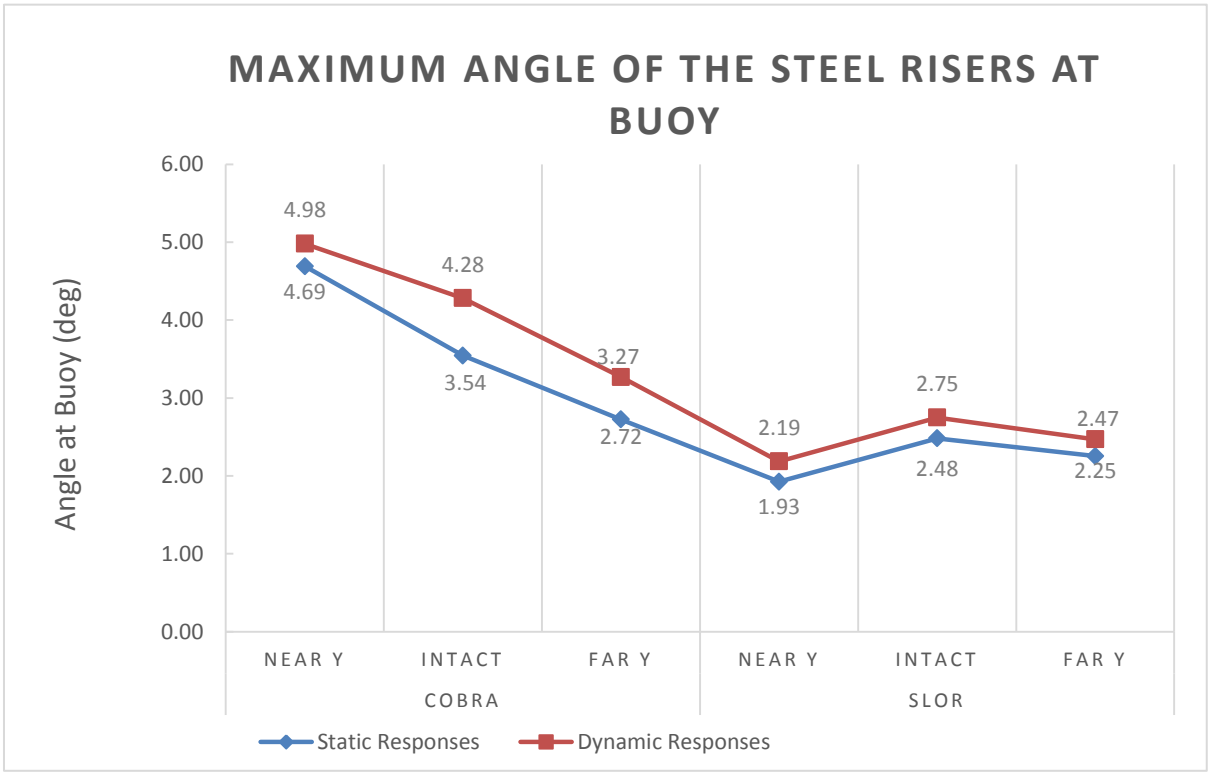

Figure 7-21 Static and Dynamic Response of Steel Riser Angles at Buoys

As expected, Figure 7-21 proves that the dynamic responses in the buoyancy module behavior are considered minor, with the maximum angle deviations at around 0.74^0. The hydrodynamic effects from the sea surface are relatively low in the buoyancy module which is located in 300 m water depth. Finally, this result seems to be consistent with other research which can be found in Sections 7.5.2 and 7.5.1.

Taken together, these results provide an important insight into a conclusion that the uncoupled riser configurations are suitable to decouple the excessive vessel motions in harsh environmental conditions such as the Norwegian Sea. As described in Section 7.5.2, it has been suggested that the buoyancy module may be located in deeper water depths to reduce the hydrodynamic effect from waves as well as floater motions. In general, the riser configurations in 1500 m water depth (i.e. the SLOR and the COBRA configurations) have sufficient capacity to perform during operating conditions. However, for the SLOR configurations, it can thus be suggested that the declination angle in the Top Tensioned Riser

shall be limited to the lower degree in order to avoid the high stresses at the bottom connection point.

7.5.4 Mooring Line of COBRA Configurations

This section examines the effects of the wave frequency (WF) in the mooring line. Two mooring lines are used to maintain the buoyancy position as intended. The arrangements of the mooring lines in three different water depths are described in Section 7.4. As described in Section 7.4.4, static equilibrium was established in mooring lines prior to performing the dynamic analysis. The results of the dynamic analysis are presented in Table 7-18 and Figure 7-22.

Table 7-18 Dynamic Responses on Mooring Line

Parameter	COBRA		
	Near Y	Intact	Far Y
Water Depth of 400 m			
Maximum Mooring Tension (kN)	2007.27	2036.01	2039.71
Water Depth of 1000 m			
Maximum Mooring Tension (kN)	1453.57	1519.26	1512.74
Water Depth of 1500 m			
Maximum Mooring Tension (kN)	1053.62	1161.61	1155.79

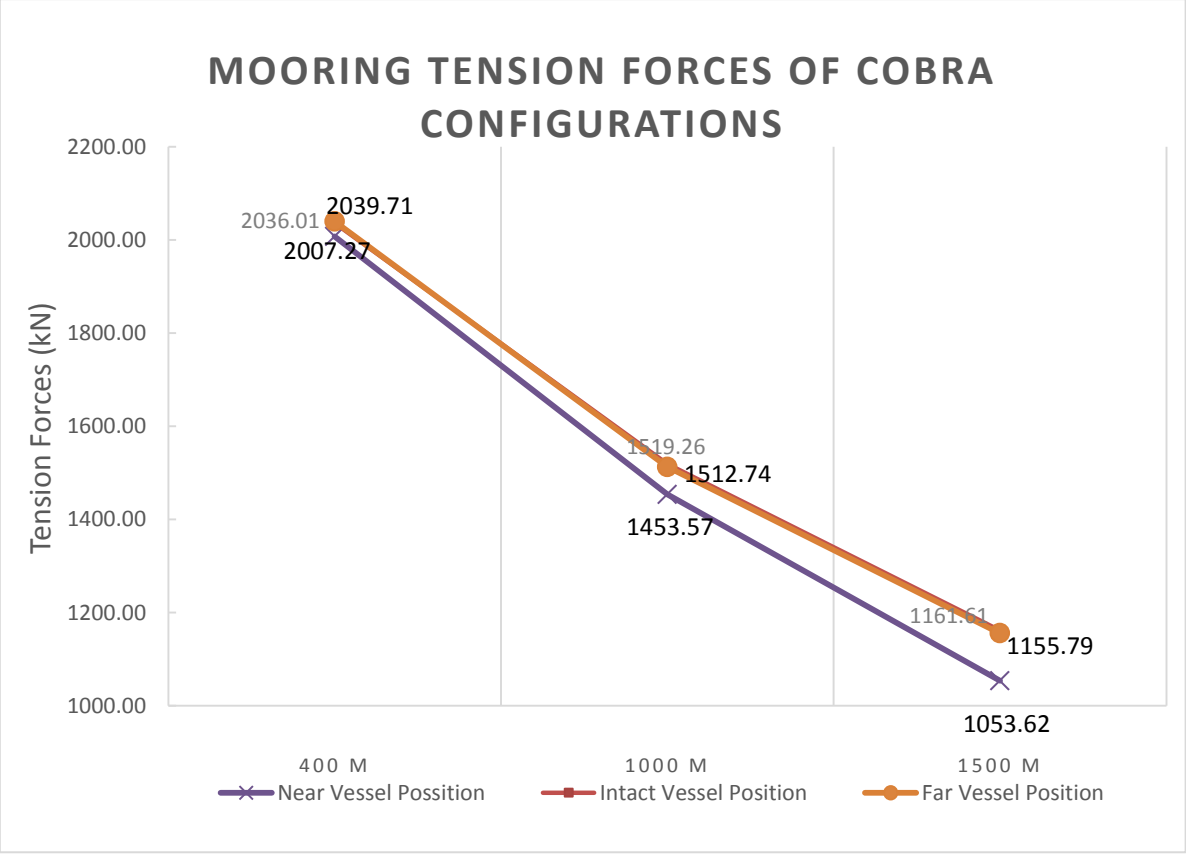

Figure 7-22 Dynamic Responses of Mooring Tensions for Each Vessel Position

As can be seen in Table 7-18, similar trends to those of the static response are established (refer to Section 7.4.4). The maximum tension load of 2039.71 kN in 400 m water depth is observed in the far vessel position. Figure 7-22 shows that there has been a gradual decrease in the level of maximum tension forces as the water depth increases. This result may explain by the fact that the buoyancy module is identically designed for all water depths. Meanwhile, the tension forces in the steel risers increase when the water depth increases. Thus, the mooring tension forces reduce as the water depth increases.

In order to examine the effect of wave frequency (WF) motions, Figure 7-23 compares the static and dynamic responses of mooring tensions.

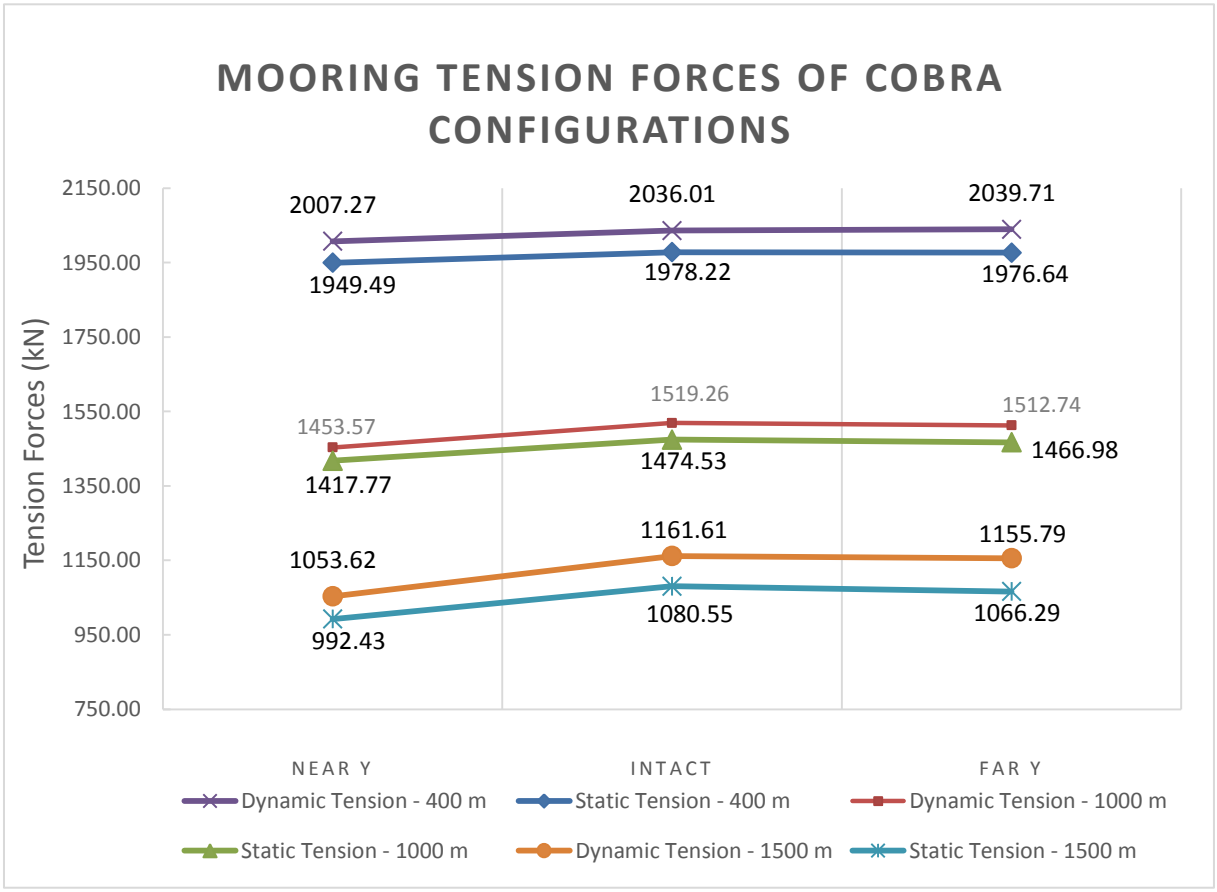

Figure 7-23 Static and Dynamic Responses of Mooring Tensions

From Figure 7-23, we can see that the dynamic responses in the mooring lines are slightly higher in the deeper water depths. The escalation rate of tension forces can reach up to 8% in 1500 m water depth and drop to 3 % in 400 m water depth. These findings suggest that the tension forces on mooring line shall be set higher to obtain fewer dynamic effects. This implies that relatively large buoyancy forces are required to attain high tension forces in the mooring line. However, this will result in improper design of the buoyancy modules. The optimum design may be obtained by a sensitivity study to design a suitable length for mooring lines and the lower tension of the steel risers; thus the proper design of the buoyancy module may be achieved.

7.6 Discussion

The main aim of this section is to present the summary results and discussions from the comparison study of the uncoupled riser configurations (i.e. SLOR and COBRA) in three different water depths; 400 m, 1000 m, and 1500 m. The summary results and discussions are described as follows:

- In general, the COBRA and the SLOR configurations have sufficient strength capacity to sustain all design load conditions in accordance with ultimate limit state (ULS) design.

- According to the results in Section 7.5, overall, the SLOR and the COBRA riser configurations perform an excellent job of decoupling excessive vessel motion in harsh environmental conditions, especially in the Norwegian Sea. Furthermore, the use of a flexible jumper as a connection between the buoyancy modules and the vessel effectively reduces the wave frequency (WF) effects of the vessel motions.

- According to Section 6.6, it has been observed in Section 7.5 that the flexible jumper arrangements for both riser configurations do not comply with the minimum design acceptance criteria in respect of the maximum departure angle. The highest departure angle of 16.71^0 in the SLOR configurations, which is more than the maximum allowable departure angle of 12.5^0, is observed in the far vessel position.

  The failure to comply with the maximum allowable departure angle can be solved by the following proposed solution. There is a possibility to introduce a larger opening on the 'Riser Guide Tube'. In the example, the proposed 'Riser Guide Tube' opening of 20^0 is used to accommodate the high departure angle of flexible jumpers during the far vessel position. Thus, the acceptance criteria for the departure angle of flexible jumpers can be revised to become 20^0 instead of the 12.5^0 from the previous acceptance criteria.

- As can be seen in Figure 7-8, Figure 7-13, and Figure 7-18, the dynamic effects at the sub-surface buoy are lower compared to the dynamic effects at the vessel. It is possible, therefore, that the use of flexible jumpers is effective in reducing vessel motions due to harsh environmental conditions. The results agree with the main function of the flexible jumper as described in Section 2.3.1.

- As described in Section 7.5.2, the hydrodynamic effects from the sea surface are reduced when the water depth increases. Thus, it is suggested that the sub-surface buoyancy module be set in deeper water depths away from the wave zone to reduce the hydrodynamic effects from the sea surface.

- The analysis results of the low frequency (LF) motions which are represented by the vessel offset, indicate that there is a strong relationship between the vessel offset and the minimum bending radius (MBR) of the flexible jumpers. According to the static

and the dynamic response results, the bending radius of the flexible jumpers increases when the distance from the vessel to the subsurface buoyancy module increases. Therefore, for both riser configurations in all water depths, the minimum bending radius of the flexible jumper is always observed in the near vessel condition.

- The studies have found that for the flexible jumper, the departure angle value on the vessel corresponds with the tension value on the flexible jumpers; a higher angle value results in higher tension loads. In consequence, the tension load at the vessel shall be carefully controlled because it may affect the hang off capacity of the turrets. In respect of turret designs, the lower tension load may be achieved by limiting the departure angle at the vessel.

- The results of the static and dynamic responses in the COBRA configurations show that a short layback distance in shallow water depth results in high bending stress near the 'Touch Down Point'. Thus, in order to reduce the bending stress, the COBRA configuration requires a broader area to lay down the steel risers which radially spread around the vessel.

  Furthermore, for the COBRA riser configurations, the steel riser angles at the buoy increase when the distance from the vessel to the subsurface buoyancy module decreases. This result may be explained by the fact that the highest vertical forces in the flexible jumper occurs in the near vessel position, which will pull the buoyancy module towards the horizontal position.

- The results of this chapter conclude that the COBRA riser configurations perform better when compared to the SLOR riser configurations. This is mainly due to several factors; the SLOR configurations should be examined with caution for items such as large declination angles at the buoy, and the buoyancy force requirements in order to configure the top-tensioned risers. As can be seen in Section 7.5, in the SLOR configurations, the small values of the declination angle at the buoyancy module results in high bending stress at the bottom connection point. To achieve a lower declination angle, the SLOR configurations require a relatively massive sub-surface buoyancy module to produce sufficient buoyancy force to keep the steel riser as straight as possible. On the other hand, the COBRA configurations show better behavior in dynamic response in respect of the lower stresses and the lower buckling UF at the steel risers for the deeper water depths. This finding suggests that in general, for the Norwegian Seas conditions, the steel riser arrangement in the COBRA configurations shows excellent dynamic behavior and robust design.

8. Accidental Study in Case of Iceberg Approach

8.1 Introduction

The main purpose of this chapter is to check the riser performances in the event of an iceberg approach in accordance with the Accidental Limit State (ALS). As described in DNV OS F201 (DNV, 2010a), the accidental conditions should be considered in the design stages in order to avoid a catastrophic accident in the riser system. Therefore, the design parameters in the ALS conditions shall be appropriately selected according to DNV OS F201 (DNV, 2010a), such as load effect factors, safety class resistance factor and material resistance factor which are listed in Table 4-3, Table 4-4 and Table 4-5, respectively.

The accidental analysis that is performed in this thesis is to examine the riser configurations in the case of an iceberg approach. Two solutions have been suggested in order to avoid iceberg collisions with the vessel; these are drift-off/side-step from the vessel or disconnecting the turret by using a disconnectable turret system. Each riser component is checked, and it is ensured that it conforms to the acceptable criteria in the event of an iceberg approach, according to Section 6.6. Two distinct water depths have been chosen (i.e. 400 m, and 1500 m) to compare the capability of the riser configurations in the different environmental conditions.

The solutions of the riser arrangements in ALS conditions are presented in two parts. The first part is described in Section 8.2 which will present vessel ‘drift off’ as a solution in the case of ice-berg approaches. The two riser configurations (SLOR and COBRA) are examined in two different water depths; at 400 m and 500 m. A similar riser arrangement to that used in Section 7.4.1 for 400 m water depth and in Section 7.4.3 for 1500 m water depth. To obtain the optimum riser arrangement during the accidental event, a sensitivity study is performed with regard to the minimum design criteria which are described in Section 6.6. The main purpose of the sensitivity study is to investigate the maximum distance of the vessel that could be reached by ‘drift off’ from the initial position to avoid the iceberg collisions. The vessel ‘drift off’ solution is the main concern of this thesis. Thus, from the initial conditions, the riser arrangements are designed in such a manner that the components are prepared to accommodate the possibility of vessel drift-off during the accidental event.

Section 8.3 presents the second solution for the riser configurations to avoid collision with icebergs, which is disconnecting the turret by using a disconnectable turret system. As described previously, two different water depths are purposely chosen to examine the behavior of riser performances during the accidental event. Similar riser configurations are established for 400 m and 1500 m water depth (refer to Section 7.3), except for the length of the flexible jumpers, which should be reduced to best suit the arrangement of the disconnectable system.

A three-hour dynamic simulation with 0.02-second time step is performed in accordance with Section 7.5. This method is used to simulate the three-hour storm duration in less time. Further dynamic analysis is presented in this chapter after static equilibrium is achieved by

analyzing the static responses. For the static responses, the summary results are provided in Appendix C.

8.2 Vessel Drift-Off

In the event of an iceberg approach, the vessel is expected to drift off from the initial position to avoid a collision. The maximum side-stepping distance is achieved by performing a sensitivity study on the riser configurations, taking into consideration the acceptance criteria in Section 6.6. To ensure the riser components are free form clashing during the accidental conditions, it is necessary to maintain sufficient clearance between each riser component. The minimum clearance between riser components is 7.0 m, which is measured from center to center of the riser components. The minimum clearance of 7.0 m is considered sufficient in the dynamic response analysis since the outside diameter of the flexible jumpers is 424 mm and the outside diameter of the steel risers is 306 mm.

The following sections describe the dynamic responses of accidental limit state (ALS) for the SLOR and the COBRA configurations. As described in the previous section, the riser configurations are installed in two distinct water depths (i.e. 400 m and 1500 m). The selected water depths are used to examine the maximum distance a vessel could drift off during the accidental event. The riser components, which comprise flexible risers and steel risers, are compared and checked in order to satisfy the minimum clearances and the minimum requirements in accordance with Section 6.6. In addition, the summary results of mooring lines for the COBRA configurations are presented in Appendix B.

8.2.1 Vessel Drift-Off in Water Depth of 400 m

According to Table 7-3 and Table 7-4, the riser arrangements in 400 m water depth configure the buoyancy module in 200 m water depth and 200 m shifted from the center-line of the vessel. For the initial riser configurations of SLOR and COBRA in 400 m water depth, refer to Figure 7-1 and Figure 7-2, respectively.

A sensitivity study is performed to obtain the maximum drifting distance of the vessel to avoid an iceberg collision. The study concludes that a 100 m drift is set as the maximum distance which the vessel could be reached to side-stepping in case of an ice-berg approach. The following paragraphs present the dynamic results of the riser configurations in the accidental events.

Flexible Jumper

According to Section 7.3, a flexible jumper length of 575 m is used to connect the steel riser section from the buoyancy module to the surface facility. The flexible jumpers are divided into three sections in accordance with the marine growth factor that should be applied on each section as described in Table 6-3. A similar division of the flexible jumpers to that used in Section 7.4.1 is used in this study.

The acceptance criteria of the flexible jumper shall also be fulfilled during the accidental cases. No compression load is allowed in the flexible jumper and the minimum bending radius

of 5.0 m shall be satisfied. In addition, a 7.0 m clearance radius of the flexible jumpers should be secured in order to avoid clashing during the accidental event. The dynamic results obtained from this study are presented in Table 8-1.

Table 8-1 Dynamic Response on Flexible Jumpers (400 m WD)

Parameter	COBRA		SLOR	
	Near Y	Far Y	Near Y	Far Y
Angle at vessel (deg)[1]	8.64	16.51	8.10	17.71
Angle at buoy (deg)[1]	6.42	15.19	7.51	17.49
Minimum bending radius (m)	7.50	47.77	10.55	55.66
Minimum clearance (m)	7.98	34.27	8.77	15.30
Maximum water depth (m)[2]	385.53	343.92	381.50	336.65
Minimum tension (kN)	20.83	111.40	29.66	125.76
Maximum tension at vessel (kN)	1476.47	1516.92	1472.63	1529.92
Maximum tension at buoy (kN)	679.73	731.48	685.39	749.19

Notes:
[1)] The angle is measured relative to the vertical axis and taken from the max. value of the responses.
[2)] The distance is measured from Mean Sea Level (MSL).

The results, as shown in Table 8-1, indicate that the minimum tension load and the minimum bending radius satisfy the minimum design requirements. Interestingly, the tension load corresponds with the bending radius where the minimum value is always observed in the near vessel position (refer to Section 7.6). A minimum tension load of 20.83 kN is found in the COBRA configurations in correspondence with a minimum bending radius of 7.50 m. Furthermore, it can be seen in Table 8-1 that the minimum clearance of the flexible jumper is 7.98 m for the COBRA configurations in the near vessel position.

However, the flexible jumper angles at the vessel for both riser configurations do not comply with the acceptance criteria of the departure angle, which is 12.5^0. The maximum departure angle observed in the SLOR configurations is 17.71^0 in the far vessel position. According to Section 7.6, a 20^0 'Riser Tube' opening is proposed to accommodate the higher departure angle of the flexible jumpers during far vessel position. The static riser arrangements for the vessel drift-off case can be found in Figures 8-1 and 8-2 for the SLOR and the COBRA configurations respectively.

This study has found that generally the flexible jumpers for both riser configurations are able to perform vessel drifting of 100 m in the event of an iceberg approach, although, a larger 'Riser Tube' opening is required to accommodate a higher departure angle in the far vessel position. Moreover, the clearance radius of the flexible jumper fulfills the minimum clearance criteria. Therefore, it can be ensured that the flexible jumper arrangements are free from any clashing issue during the accidental events.

Steel Riser

Two different steel riser arrangements are used for the SLOR and the COBRA configurations. As described in Section 7.4.1, the top-tensioned riser and steel catenary riser are configured for the SLOR and the COBRA steel riser arrangements, respectively. By this means, contrasting results are expected in the dynamic responses, especially in respect of the tension forces. In these cases, the steel risers should also satisfy the minimum design criteria as described in Section 6.6.

The results of dynamic responses due to the vessel side-stepping are compared between the SLOR and the COBRA configurations in Table 8-2.

Table 8-2 Dynamic Response on Steel Risers (400 m WD)

Parameter	COBRA		SLOR	
	Near Y	Far Y	Near Y	Far Y
Angle at buoy (deg)[1]	4.69	2.96	2.27	2.12
Maximum tension at buoy (kN)	326.96	280.65	4870.88	4909.04
Minimum tension at seabed (kN)	62.08	13.74	4392.46	4374.86
von Mises stress at buoy (Mpa)	149.71	149.69	168.22	168.50
von Mises stress on steel riser (Mpa)	121.40	120.45	127.49	127.51
von Mises stress at seabed (Mpa)	137.26	148.70	126.92	126.90
Maximum buckling UF at buoy	0.05	0.05	0.10	0.10
Maximum buckling UF at steel riser	0.61	0.68	0.05	0.05
Maximum buckling UF at seabed	0.22	0.26	0.04	0.04

Note:
[1)] The angle is measured relative to the buoy and taken from the max. value of the responses.

From the data in Table 8-2, the results show that the steel risers for both configurations have sufficient strength to perform in the accidental conditions. The maximum bucking utilization factor (UF) in the COBRA configurations is 0.68 during the far vessel position, which satisfies the acceptance criteria of the buckling UF. The COBRA's steel riser behavior is recognized in this study to be similar to that observed in the results in Section 7.5.1. The short lay-back distance for the COBRA configurations in 400 m water depth results in high bending stress near 'Touch Down Point'. As expected, the distinct tension forces are observed in the SLOR and the COBRA configurations due to the different arrangement of the steel risers.

The static riser arrangements for the SLOR and COBRA configurations for the drift off case in 400 m water depth are presented in Figure 8-1 and Figure 8-2 respectively.

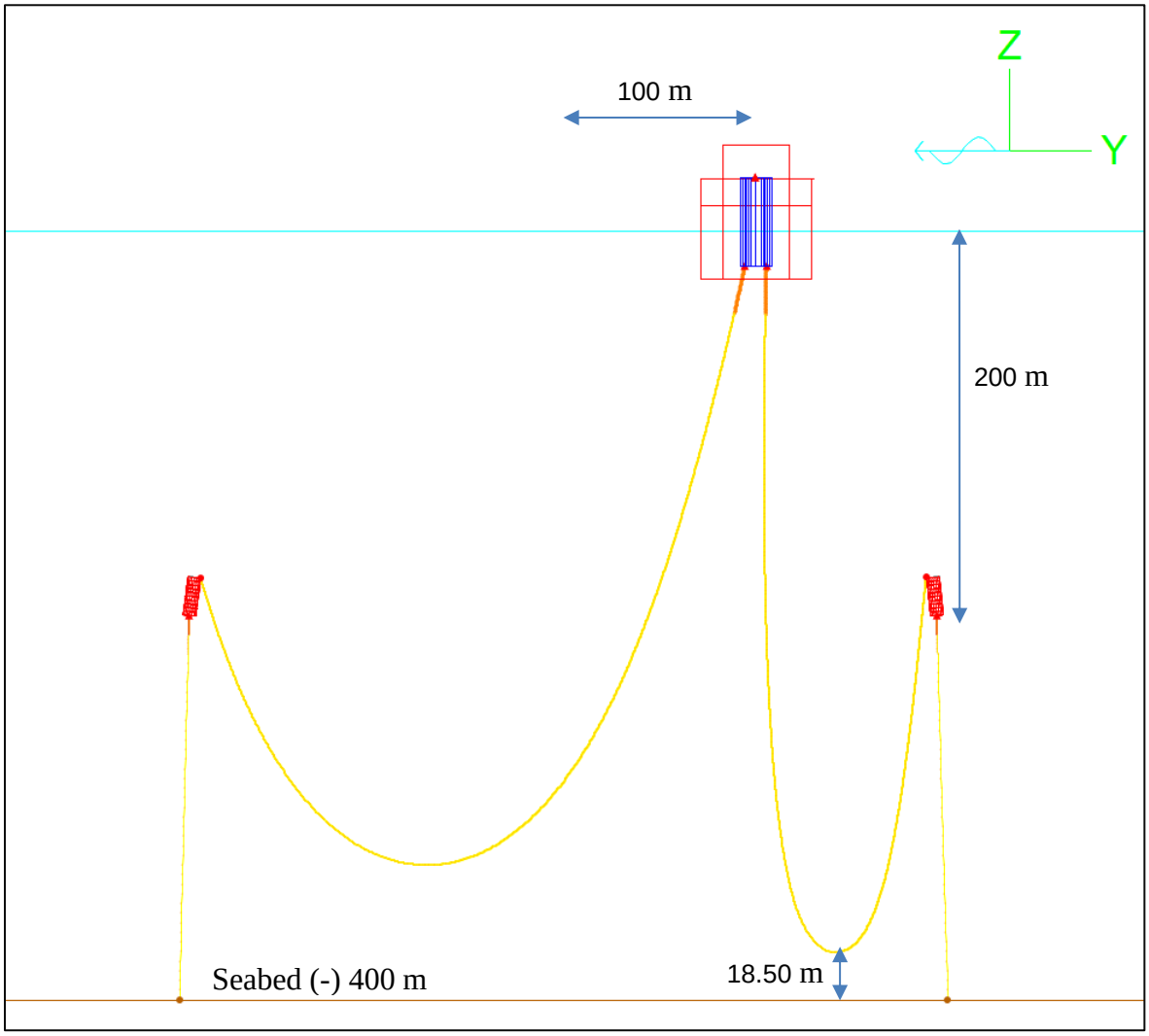

Figure 8-1 Static Riser Configurations in 400 m Water Depth (SLOR Configurations)

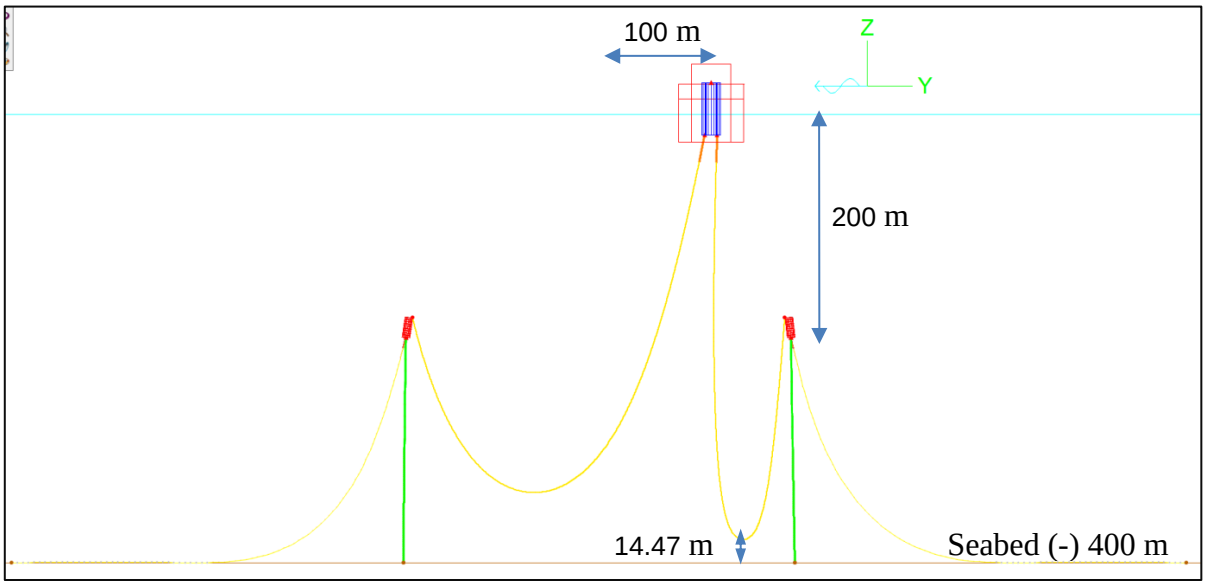

Figure 8-2 Static Riser Configurations in 400 m Water Depth (COBRA Configurations)

Taken together with the flexible jumper results, the present results indicate that both riser configurations have the ability to perform a 100 m drift-off in the event of an iceberg approach. It has been suggested that the larger 'Riser Guide' opening of 20^0 is required in both riser configurations to accommodate the larger departure angle of the flexible jumpers at the vessel. In general, the results in this study produce similar riser behavior to that of the base case study for the riser configurations in 400 m water depth, as described in Section 7.5.1.

8.2.2 Vessel Drift Off in Water Depth of 1500 m

The riser arrangements in this study are adopted from the base case riser arrangements from the ULS study in 1500 m water depth. According to Section 7.4.3, for the riser configurations in 1500 m water depth, the subsurface buoyancy modules are located in 300 m water depth and shifted 350 m from the center line of the vessel. The initial riser arrangements in 1500 m water depth for the SLOR and the COBRA configurations can be found in Figure 7-6 and Figure 7-5, respectively.

As described in the previous section, a sensitivity study is performed to obtain the maximum drift-off distance of the vessel in order to avoid iceberg collision. The minimum design requirements, which are described in Section 6.6, are used as design limitations to verify the acceptance of the sensitivity study. The minimum clearances of 7.0 m should be satisfied in order to ensure the riser is free from any clashing issue. Based on the study for both riser configurations in 1500 m water depth, a 250 m vessel drifting can be achieved in the event of an iceberg approach.

The summary results and discussions for the dynamic responses of the riser configurations in 1500 m water depth are presented in the following paragraphs. In addition, the summary results of the mooring lines for the COBRA configurations can be found in Appendix C.

Flexible Jumper

Similar arrangements to those of the base case study are used for this accidental case. The general arrangements of flexible jumpers in 1500 m water depths are described in Section 7.4.3. The flexible jumpers are divided into three different sections to consider the marine growth effect on the jumpers (refer to Table 6-3).

The flexible jumpers shall have the acceptable design limitation to perform the operational function in the accidental conditions. Therefore, the minimum design requirement with sufficient clearance should be satisfied in the flexible jumper, as described in Section 6.6. The results obtained from the dynamic analysis of the flexible jumpers in the SLOR and the COBRA configurations are presented in Table 8-3.

Table 8-3 Dynamic Response on Flexible Jumpers (1500 m WD)

Parameter	COBRA		SLOR	
	Near Y	Far Y	Near Y	Far Y
Angle at vessel (deg)[1]	6.90	19.31	7.72	17.07
Angle at buoy (deg)[1]	4.18	21.64	2.52	17.26
Minimum bending radius (m)	14.31	129.14	5.75	99.72
Minimum clearance (m)	8.23	20.46	7.97	18.96
Maximum water depth (m)[2]	641.47	532.46	650.06	555.71
Minimum tension (kN)	37.82	296.14	13.03	241.86
Maximum tension at vessel (kN)	2501.81	2607.54	2496.64	2575.39
Maximum tension at buoy (kN)	1166.79	1340.07	1157.10	1278.71

Notes:
[1)] The angle is measured relative to the vertical axis and taken from the max. value of the responses.
[2)] The distance is measured from Mean Sea Level (MSL).

The results of this study indicate that the flexible jumpers in both riser configurations have sufficient strength and capacity to sustain the designated loads during the vessel's drift-off from the initial position. By using these configurations, the flexible jumper is confirmed safe to perform a 250 m vessel drift-off in the event of an iceberg approach. As can be seen in Table 8-3, there is no compression load observed at the flexible jumpers. Furthermore, the minimum bending radius and the minimum clearance radius of the flexible jumpers fulfill the minimum design requirements. Based on the dynamic response results in the accidental case, the COBRA configurations have better riser performances than the SLOR configurations. These are indicated by the minimum bending radius (5.75 m) and the minimum clearance radius (7.97 m), which are observed in the SLOR riser configurations.

Unfortunately, the departure angles for both riser configurations in the far vessel position are higher than the maximum requirements as described Section 6.6. A maximum departure angle of 19.31^0 in the COBRA configurations is observed in the far vessel position. The proposed solution is presented in Section 7.6; a 20^0 'Riser Tube' opening may be used to accommodate the high departure angle in the far vessel position. The static riser configurations are presented in Figure 8-4 and Figure 8-5 to illustrate the riser arrangements during the 250 m vessel side-stepping.

In general, the flexible jumpers for the SLOR and the COBRA configurations are sufficiently acceptable enough to perform a 250 m drifted-off to avoid an ice-berg collision during the accidental conditions with a note that the 'Riser Tube' opening of 20^0 should be used to accommodate a higher departure angle in the far vessel position. As described in Table 8-3, the clearance radius of the flexible jumper is sufficient to ensure that, according to the analysis results, the clashing issue in the flexible jumper will not occur during the accidental conditions. Therefore, the riser configurations have an acceptable design in respect of vessel drift off solutions.

Steel Riser

The description of the steel riser arrangements of the SLOR and the COBRA configurations that are used in 1500 m water depth can be found Section 7.4.3. According to the dynamic results in ULS conditions (refer to Section 7.5.3), the steel riser is expected to have a robust design due mainly to the fact that the vessel motion effects are already decoupled by the arrangement of a flexible jumper and a buoyancy module. In this study, the vessel drifts off from the initial position to avoid an iceberg collision. By means of these, a 250 m vessel offset is applied to observe the performance of the steel risers in the accidental conditions.

The results obtained from the dynamic responses due to vessel side-stepping in the SLOR and the COBRA configurations are presented in Table 8-4.

Table 8-4 Dynamic Response on Steel Riser (1500 m WD)

Parameter	COBRA		SLOR	
	Near Y	Far Y	Near Y	Far Y
Angle at buoy (deg)[1]	7.18	2.06	1.26	4.45
Maximum tension at buoy (kN)	1731.73	1802.34	4310.42	4439.31
Minimum tension at seabed (kN)	338.36	313.08	2853.27	2830.54
von Mises stress at buoy (Mpa)	149.01	149.24	161.51	162.37
von Mises stress on steel riser (Mpa)	118.61	118.60	123.35	123.56
von Mises stress at seabed (Mpa)	116.43	116.61	278.75	281.46
Maximum buckling UF at buoy	0.06	0.06	0.08	0.08
Maximum buckling UF at steel riser	0.25	0.25	0.30	0.31
Maximum buckling UF at seabed	0.12	0.12	0.17	0.17

Note:
[1)] The angle is measured relative to the buoy and taken from the max. value of the responses.

As expected, the steel risers for both riser configurations have an acceptable design in the accidental conditions which are indicated by lower values of buckling utilization factor (UF). From the results in Table 8-4, a maximum buckling UF of 0.31 in the SLOR configurations is observed in the far vessel position. However, for the SLOR configurations, the top steel riser angle should be examined with caution. According to Section 7.6, the small values of the declination angle at the buoyancy module result in high von Mises stress at the bottom connection point. The maximum stress observed in the SLOR configurations is 281.46 MPa in the far vessel position. On the other hand, the sufficient lay back distance in the COBRA configurations results in lower von Mises stress in the steel catenary risers. These findings agree with the results in the earlier study (refer to Section 7.5.3). In general, the steel riser arrangements for both configurations have sufficient capacity to perform a 250 m vessel side-stepping in the event of an ice-berg approach.

The static riser arrangements for the SLOR and COBRA configurations for the drift-off case in 1500 m water depth are presented in Figure 8-3 and Figure 8-4, respectively.

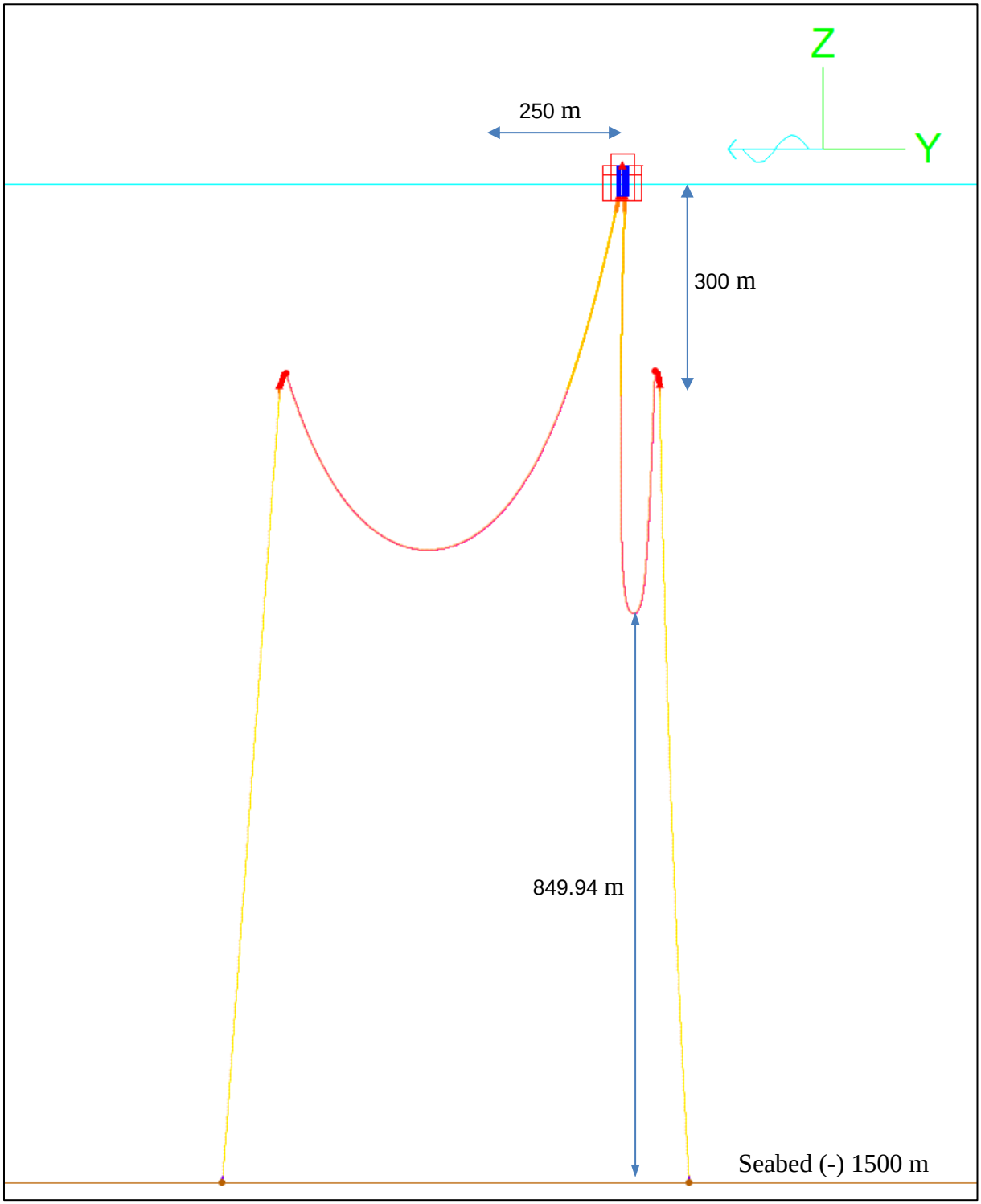

Figure 8-3 Static Riser Configurations in 1500 m Water Depth (SLOR Configurations)

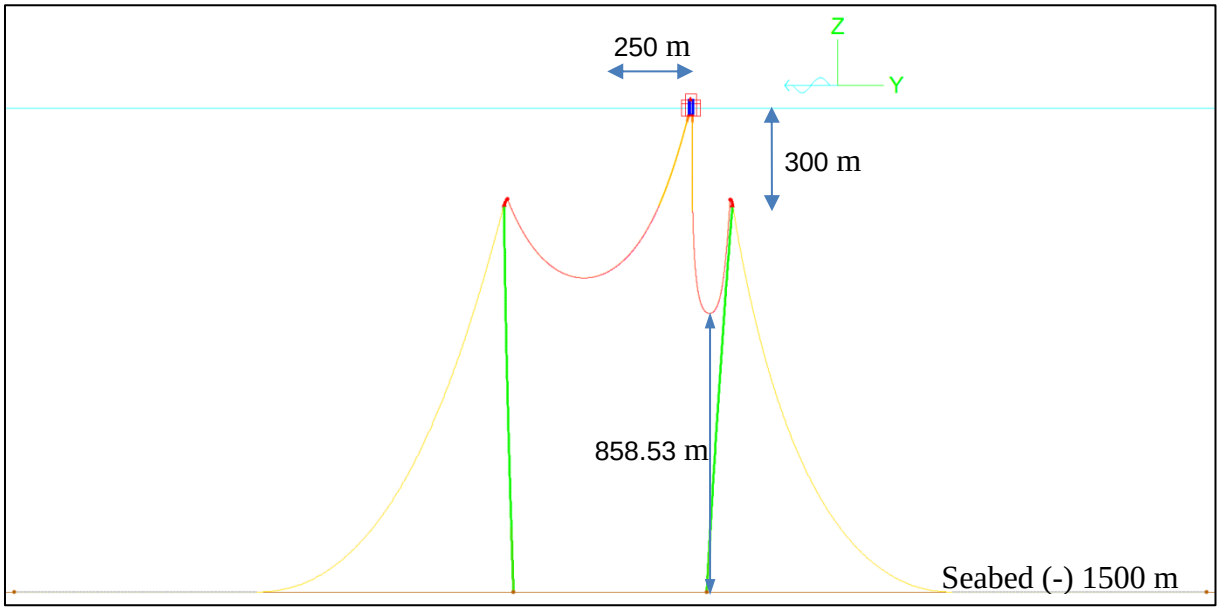

Figure 8-4 Static Riser Configurations in 1500 m Water Depth (COBRA Configurations)

The results of this study show that, the uncoupled riser configurations in 1500 m water depth are capable of 250-m drift-off in line with the riser lay directions in order to avoid an iceberg collision. The study has demonstrated, for the first time, that the uncoupled riser configurations in 1500 m water depth have the ability to side-step as an accidental solution in the event of an iceberg approach. In addition, the 'Riser Guide' opening of 20^0 is suggested for both riser configurations to accommodate the larger departure angle of the flexible jumpers.

8.3 Disconnecting Turret System

The disconnectable turret system is an alternative design, allowing the turret to disconnect and the vessel to sail away to avoid iceberg collisions. The turret shall be designed to have a buoyancy module with sufficient buoyancy forces in order to support the flexible jumpers in the water during the disconnecting operation. The main aim in this analysis is to ensure all riser components remain safe and have sufficient strength to sustain the design loads during the accidental conditions. The detail of disconnecting and reconnecting the turret systems is not the main focus in this thesis. Therefore, this thesis only confirms the adequacy of the riser components and the minimum buoyancy forces that are required in the event of an iceberg approach.

As mentioned in Section 6.5, the riser configurations are examined for the water depth of 400 m and 1500 m to evaluate the accessibility of the turret system in two distinct environmental conditions. Similar riser arrangements of the SLOR and the COBRA configurations to those described in Section 7.4.1 and 7.4.3 are used in this study, except the flexible jumper lengths should be modified to best suit the riser arrangements for the disconnectable turret system. In fact, a shorter flexible jumper length compared to the previous study (refer to Section 8.2) is required since the vessel drift-off is not applicable for this turret system. The revised riser

arrangements for the SLOR and COBRA configurations are presented in Table 8-5 and Table 8-6, respectively.

Table 8-5 SLOR Configuration for Disconnectable Turret System

Parameters	Water Depth	
	400 m	1500 m
Flexible Jumper Length	375	650
Steel Riser Length	200	1200
Buoyancy Location (m)[1]	200	300
Buoyancy Shift (m)[2]	200	350

Notes:
1) Location is measured from a vertical distance relative to MSL.
2) Shifting is measured from a horizontal distance relative to the centerline of the vessel.

Table 8-6 COBRA Configuration for Disconnectable Turret System

Parameters	Water Depth	
	400 m	1500 m
Flexible Jumper Length	375	650
Steel Riser Length	470	2270
Buoyancy Location (m)[1]	200	300
Buoyancy Shift (m)[2]	200	350
Mooring Length (m)[3]	200	1200

Notes:
1) Location is measured from a vertical distance relative to MSL.
2) Shifting is measured from a horizontal distance relative to the centerline of the vessel.
3) Mooring length is measured for each line.

The dynamic responses of the riser configurations are analyzed in accordance with the accidental limit state (ALS) conditions. The analysis results are divided into two sections according to the different water depths. In brief, Section 8.3.1 and Section 8.3.2 present the summary results and discussions of the dynamic responses for the riser configurations in 400 m and 500 m water depths, respectively. In each section, the results of the flexible jumpers and the steel risers for the SLOR and the COBRA configurations will be discussed. In addition, the mooring line results for the COBRA configurations are presented in Appendix C.

8.3.1 Disconnectable Turret in Water Depth of 400 m

The riser arrangements are configured by using similar arrangements to those for the intact conditions, except the flexible jumper length is reduced in order to satisfy the minimum length of flexible jumper in the ULS conditions. The arrangements of the SLOR and the COBRA configurations for the disconnectable turret system in 400 m water depth can be found in Table 8-5 and Table 8-6, respectively.

At the time when the buoyancy module of the turret is launched into the water, it is expected that the turret will have the same elevation as the subsurface buoyancy module (i.e. in 200 m water depth). To attain that elevation, a minimum buoyancy force is suggested in this report as a preliminary input for designing the disconnecttable buoyancy module on the turret system. The dynamic results of the flexible jumpers and the steel risers for the SLOR and the COBRA configurations during the disconnectable operation are presented in the following paragraphs.

Flexible Jumper

The flexible jumpers are modeled in two sections to represent the different marine growth effects in respect of water depths. Therefore, similar flexible jumper properties to those used in Section 7.4.1 are used in this study. Similar acceptance criteria to those in Section 6.6 are also applicable in this accidental study, because the riser components are expected to be operated in normal conditions after the turret system is reconnected to the vessel. The dynamic results of the flexible jumpers for the SLOR and COBRA configurations during disconnection of the turret are presented in Table 8-7.

Table 8-7 Dynamic Responses on Flexible Jumpers (400 m WD)

Parameter	COBRA	SLOR
Angle at vessel (deg)[1]	10.76	12.36
Minimum bending radius (m)	15.39	21.62
Maximum water depth (m)[2]	378.28	370.21
Minimum tension (kN)	48.32	67.27
Maximum tension at vessel (kN)	1210.82	1195.38
Maximum tension at buoy (kN)	1210.82	1195.38

Notes:
[1)] The angle is measured relative to the vertical axis and taken from max. angle value of the responses prior to the turret launching.
[2)] The distance is measured from Mean Sea Level (MSL).

The results in Table 8-7 indicate that the flexible jumpers have sufficient capacity to perform disconnectable turret operations. A minimum bending radius of 15.39 m is observed in the COBRA configurations in accordance with the minimum tension of 48.32 kN. In the water depth of 400 m, the lowest part of the flexible jumper is located at 378.28 m below the sea surface. Furthermore, a maximum departure angle prior to launch of 12.36^0 is found in the SLOR configurations. From these findings, according to Section 6.6, it is clear that all design parameters of the flexible jumpers in 400 m water depth satisfy the minimum design requirements.

In addition, it is important to provide the final geometry of the turret buoyancy module in the water in order to ensure that the riser configurations are sufficiently safe to perform the disconnectable turret operations. Table 8-8 provides information of the turret geometry in the water after disconnection from the vessel.

Table 8-8 Turret Geometry (400 m WD)

Parameter	COBRA	SLOR
Required Buoyancy Forces at Turret (kN)	1203.28	1203.28
Maximum Water Depth at Turret (m)[1]	213.93	212.42

Note:
[1)] The distance is measured from Mean Sea Level (MSL).

As can be seen from Table 8-8, a similar buoyancy force of 1203.28 kN is required in both configurations. From these results it seems possible that an identical flexible jumper length can be used for this study (refer to Table 8-5 and Table 8-6). As expected, the deepest position of the disconnectable turret is located almost in the same elevation with the subsurface buoyancy modules. As described in Table 8-8, the turret elevation in the COBRA configurations (213.93 m) is slightly deeper than the turret position in the SLOR configurations (212.42 m).

Steel Riser

As explained previously, the steel riser is expected to have contrasting dynamic results due to the fact that the steel riser arrangements for the SLOR and the COBRA differ in every aspect. Similar steel riser arrangements for each riser configurations to those described in Section 7.4.1 are used in this study.

The following table presents the dynamic results of the steel risers in the SLOR and the COBRA configurations during the disconnecting operation.

Table 8-9 Dynamic Responses on Steel Risers (400 m WD)

Parameter	COBRA	SLOR
Angle at buoy (deg)[1]	5.16	3.80
Maximum tension at buoy (kN)	344.76	5151.83
Minimum tension at seabed (kN)	4.80	4384.67
von Mises stress at buoy (Mpa)	149.72	170.30
von Mises stress on steel riser (Mpa)	121.33	128.28
von Mises stress at seabed (Mpa)	155.27	127.73
Maximum buckling UF at buoy	0.05	0.09
Maximum buckling UF at steel riser	0.72	0.04
Maximum buckling UF at seabed	0.27	0.04

Notes:
[1)] The angle is measured relative to the buoy and taken from max. angle value of the responses.

As shown in Table 8-9, a maximum buckling utilization factor (UF) of 0.72 is observed in the COBRA configurations. Moreover, in accordance with the maximum buckling UF, a maximum von Mises stress of 155.27 MPa is found in the 'Touch Down Point' of the COBRA configurations. Interestingly, the results from this table will now be compared to the

results in Table 7-6 to discover whether a similar response from the steel riser is observed in the vessel intact position.

As expected, a contrasting result is obtained in the SLOR's steel riser configurations. The top-tensioned steel riser arrangement in the SLOR configuration produces the maximum tension of 5151.83 kN. Due to this high tension force in the steel risers, a low buckling UF of 0.09 is found in the SLOR configurations. The final riser arrangements of the disconnectable turret are illustrated in and Figure 8-5 and Figure 8-6 for the SLOR and the COBRA configurations, respectively.

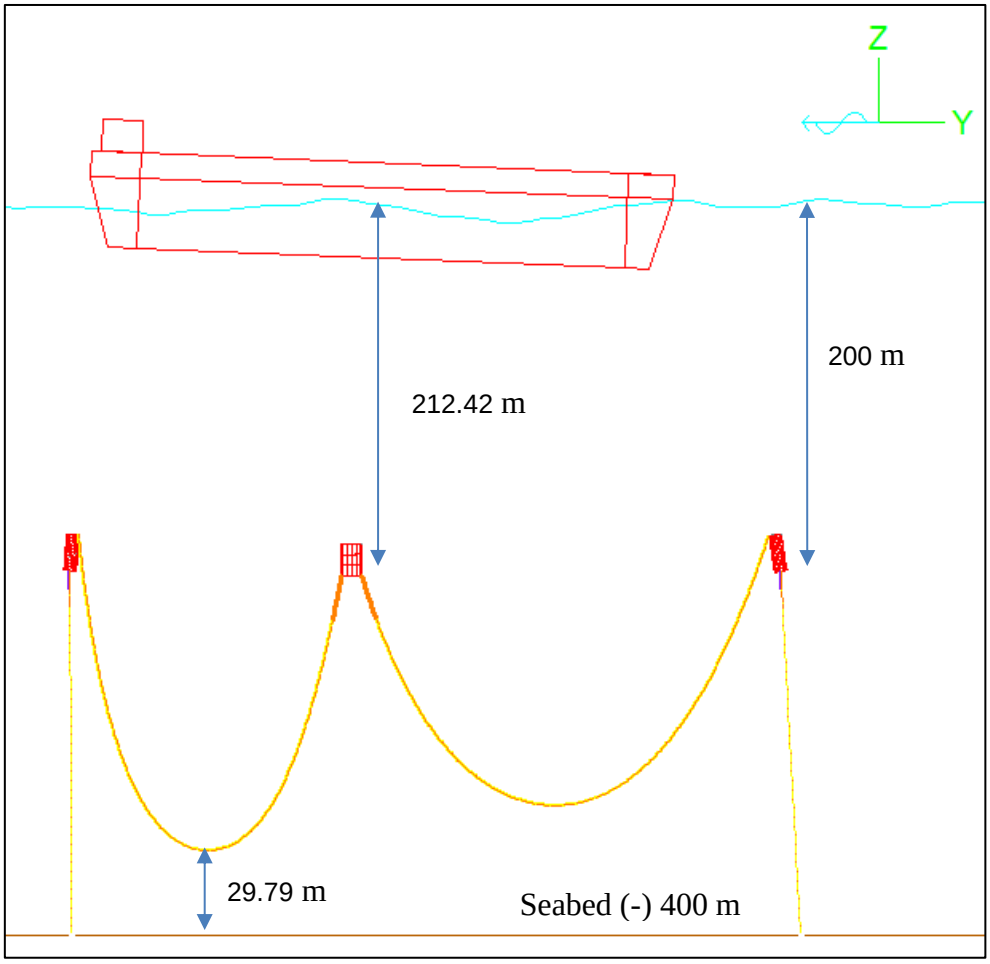

Figure 8-5 Final Turret Positions in 400 m Water Depth (SLOR Configurations)

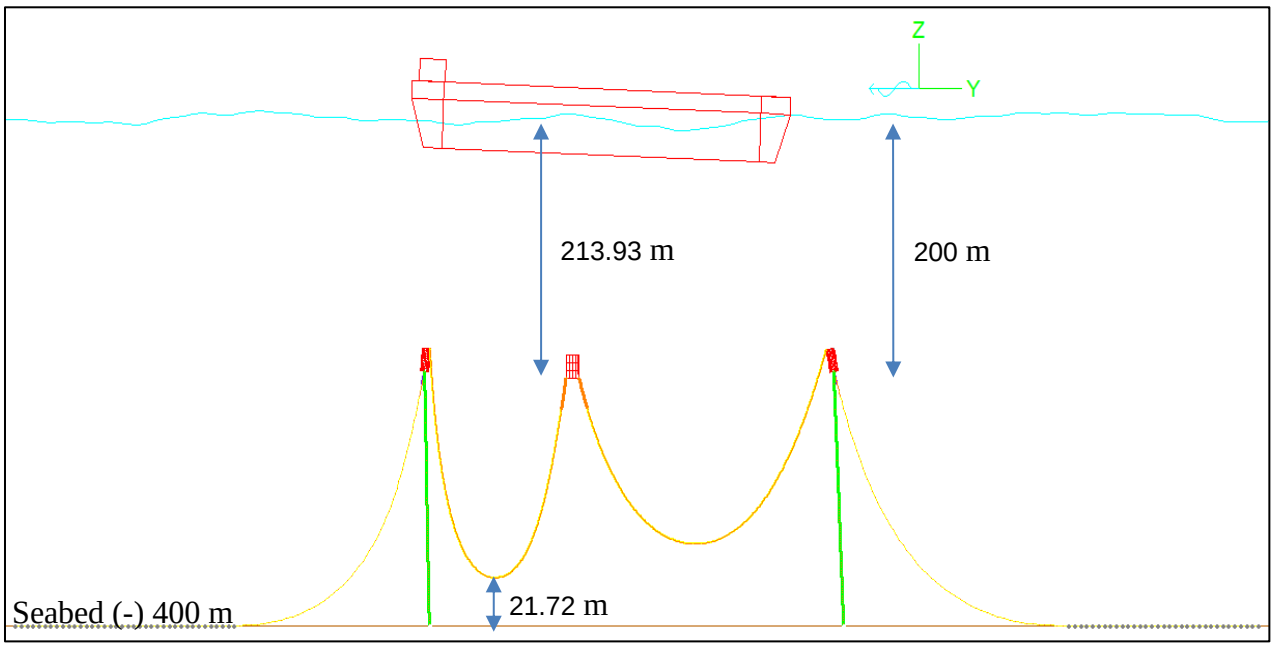

Figure 8-6 Final Turret Positions in 400 m Water Depth (COBRA Configurations)

From the results in Table 8-9, it is confirmed that the steel risers in both riser configurations have sufficient strength to perform the disconnectable turret operation in the event of an iceberg approach. This study has shown that similar riser behavior can also be found in the steel riser responses in 400 m water depth during intact condition (refer to Table 7-6).

8.3.2 Disconnectable Turret in Water Depth of 1500 m

It can be seen in Table 8-5 and Table 8-6 that the flexible jumper length is reduced to 650 m from 1000 m in the base case study (refer to Section 7.3). In this study, the disconnectable turret system is used to disconnect the turret in the event of an iceberg approach; thus there is no requirement for the vessel to side-step at a certain distance. Therefore, the flexible jumper length is set only to satisfy the minimum requirement of departure angles (refer to Section 6.6).
As described in Section 8.3.1, the same principle of the disconnectable turret is also applied for this water depth. In ideal conditions, the buoyancy module of the turret is going to be set at the same elevation as that of the subsurface buoyancy module, which is in 300 m water depth. The riser components are also confirmed to have similar design requirements to those described in Section 6.6. By this means, the riser configurations are expected to normally operate right after the reconnecting operations.

Flexible Jumper

The dynamic response analysis will ensure that the flexible jumper has sufficient strength and suitable configurations to perform the disconnectable operation in accordance with accidental limit state (ALS) conditions. In this section, the minimum buoyancy requirement is also suggested for the turret design in order to maintain the flexible jumpers in the designated water depth.

Similar flexible jumper geometries and properties to those employed in Section 7.4.3 are used in this study. The results obtained from the dynamic response of flexible jumpers for both riser configurations are presented in Table 8-10.

Table 8-10 Dynamic Responses on Flexible Jumpers (1500 m WD)

Parameter	COBRA	SLOR
Angle at vessel (deg)[1]	12.42	11.00
Minimum bending radius (m)	53.53	41.03
Maximum water depth (m)[2]	573.64	584.01
Minimum tension (kN)	107.13	80.96
Maximum tension at vessel (kN)	1929.49	1915.19
Maximum tension at buoy (kN)	1104.36	1083.94

Notes:
1) The angle is measured relative to the vertical axis and taken from max. angle value of the responses prior to the turret launching.
2) The distance is measured from Mean Sea Level (MSL).

From the results in Table 8-10, it is clear that the flexible jumpers in both riser configurations satisfy the minimum design requirement which is described in Section 6.6. This is indicated by the following parameters: no compression load is observed on the flexible jumpers and the minimum bending radius of 41.03 m is found in the SLOR configurations. Furthermore, a maximum departure angle of 12.42^0 in the COBRA configurations fulfills the requirement of the departure angle at the vessel. In addition, the lowest flexible jumper position when the turret is disconnected is 584.01 m below the sea surface.

For the disconnectable turret system, an additional result is provided in Table 8-11. In this table, the final position of the turret is ensured at the intended elevation. Furthermore, the current study also suggests the preliminary data for designing the buoyancy module in the turret system. The information about the turret geometry during the dynamic responses is presented in Table 8-11.

Table 8-11 Turret Geometry (1500 m WD)

Parameter	COBRA	SLOR
Required Buoyancy Forces at Turret (kN)	2134.91	2134.91
Maximum Water Depth at Turret (m)[1]	297.74	297.76

Note:
1) The distance is measured from Mean Sea Level (MSL).

As described in Table 8-11, a buoyancy force of 2134.91 kN is required to maintain the position of the turret system in the designated water depth. Similar buoyancy forces are required to support an identical flexible jumper for both riser configurations. As expected, the final position of the disconnectable turret is located almost in the same elevation as that of the subsurface buoyancy module which is located in 300 m water depth. The minimum water depth for the turrets in the water is around 298 m below the sea surface.

Steel Riser

The dynamic results in steel risers are expected to be identical with the initial configurations in the base case condition, since the steel risers in the uncoupled riser configurations are less affected by the wave frequency (WF) from the floater motions. Furthermore, in this study the flexible jumper is disconnected from the vessel. Thus, after the disconnecting operations, the flexible jumper is free from the vessel motion effects.

The detailed description of the uncoupled riser configurations, which are used in this study, can be found in Section 7.4.3. Table 8-12 presents the dynamic response summary of the steel risers for SLOR and COBRA, respectively.

Table 8-12 Dynamic Responses on Steel Riser (1500 m WD)

Parameter	COBRA	SLOR
Angle at buoy (deg)[1]	3.96	3.75
Maximum tension at buoy (kN)	1922.92	5074.60
Minimum tension at seabed (kN)	260.46	2944.75
von Mises stress at buoy (Mpa)	149.61	166.95
von Mises stress on steel riser (Mpa)	118.90	125.50
von Mises stress at seabed (Mpa)	117.79	299.48
Maximum buckling UF at buoy	0.06	0.09
Maximum buckling UF at steel riser	0.30	0.36
Maximum buckling UF at seabed	0.13	0.20

Notes:
[1)] The angle is measured relative to the buoy and taken from max. angle value of the responses.

As shown in Table 8-12, it can be concluded that the analysis results for the steel risers in both configurations satisfy the minimum design requirement which is described in Section 6.6. The maximum buckling utilization factor (0.36) and von Mises stress (299.48 MPa) are observed in the SLOR riser configurations. This is mainly due to the relatively high declination angle (3.75^0) occurring on the top-tensioned riser configurations in 1500 m water depth. For the SLOR configurations in deep water, the small riser top angle can cause higher stress at the bottom connection point.

In contrasts, the COBRA configurations have relatively lower buckling UF and von Mises stress in comparison to the SLOR configurations. It can thus be suggested that the longer lay back distance in 1500 m water depth may reduce the bending stress near the 'Touch Down Point'. The findings of this study produce similar results to those of the steel risers for the base case study in 1500 m water depth (refer to Section 7.5.3). The final arrangements for both riser configurations are illustrated in the following figures.

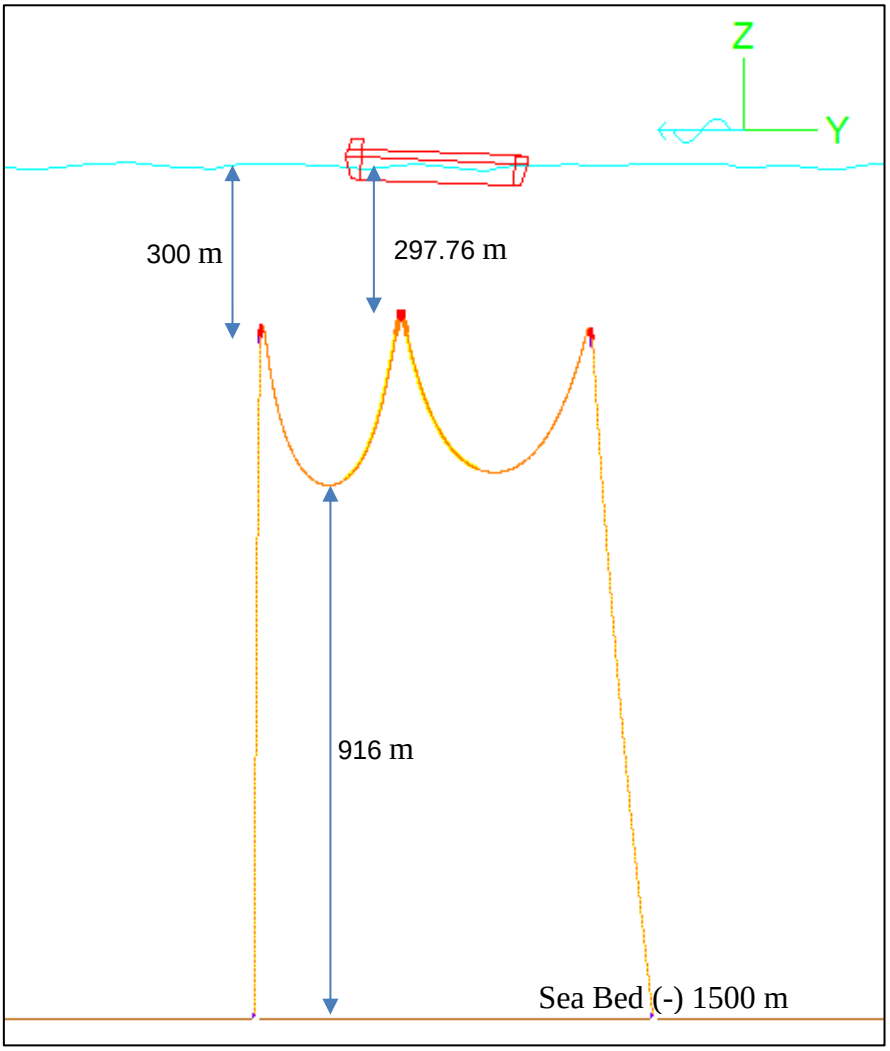

Figure 8-7 Final Turret Positions in 1500 m Water Depth (SLOR configurations)

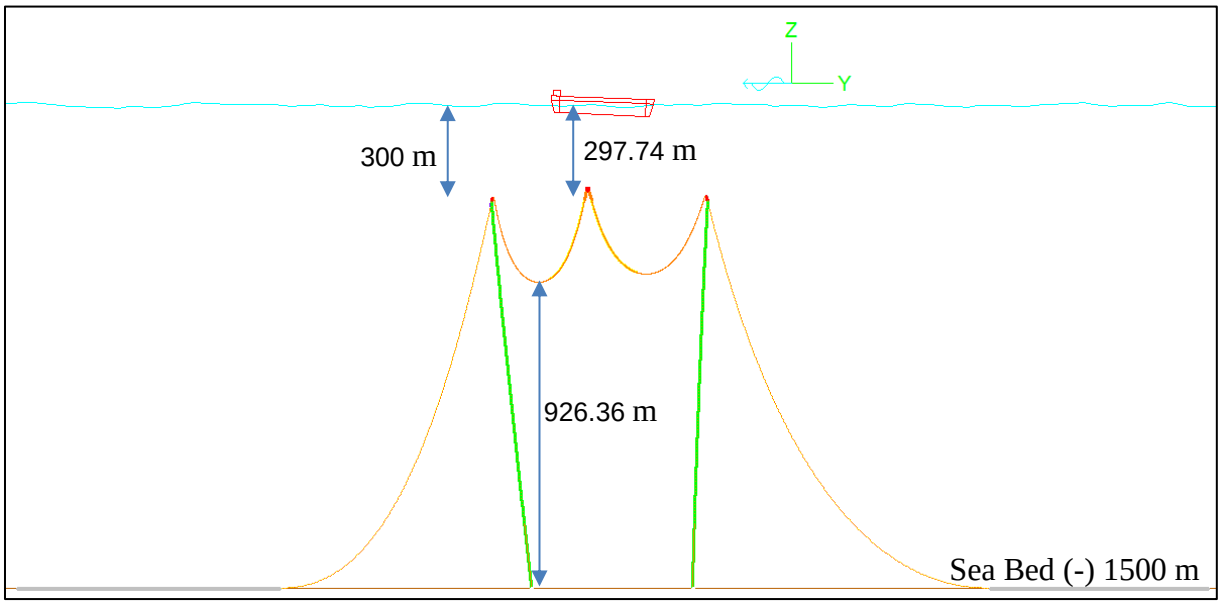

Figure 8-8 Final Turret Positions in 1500 m Water Depth (COBRA configurations)

This study has found that all riser components for both riser configurations have the capacity to perform the disconnectable turret operations in the event of an iceberg approach. Furthermore, these results indicate that there are similarities between the behavior of steel risers in the current study and those described in Section 7.5.3. Thus, it can be concluded that the steel risers on the uncoupled riser configurations may not be affected by the vessel motions.

8.4 Discussion

The purpose of this section is to present the summary results and discussions of the two suggested solutions to avoid iceberg collisions. In this thesis, an iceberg approach is considered as an accidental limit state (ALS). Therefore, the riser configurations should satisfy the minimum design requirements in order to avoid a catastrophic accident in the riser system. Two distinct water depths are applied in the accidental conditions to investigate suitable solutions for the SLOR and the COBRA configurations. The following paragraphs present the summary results and discussions of the riser configurations in the event of an iceberg approach.

- By using the riser arrangements as described in Table 7-3 for the SLOR configurations and Table 7-4 for the COBRA configurations, in 400 m water depth, the riser configurations have sufficient capacity to perform a 100-m drift-off from the initial vessel position in accidental conditions. For water depth of 1500 m, the riser configurations could reach a side-stepping of up to 250 m from the initial position with the acceptable design limitation for all riser components. These studies were performed in order to avoid the collision in the event of an iceberg approach.

- As an alternative solution, the new riser arrangements are set up based on Table 8-5 for the SLOR configurations and on Table 8-6 for the COBRA configurations in order to use participate in the disconnectable operations. According to the results in Section 8.3, both riser configurations have sufficient strength and capacity to perform the disconnectable turret operation in the event of an iceberg approach. The different required buoyancy modules on the turret are presented in Table 8-8 and Table 8-11 for the riser configurations in 400 m and 500 m water depths, respectively.

- Based on the analysis results for the drift-of case, a 20^0 'Riser Guide' opening is required in order to accommodate the higher departure angle at the vessel for both riser configurations in all water depths. However, a 12.5^0 'Riser Guide' opening is sufficient for use in the disconnectable turret system in all water depths.

- The results of this study conclude that, in the shallower water depth (i.e. less than 1000 m WD), the disconnectable turret system is a more favorable to use as a solution to avoid an ice berg collision in the accidental conditions. The maximum drift-off distance (i.e. 100 m) for both riser configurations in 400 m water depth is considered insufficient to avoid an iceberg collision. The reason for this is a limitation of water

depth; shallow water depth (less than 1000 m) cannot accommodate the length of the flexible jumpers which allow the vessel to side-step at the sufficient distance.

- According to the investigations into the riser configurations in 1500 m water depth, it can be concluded that the vessel drift off solution is a more beneficial solution in the event of an iceberg approach. The ability of both riser configurations to side-step up to 250 m is considered sufficiently acceptable to avoid an iceberg collision during the accidental conditions. Furthermore, the maximum drift-off distance is allowed to increase to a certain degree by modifying the initial riser arrangements in deeper water depth (i.e. more than 1000 m WD); for example, a longer distance can be used to shift the sub-surface buoyancy module further away from the center line of the vessel. It is possible, therefore, that plenty of room is available for the longer flexible jumpers installed in both riser configurations since the minimum clearance of the flexible jumper to the seabed in the current riser configuration is 850 m (refer to Figure 8-7).

  On the other hand, the disconnectable turret system in 1500 m water is also acceptable for use in for both riser configurations. However, this turret system requires high maintenance and operating cost to reconnect and assemble the turret system prior to proceeding with normal operations. Moreover, in terms of cost-effectiveness, it should also be taken into consideration that the production rate is affected during the disconnectable operation (Huang & Judge, 1996). Although the study has successfully demonstrated that the riser components sufficiently fulfill the minimum requirement, there are certain limitations in terms of economy aspects which it is necessary to consider in this system.

9. Conclusions and Recommendation

9.1 Conclusion

The Norwegian Sea has a unique physical environment which is characteristic in comparison to other areas. The area, which is situated in water depths not more than 2000 m, has the largest maximum wave height among other sea regions such as Campos Basin in Brazil, Gulf of Mexico, and West of Africa. By means of that, the Norwegian Sea is categorized as a hostile environmental area. In recent oil and gas, developments the industry demands advanced solutions to access the hydrocarbons in the deeper waters and harsh environmental conditions. However, none of the deep water riser configurations are installed in conditions which have similar environmental characteristics with the Norwegian Sea.

To overcome the challenges, the uncoupled riser configuration is introduced as a riser configuration which has the capability to decouple the floater motion effects from the sea surface. The combination of environmental loadings (i.e. wave loads, wind speeds and current loads) may create severe vessel motions in the low frequency (LF) as well as in the wave frequency (WF) range. Two types of uncouple riser configurations (SLOR and COBRA) are therefore purposely selected to investigate the robustness of the riser designs in the Norwegian Sea conditions.

In general, the selected uncoupled riser concepts show excellent capabilities in decoupling excessive vessel motions in the harsh environmental conditions, particularly in the Norwegian Sea. The use of flexible jumpers is effective in reducing the vessel motion effects, thus only minimum dynamic forces are being transferred to the lower part of the riser configurations. High departure angles of the flexible jumpers at the vessel indicate that the Norwegian Seas has harsh environmental conditions such as maximum wave heights exceeding 30 m, and sea current speed reaching 1.8 m/s. As described earlier, the combinations of environmental loadings significantly affect the floater motions at the sea surface. Therefore, by using the arrangements of a flexible jumper and a sub-surface buoyancy module, the vessel motion effects on the riser configurations are effectively reduced.

The analysis of the COBRA configurations have shown that the catenary riser shape is a robust and effective design due mainly to long layback distance in the deeper water depths. Lower bending stresses at the ‘Touch Down Point’ area are observed when the water depth increases. In addition, with the presence of the mooring lines of the COBRA buoyancy module, which are tethered down to the seabed, an excellent sub-surface buoyancy module behavior is produced. The equilibrium forces between the flexible jumper, the steel riser, and the mooring line lead to efficient sub-surface buoyancy module geometries.

The SLOR configurations, which are studied for three different water depths, suggest that this riser configuration has better performances in shallower water depths. The top-tensioned riser sections are supposed to be fully tensioned with a minimum declination angle in order to represent a robust design. In the deeper waters, a small value of riser declination angle at the buoyancy module results in high bending stresses at the bottom connection point. Therefore,

the SLOR configurations require a relatively massive sub-surface buoyancy module to produce sufficient amount of buoyancy forces in order to minimize the declination angle of the steel risers. The bigger subsurface buoyancy module may be associated with an inefficient design of the module in respect of design complexity, high construction and installation costs and high maintenance cost. Ultimately, it will also affect the time schedule.

In terms of the installation point of view, for both riser configurations it would be an advantage to preinstall the steel riser sections prior to connecting to the surface facility by using the flexible jumpers. Meanwhile, for the Norwegian Sea conditions, the COBRA configurations have a more robust and efficient design in comparison to the SLOR configurations during the operating conditions.

The accidental limit state (ALS) case in this thesis considers the possibility of drifting icebergs. Based on the analysis results in Chapter 8, in order to avoid iceberg collision, a disconnectable turret system is more favorable to apply for both riser configurations in the shallower water depth (i.e. less than 1000 m WD). However, regarding economic aspects, the drift off solution is the most cost-effective solution for both riser configurations to avoid the collision in the event of an iceberg approach in the deeper waters (i.e. more than 1000 m WD).

In summary, this thesis suggests that for the application of the riser concepts in the Norwegian Sea, the COBRA configuration is feasible to operate in water depths more than 1000 m with the hostile environmental conditions. In the accidental conditions, the COBRA configuration has sufficient capacity to allow a 250 m (or more) side-stepping in the event of an iceberg approach. In addition, the steel riser sections in the COBRA configuration can be installed in advance prior to arrival of the host facility. Therefore, these studies could serve as a base for advanced research of using the COBRA configurations as a future solution for the uncoupled riser configurations in deep water conditions.

9.2 Recommendation

It is recommended that further research be undertaken in the following areas:

- There is abundant room for further studies in determining the different configurations and arrangements of the mooring lines in the COBRA configurations to accommodate the forces acting from the perpendicular to the riser lay directions.
- A further study with more focus on the sub-surface buoyancy module location may take into account the reduced effects away from the wave zone area. In fact if the buoyancy module is located in deeper waters, this will reduce the hydrodynamic effects from the sea surface.
- In order to satisfy the departure angle requirements, a longer section of the flexible jumper may be used. Further studies, which take these variables into account, will need to be undertaken. In addition, a longer flexible jumper may increase the maximum side-stepping distance of the vessel in the event of an iceberg approach.

- In the Accidental Limit State, further investigations should be undertaken to study the cross drift-off case in which the vessel has to be shifted perpendicularly to the riser lay directions in the event of iceberg approaches.

- More comprehensive results may be achieved by applying current loads and wave loads omni-directionally for the global analysis of the riser configurations. It may give different riser analysis results and show different riser behaviors in the various load directions.

- Based on Karunakaran & Baarholm, 2013, the COBRA configurations have very robust fatigue performances. To confirm that these results are also applicable for the selected riser configurations in the Norwegian Sea, a fatigue analysis should performed as a further study to ensure that presence of sufficient fatigue life of the steel riser sections.

10. References

About Flow Assurance. (2007). Retrieved from http://www.statoil.com website: http://www.statoil.com/en/TechnologyInnovation/FieldDevelopment/FlowAssurance/Pages/default.aspx

Amundsen, B., & Lie, E. (2012). Westerently Storm Warm Norway. Retrieved from http://www.forskningsradet.no/ website: http://www.forskningsradet.no/en/Newsarticle/Westerly_storms_warm_Norway/1253979657686

Bai, Y., & Bai, Q. (2010). *Subsea Structure Engineer Handbook*. Huston, USA: Elsevier Inc.

Baltrop, N. D. P. (1998). *Floating Structure : A Guide for Design and Analysis* (Vol. 2). London: The Center for Marine and Petroleum Technology.

Chakrabarti, S. K. (2005). *Handbook of Offshore Engineering* (1st ed. Vol. I). Illinois, USA: Elsevier.

de Ruiter, J., & Fox, D. A. (1975). *Site Investigations For North Sea Forties Field, OTC-2246-MS*. Paper presented at the OTC, Dallas, Texas, USA.

Dean, R. G., & Dalrymple, R. A. (1984). *Water Wave Mechanics For Engineer and Scientists* (Vol. 2). Singapore: World Scientific.

DNV. (2010a). DNV-OS-F201: Dynamic Riser. Norway: Det Norske Veritas.

DNV. (2010b). DNV-RP-C205: Environmental Conditions and Environmental Loads. Norway: Det Norske Veritas.

DNV. (2012). DNV-RP-C203: Fatigue Design of Offshore Steel Structures. Norway: Det Norske Veritas AS.

DNV. (2013). DNV-OS-F101: Submarine Pipeline System. Norway: Det Norske Veritas AS.

Gudmestad, O. T., & Karunakaran, D. (2012). *Challenges Faced by the Marine Contractors Working in Western and Southern Barents Sea, OTC-23842-MS*. Paper presented at the ATC, Houston, Texas, USA.

Gudmestad, O. T., Olufsen, A., & Strass, P. (1995). *Challenges For the Development of Hydrocarbon Fields In the Barents Sea, ISOPE-I-95-170*. Paper presented at the International Offshore and Polar Engineering Confrence, The Hague, The Netherlands.

Howells, H., & Hatton, S. A. (1997). *Challenges for Ultra-Deep Water Riser System*. Paper presented at the Floating Production System IIR, London.

Huang, K., & Judge, S. (1996). *Turret Mooring System Design and Analysisfor Harsh Environments, OTC-8260-MS*. Paper presented at the OTC, Houston, Texas, USA.

Journee, J. M. J., & Massie, W. W. (2001). *Offshore Hydrodynamics* (1st ed.). Delft, Netherland: Delft University of Technology.

Journee, J. M. J., & Massie, W. W. (2002). *Ship Hydromechanics*. Delft, Netherland: Delft University of Technology.

Karunakaran, D. N., & Baarholm, R. (2013). *COBRA: An Uncoupled Riser System for Ultradeep Water in Harsh Environment, OTC-23986-MS*. Paper presented at the OTC, Houston, Texas, USA.

Lappegaard, O. T., Solheim, B. J., & Plummer, F. B. (1991). *Snorre Project Strategies and Status, OTC-6626-MS*. Paper presented at the OTC, Houston, Texas, USA.

Lien, T. (2010). Riser System. Retrieved from http://subsea1.com website: http://subsea1.com/index/page?page_id=11018

Maclure, D., & Walters, D. (2006). *Freestanding Risers in The Gulf of Mexico - A Unique Solution for Challenging Field Development Configurations*.

McGrail, J., & Lim, F. (2004). *SLOR vs. SCR for Deepwater Applications*. Paper presented at the International Offshore and Polar Engineering Confrence, Toulon, France.

NORSOK. (2007). N-003: Action and Action Effects. Norway: Standards Norway.

NPD, N. P. D. (2013). *FACTS 2013: The Norwegian Petroleum Sector* L. Alveberg & E. V. Melberg (Eds.),

Nurwanto, T. (2012). *COBRA Riser Concept for Ultra Deepwater Condition.* (MSc), University of Stavanger, Stavenger, Norway.

Orcina. (2013). Orcaflex Manual (Version 9.7a). Cumbria, UK: Orcina Ltd.

Rahmastorf, S. (2003). The Current Climate. Retrieved from http://www.nature.com/nature website: http://www.pik-potsdam.de/~stefan/Publications/Nature/nature_concept_03.pdf

Reitze, G., Mandeville, R. J. R., & Streit, P. (2011). *Installing the World's Deepest FSHR's, for the GOM Cascade & Chinook Development, OTC-21395-MS*. Paper presented at the OTC, Houston, Texas, USA.

Seymour, B., Zhang, H., & Wibner, C. (2003). *Integrated Riser and Mooring Design for the P-43 and P-48 FPSOs, OTC-15140-MS*. Paper presented at the OTC, Houston, Texas, USA.

Stewart, R. H. (2008). *Introduction To Physical Oceanography*. Texas, USA: Texas A & M University.

Totland, T., Pettersen, O. A., Grini, P. G., & Utengen, S. F. (2007). *The Norwegian Sea: The Development of a New Offshore Region, OTC-18956-MS*. Paper presented at the OTC, Houston, Texas, USA.

Appendix A – Wall Thickness Design Calculation

Wall Thickness Design Calculation

1 Data

1.1 Geometry Data

Pipe inside diameter	ID	254	mm
Pipe wallthickness	WT	26	mm
Pipe outside diameter	OD	306	mm
Fabrication tolerance		1%	
	t_{fab}	0.26	mm
Corrotion allowance	t_{corr}	3	mm
Ovality	f_0	2%	

1.2 Material Data, X56

Yield stress	F_y	448.2	MPa
Tensile stress	F_u	530.9	MPa
Young modulus	E	207000	MPa
Poison ratio	v	0.3	
Anisotropy factor		0.95	
Hardening factor		0.92	
Fabrication factor	α_{fab}	0.85	
Material sesistance factor (ULS)	γ_m	1.15	

1.3 Load Data

Water depth	h	1500	m
Water mass density	ρ_w	1025	kg/m^3
Incidental to desing pressure ratio	γ_{id}	1.1	
Load condition factor		1.07	
Stain		3%	

Operating Condition

Desing pressure	P_d	500	bar
		50	MPa
Content density	ρ_i	800	kg/m^3

Test Condition

Test pressure	P_t	550	bar
		55	MPa
Content density	ρ_i	1025	kg/m^3

2 Failure Mode

2.1 Brust

2.1.1 Brust in Operating Condition

Safety class resistance factor (High)	γ_{SC}	1.26	

Wall thickness during operating condition

$$t_1 = t_{nom} - t_{fab} - t_{corr}$$ 22.74 mm

Local internal design pressure

$$P_{Id} = \gamma_{id}.P_d$$ 55.00 MPa

Local incidental pressure

$$P_{li} = P_{Id} + 0.1\,.P_d$$ 60.00 MPa

External pressure

$$P_e = \rho_w.g.h$$ 15.08 MPa

Minimum requirement of brust pressure

$$P_b(t) = (P_{li} - P_e).\gamma_m.\gamma_{SC}$$ 65.08 MPa

Brust pressure resistance on the pipe

$$P_b(t_1) = \frac{2}{\sqrt{3}} \cdot \frac{2.t_1}{D - t_1} \cdot min\left(f_y; \frac{f_u}{1.15}\right)$$ 83.10 MPa

Unity Check

$$UC = \frac{P_b(t)}{P_b(t_1)}$$ 0.78

2.1.1 **Brust in Test Condition**

Safety class resistance factor (Test) γ_{SC} 1

Wall thickness during operating condition

$$t_1 = t_{nom} - t_{fab}$$ 25.74 mm

Local internal design pressure

$$P_{Id} = \gamma_{id}.P_t$$ 60.50 MPa

Local incidental pressure

$$P_{li} = P_{Id} + 0.1\,.P_t$$ 66.00 MPa

External pressure

$$P_e = \rho_w.g.h$$ 15.08 MPa

Minimum requirement of brust pressure

$$P_b(t) = (P_{li} - P_e).\gamma_m.\gamma_{SC}$$ 58.55 MPa

Brust Pressure resistance in the pipe

$$P_b(t_1) = \frac{2}{\sqrt{3}} \cdot \frac{2.t_1}{D - t_1} \cdot min\left(f_y; \frac{f_u}{1.15}\right)$$ 95.06 MPa

Unity check (UC)

$$UC = \frac{P_b(t)}{P_b(t_1)}$$ 0.62

2.2 **Collapse**

Safety class resistance factor (High) γ_{SC} 1.26

Wall thickness during operating condition

$$t_1 = t_{nom} - t_{fab} - t_{corr}$$ 22.74 mm

For the worst condition, It is considered that there is no content in the pipe

P_{min} 0 MPa

External pressure

$$P_e = \rho_w.g.h$$ 15.08 MPa

Minimum requirement of colapse pressure

$$P_c(t) = (P_e - P_{min}).\gamma_m.\gamma_{SC}$$ 21.86 MPa

Plastic collapse pressure

$$P_p(t_1) = 2 \cdot \frac{t_1}{D} \cdot f_y \cdot \alpha_{fab}$$ 56.62 MPa

Elastic collapse pressure

$$P_{el}(t_1) = \frac{2.E.\left(\frac{t_1}{D}\right)^3}{1-v^2} \qquad 186.71 \text{ MPa}$$

Colapse pressure resistance on the pipe

$$\frac{\left(P_c(t_1) - P_{el}(t_1)\right).\left(P_c{}^2(t_1) - P_p{}^2(t_1)\right)}{P_c(t_1)} = P_{el}(t_1).P_p(t_1).f_0 \cdot \frac{D}{t_1}$$

$P_c(t_1)$ 47.33 MPa

Unity Check

$$UC = \frac{P_b(t)}{P_b(t_1)} \qquad 0.46$$

2.3 **Propagating Buckling**

Safety class resistance factor (High) γ_{SC} 1.26

Propagating buckling factor γ_C 1

Buckling propagation is not allowed

Wall thickness during test condition for buckling check

$$t_2 = t_{nom} \qquad 26 \text{ mm}$$

For the worst condition, It is considered that there is no content in the pipe

P_{min} 0 MPa

External pressure

$$P_e = \rho_w.g.h \qquad 15.08 \text{ MPa}$$

Minimum requirement of propagating buckling pressure

$$P_{pr} = (P_e - P_{min}).\gamma_c.\gamma_m.\gamma_{SC} \qquad 21.86 \text{ MPa}$$

Propagating buckling resistance on the pipe

$$P_{pr}(t_2) = 35 \cdot f_y \cdot \alpha_{fab} \cdot \left(\frac{t_2}{D}\right)^{2.5} \qquad 28.06 \text{ Mpa}$$

Unity Check (UC)

$$UC = \frac{P_b(t)}{P_b(t_1)} \qquad 0.78$$

3 **Conclusion**

According to the above calculations, the riser wallthickness has sufficient strength to resist the internal and external net overpressure. In addition, the pipe wall thickess also satisfies the minimum requirement to avoid propagating buckling along the pipes.

Appendix B – Base Case Result

B.1 Static Response (ULS)

B.1.1 Riser Configurations in 400 m Water Depth

Flexible Jumper

Parameter	COBRA			SLOR		
	Near Y	Nominal	Far Y	Near Y	Nominal	Far Y
Maximum angle at vessel (deg)	1.29	7.02	10.24	0.72	7.87	11.32
Maximum angle at buoy (deg)	5.27	9.48	11.75	6.35	6.99	13.99
Maximum tension at vessel (kN)	1193.72	1198.46	1205.53	1192.81	1199.05	1208.75
Maximum tension at buoy (kN)	664.76	669.00	675.91	667.38	673.05	682.53
Minimum bending radius (m)	11.58	27.38	48.41	15.54	33.14	56.51

Steel Riser

Parameter	COBRA			SLOR		
	Near Y	Nominal	Far Y	Near Y	Nominal	Far Y
Maximum angle at buoy (deg)	3.47	2.45	1.87	1.56	2.21	1.32
Maximum tension at buoy (kN)	311.39	317.42	271.87	4748.43	4754.73	4761.20
Minimum tension at seabed (kN)	71.76	21.38	30.07	4533.36	4516.12	4522.63

B.1.2 Riser Configurations in 1000 m Water Depth

Flexible Jumper

Parameter	COBRA			SLOR		
	Near Y	Nominal	Far Y	Near Y	Nominal	Far Y
Maximum angle at vessel (deg)	0.13	6.66	8.46	1.00	7.45	9.29
Maximum angle at buoy (deg)	5.89	8.62	10.51	7.07	9.81	11.82
Maximum tension at vessel (kN)	1843.79	1848.31	1855.08	1925.24	1931.94	1938.75
Maximum tension at buoy (kN)	990.80	995.19	1000.83	1068.41	1073.10	1082.45
Minimum bending radius (m)	25.85	41.72	64.51	35.35	52.48	77.26

Steel Riser

Parameter	COBRA			SLOR		
	Near Y	Nominal	Far Y	Near Y	Nominal	Far Y
Maximum angle at buoy (deg)	4.14	3.41	1.86	2.17	2.83	2.49
Maximum tension at buoy (kN)	1069.36	1085.52	992.90	4352.11	4360.88	4367.58
Minimum tension at seabed (kN)	251.98	267.47	178.68	3537.28	3545.17	3577.41

B.1.3 Riser Configurations in 1500 m Water Depth

Flexible Jumper

Parameter	COBRA			SLOR		
	Near Y	Nominal	Far Y	Near Y	Nominal	Far Y
Maximum angle at vessel (deg)	1.27	7.98	9.66	0.24	6.98	8.46
Maximum angle at buoy (deg)	7.24	9.69	12.33	5.57	7.68	9.98
Maximum tension at vessel (kN)	2006.11	2017.76	2025.21	2002.25	2007.44	2012.32
Maximum tension at buoy (kN)	1143.85	1145.78	1157.41	1142.19	1144.23	1155.76
Minimum bending radius (m)	39.14	55.60	85.65	28.03	42.07	71.08

Steel Riser

Parameter	COBRA			SLOR		
	Near Y	Nominal	Far Y	Near Y	Nominal	Far Y
Maximum angle at buoy (deg)	4.69	3.54	2.72	1.93	2.48	2.25
Maximum tension at buoy (kN)	1788.09	1815.01	1668.98	4274.78	4282.96	4288.20
Minimum tension at seabed (kN)	384.07	443.15	284.61	2922.54	2903.58	2934.46

B.1.4 COBRA's Mooring Line

Parameter	COBRA		
	Near Y	Intact	Far Y
Water Depth of 400 m			
Maximum Mooring Tension (kN)	1949.49	1978.22	1976.64
Water Depth of 1000 m			
Maximum Mooring Tension (kN)	1417.77	1474.53	1466.98
Water Depth of 1500 m			
Maximum Mooring Tension (kN)	992.43	1080.55	1066.29

B.2 Dynamic Response (ULS)

B.2.1 Riser Configurations in 400 m Water Depth

Flexible Jumper

Parameter	COBRA			SLOR		
	Near Y	Intact	Far Y	Near Y	Intact	Far Y
Maximum angle at vessel (deg)	8.14	12.89	15.59	7.53	13.73	16.71
Minimum angle at vessel (deg)	0.00	0.00	6.68	0.00	0.00	7.83
Maximum at buoy (deg)	7.38	12.08	13.24	8.57	13.65	15.49
Minimum at buoy (deg)	3.93	2.87	9.27	5.01	4.48	11.71
Minimum bending radius (m)	10.07	22.47	41.92	13.67	27.82	48.81
Maximum water depth (m)	382.55	367.67	349.20	378.07	362.08	342.29
Minimum tension (kN)	28.42	58.69	101.87	38.38	70.99	116.30
Maximum tension at vessel (kN)	1479.31	1468.50	1509.24	1474.80	1468.21	1519.82
Maximum tension at buoy (kN)	683.50	708.39	721.98	690.25	718.00	736.24

Steel Riser

Parameter	COBRA			SLOR		
	Near Y	Intact	Far Y	Near Y	Intact	Far Y
Maximum angle at buoy (deg)	4.48	5.00	3.48	2.41	3.08	1.81
Minimum angle at buoy (deg)	2.00	0.96	0.99	0.96	0.00	0.44
Maximum tension at buoy (kN)	328.41	335.53	277.51	4879.63	4899.18	4901.19
Minimum tension at Steel Riser (kN)	63.26	3.28	11.37	4390.35	4356.08	4386.01
von Mises stress at buoy (Mpa)	149.71	149.72	149.69	168.29	168.43	168.44
von Mises stress on steel riser(Mpa)	121.41	121.44	120.43	127.51	127.55	127.50
von Mises stress at seabed (Mpa)	137.25	155.91	148.31	126.95	127.00	126.89
Maximum buckling UF at buoy	0.05	0.05	0.05	0.10	0.10	0.10
Maximum buckling UF at steel riser	0.67	0.79	0.76	0.05	0.05	0.05
Maximum buckling UF at seabed	0.24	0.30	0.28	0.04	0.04	0.04

B.2.2 Riser Configurations in 1000 m Water Depth

Flexible Jumper

Parameter	COBRA			SLOR		
	Near Y	Intact	Far Y	Near Y	Intact	Far Y
Maximum angle at vessel (deg)	5.77	11.75	13.17	4.91	12.46	13.90
Minimum angle at vessel (deg)	0.00	0.00	5.44	0.00	0.00	6.31
Maximum at buoy (deg)	6.62	9.48	10.82	7.77	10.59	12.13
Minimum at buoy (deg)	5.63	6.06	9.59	6.83	7.53	11.02
Minimum bending radius (m)	24.13	38.11	54.09	33.27	48.26	65.68
Maximum water depth (m)	580.89	566.23	546.43	597.60	582.52	560.68
Minimum tension (kN)	62.74	100.91	140.51	85.87	127.07	167.95
Maximum tension at vessel (kN)	2283.55	2268.76	2305.37	2381.89	2371.93	2415.96
Maximum tension at buoy (kN)	1026.14	1047.95	1058.85	1110.81	1133.66	1147.48

Steel Riser

Parameter	COBRA			SLOR		
	Near Y	Intact	Far Y	Near Y	Intact	Far Y
Maximum angle at buoy (deg)	4.49	3.75	2.45	2.45	3.12	2.70
Minimum angle at buoy (deg)	3.71	2.32	1.48	1.95	1.27	2.11
Maximum tension at buoy (kN)	1080.20	1099.28	1004.38	4420.34	4439.95	4445.47
Minimum tension at Steel Riser (kN)	258.35	157.18	173.51	3455.39	3454.93	3457.91
von Mises stress at buoy (Mpa)	147.49	147.52	147.35	162.25	162.39	162.43
von Mises stress on steel riser(Mpa)	118.11	118.14	117.89	123.67	123.73	123.64
von Mises stress at seabed (Mpa)	120.18	124.16	122.98	298.76	299.19	299.33
Maximum buckling UF at buoy	0.05	0.05	0.05	0.09	0.09	0.09
Maximum buckling UF at steel riser	0.33	0.44	0.41	0.38	0.39	0.39
Maximum buckling UF at seabed	0.15	0.18	0.17	0.21	0.22	0.21

B.2.3 Riser Configurations in 1500 m Water Depth

Flexible Jumper

Parameter	COBRA			SLOR		
	Near Y	Intact	Far Y	Near Y	Intact	Far Y
Maximum angle at vessel (deg)	4.59	12.89	14.19	5.51	11.94	13.05
Minimum angle at vessel (deg)	0.00	0.00	6.72	0.00	0.00	5.54
Maximum at buoy (deg)	7.89	10.33	12.66	6.10	8.27	10.26
Minimum at buoy (deg)	6.91	8.46	11.51	5.34	6.51	9.22
Minimum bending radius (m)	36.84	52.75	73.17	26.33	39.55	59.52
Maximum water depth (m)	620.02	604.94	580.32	629.95	617.45	590.37
Minimum tension (kN)	93.93	140.20	186.52	68.21	106.10	156.11
Maximum tension at vessel (kN)	2481.45	2475.91	2526.10	2482.23	2465.18	2501.97
Maximum tension at buoy (kN)	1198.62	1223.40	1246.97	1177.86	1196.14	1215.53

Steel Riser

Parameter	COBRA			SLOR		
	Near Y	Intact	Far Y	Near Y	Intact	Far Y
Maximum angle at buoy (deg)	4.98	4.28	3.27	2.19	2.75	2.47
Minimum angle at buoy (deg)	4.33	3.18	2.39	1.71	1.18	1.90
Maximum tension at buoy (kN)	1821.90	1860.48	1712.88	4341.03	4361.49	4364.50
Minimum tension at Steel Riser (kN)	405.76	251.31	274.61	2824.00	2815.83	2820.89
von Mises stress at buoy (Mpa)	149.28	149.40	148.95	161.71	161.86	161.88
von Mises stress on steel riser(Mpa)	118.74	118.80	118.43	123.45	123.49	123.43
von Mises stress at seabed (Mpa)	115.58	117.93	117.51	279.39	279.77	279.84
Maximum buckling UF at buoy	0.06	0.06	0.06	0.08	0.08	0.08
Maximum buckling UF at steel riser	0.24	0.33	0.31	0.32	0.32	0.32
Maximum buckling UF at seabed	0.12	0.15	0.14	0.18	0.18	0.18

B.2.4 COBRA's Mooring Line

Parameter	COBRA		
	Near Y	Intact	Far Y
Water Depth of 400 m			
Minimum Mooring Tension (kN)	1889.79	1868.41	1919.91
Maximum Mooring Tension (kN)	2007.27	2036.01	2039.71
Water Depth of 1000 m			
Minimum Mooring Tension (kN)	1375.53	1361.07	1419.00
Maximum Mooring Tension (kN)	1453.57	1519.26	1512.74
Water Depth of 1500 m			
Minimum Mooring Tension (kN)	927.40	919.56	983.36
Maximum Mooring Tension (kN)	1053.62	1161.61	1155.79

Appendix C – Accidental Study Result

C.1 Static Response (Vessel Drift-Off)

C.1.1 Riser Configurations in 400 m Water Depth

Flexible Jumper

Parameter	COBRA		SLOR	
	Near Y	Far Y	Near Y	Far Y
Maximum angle at vessel (deg)	1.82	11.21	1.20	12.37
Maximum angle at buoy (deg)	4.43	13.68	5.41	16.10
Maximum tension at vessel (kN)	1193.13	1209.78	1192.00	1214.23
Maximum tension at buoy (kN)	664.26	679.84	666.67	687.64
Minimum bending radius (m)	8.63	55.21	12.10	64.07

Steel Riser

Parameter	COBRA		SLOR	
	Near Y	Far Y	Near Y	Far Y
Maximum angle at buoy (deg)	3.67	1.40	1.43	1.63
Maximum tension at buoy (kN)	310.17	274.54	4748.02	4764.03
Minimum tension at seabed (kN)	68.08	34.81	4532.94	4525.49

C.1.2 Riser Configurations in 1500 m Water Depth

Flexible Jumper

Parameter	COBRA		SLOR	
	Near Y	Far Y	Near Y	Far Y
Maximum angle at vessel (deg)	1.03	14.61	1.89	12.14
Maximum angle at buoy (deg)	3.62	21.36	2.11	16.94
Maximum tension at vessel (kN)	1999.78	2064.03	1997.03	2043.50
Maximum tension at buoy (kN)	1140.26	1207.09	1141.08	1177.56
Minimum bending radius (m)	15.23	146.06	6.06	115.69

Steel Riser

Parameter	COBRA		SLOR	
	Near Y	Far Y	Near Y	Far Y
Maximum angle at buoy (deg)	6.88	1.30	1.01	4.18
Maximum tension at buoy (kN)	1713.19	1730.87	4270.72	4309.78
Minimum tension at seabed (kN)	324.67	339.74	2917.27	2958.87

C.1.3 COBRA's Mooring Line

Parameter	COBRA	
	Near Y	Far Y
Water Depth of 400 m		
Maximum Mooring Tension (kN)	1949.42	1976.03
Water Depth of 150000 m		
Maximum Mooring Tension (kN)	1042.55	1042.55

C.2 Dynamic Response (Vessel Drift-Off)

C.2.1 Riser Configurations in 400 m Water Depth

Flexible Jumper

Parameter	COBRA		SLOR	
	Near Y	Far Y	Near Y	Far Y
Maximum angle at vessel (deg)	8.64	16.51	8.10	17.71
Minimum angle at vessel (deg)	0.00	7.67	0.00	8.90
Maximum at buoy (deg)	6.42	15.19	7.51	17.49
Minimum at buoy (deg)	3.08	11.32	4.05	13.90
Minimum bending radius (m)	7.50	47.77	10.55	55.66
Maximum water depth (m)	385.53	343.92	381.50	336.65
Minimum tension (kN)	20.83	111.40	29.66	125.76
Maximum tension at vessel (kN)	1476.47	1516.92	1472.63	1529.92
Maximum tension at buoy (kN)	679.73	731.48	685.39	749.19

Steel Riser

Parameter	COBRA		SLOR	
	Near Y	Far Y	Near Y	Far Y
Maximum angle at buoy (deg)	4.69	2.96	2.27	2.12
Minimum angle at buoy (deg)	2.24	0.53	0.84	0.73
Maximum tension at buoy (kN)	326.96	280.65	4870.88	4909.04
Minimum tension at Steel Riser (kN)	62.08	13.74	4392.46	4374.86
von Mises stress at buoy (Mpa)	149.71	149.69	168.22	168.50
von Mises stress on steel riser(Mpa)	121.40	120.45	127.49	127.51
von Mises stress at seabed (Mpa)	137.26	148.70	126.92	126.90
Maximum buckling UF at buoy	0.05	0.05	0.10	0.10
Maximum buckling UF at steel riser	0.61	0.68	0.05	0.05
Maximum buckling UF at seabed	0.22	0.26	0.04	0.04

C.2.2 Riser Configurations in 1500 m Water Depth

Flexible Jumper

Parameter	COBRA		SLOR	
	Near Y	Far Y	Near Y	Far Y
Maximum angle at vessel (deg)	6.90	19.31	7.72	17.07
Minimum angle at vessel (deg)	0.00	11.65	0.00	9.15
Maximum at buoy (deg)	4.18	21.64	2.52	17.26
Minimum at buoy (deg)	3.36	19.65	1.82	15.79
Minimum bending radius (m)	14.31	129.14	5.75	99.72
Maximum water depth (m)	641.47	532.46	650.06	555.71
Minimum tension (kN)	37.82	296.14	13.03	241.86
Maximum tension at vessel (kN)	2501.81	2607.54	2496.64	2575.39
Maximum tension at buoy (kN)	1166.79	1340.07	1157.10	1278.71

Steel Riser

Parameter	COBRA		SLOR	
	Near Y	Far Y	Near Y	Far Y
Maximum angle at buoy (deg)	7.18	2.06	1.26	4.45
Minimum angle at buoy (deg)	6.52	0.66	0.80	3.78
Maximum tension at buoy (kN)	1731.73	1802.34	4310.42	4439.31
Minimum tension at Steel Riser (kN)	338.36	313.08	2853.27	2830.54
von Mises stress at buoy (Mpa)	149.01	149.24	161.51	162.37
von Mises stress on steel riser(Mpa)	118.61	118.60	123.35	123.56
von Mises stress at seabed (Mpa)	116.43	116.61	278.75	281.46
Maximum buckling UF at buoy	0.06	0.06	0.08	0.08
Maximum buckling UF at steel riser	0.25	0.25	0.30	0.31
Maximum buckling UF at seabed	0.12	0.12	0.17	0.17

C.2.3 COBRA's Mooring Line

Parameter	COBRA	
	Near Y	Far Y
Water Depth of 400 m		
Minimum Mooring Tension (kN)	1892.10	1915.09
Maximum Mooring Tension (kN)	2003.89	2041.95
Water Depth of 1500 m		
Minimum Mooring Tension (kN)	979.14	935.05
Maximum Mooring Tension (kN)	1059.56	1181.29

C.3 Static Response (Disconnectable Turret System)

C.3.1 Riser Configurations in 400 m Water Depth

Flexible Jumper

Parameter	COBRA	SLOR
Maximum angle at vessel (deg)	10.48	12.29
Maximum angle at buoy (deg)	21.01	21.96
Maximum tension at vessel (kN)	886.44	886.44
Maximum tension at buoy (kN)	358.14	361.14
Minimum bending radius (m)	34.66	44.06

Steel Riser

Parameter	COBRA	SLOR
Maximum angle at buoy (deg)	2.25	2.40
Maximum tension at buoy (kN)	318.76	5084.86
Minimum tension at seabed (kN)	79.26	4869.71

C.3.2 Riser Configurations in 1500 m Water Depth

Flexible Jumper

Parameter	COBRA	SLOR
Maximum angle at vessel (deg)	12.25	10.75
Maximum angle at buoy (deg)	23.12	19.15
Maximum tension at vessel (kN)	1491.19	1477.59
Maximum tension at buoy (kN)	632.83	624.17
Minimum bending radius (m)	71.23	56.65

Steel Riser

Parameter	COBRA	SLOR
Maximum angle at buoy (deg)	2.19	2.59
Maximum tension at buoy (kN)	1692.04	4827.27
Minimum tension at seabed (kN)	287.22	3475.88

C.3.3 COBRA's Mooring Line

Parameter	COBRA
Water Depth of 400 m	
Maximum Mooring Tension (kN)	2138.48
Water Depth of 150000 m	
Maximum Mooring Tension (kN)	1329.60

C.4 Dynamic Response (Disconnectable Turret System)

C.4.1 Riser Configurations in 400 m Water Depth

Flexible Jumper

Parameter	COBRA	SLOR
Maximum angle at vessel (deg)	10.76	12.36
Minimum angle at vessel (deg)	3.04	4.89
Maximum at buoy (deg)	18.70	22.51
Minimum at buoy (deg)	14.51	18.54
Minimum bending radius (m)	15.39	21.62
Maximum water depth (m)	378.28	370.21
Minimum tension (kN)	48.32	67.27
Maximum tension at vessel (kN)	1210.82	1195.38
Maximum tension at buoy (kN)	1210.82	1195.38

Steel Riser

Parameter	COBRA	SLOR
Maximum angle at buoy (deg)	5.16	3.80
Minimum angle at buoy (deg)	0.17	0.00
Maximum tension at buoy (kN)	344.76	5151.83
Minimum tension at Steel Riser (kN)	4.80	4384.67
von Mises stress at buoy (Mpa)	149.72	170.30
von Mises stress on steel riser(Mpa)	121.33	128.28
von Mises stress at seabed (Mpa)	155.27	127.73
Maximum buckling UF at buoy	0.05	0.09
Maximum buckling UF at steel riser	0.72	0.04
Maximum buckling UF at seabed	0.27	0.04

C.4.2 Riser Configurations in 1500 m Water Depth

Flexible Jumper

Parameter	COBRA	SLOR
Maximum angle at vessel (deg)	12.42	11.00
Minimum angle at vessel (deg)	5.00	3.24
Maximum at buoy (deg)	21.39	17.68
Minimum at buoy (deg)	19.93	16.30
Minimum bending radius (m)	53.53	41.03
Maximum water depth (m)	573.64	584.01
Minimum tension (kN)	107.13	80.96
Maximum tension at vessel (kN)	1929.49	1915.19
Maximum tension at buoy (kN)	1104.36	1083.94

Steel Riser

Parameter	COBRA	SLOR
Maximum angle at buoy (deg)	3.96	3.75
Minimum angle at buoy (deg)	2.06	0.87
Maximum tension at buoy (kN)	1922.92	5074.60
Minimum tension at Steel Riser (kN)	260.46	2944.75
von Mises stress at buoy (Mpa)	149.61	166.95
von Mises stress on steel riser(Mpa)	118.90	125.50
von Mises stress at seabed (Mpa)	117.79	299.48
Maximum buckling UF at buoy	0.06	0.09
Maximum buckling UF at steel riser	0.30	0.36
Maximum buckling UF at seabed	0.13	0.20

C.4.3 COBRA's Mooring Line

Parameter	COBRA
Water Depth of 400 m	
Minimum Mooring Tension (kN)	1875.79
Maximum Mooring Tension (kN)	2143.39
Water Depth of 1500 m	
Minimum Mooring Tension (kN)	967.65
Maximum Mooring Tension (kN)	1343.01